HSE
Health & Safety Executive

A study of pile fatigue during driving and in-service and of pile tip integrity

Prepared by **MSL Engineering Limited**
for the Health and Safety Executive

OFFSHORE TECHNOLOGY REPORT
2001/018

HSE
Health & Safety Executive

A study of pile fatigue during driving and in-service and of pile tip integrity

MSL Engineering Limited
MSL House
5-7 High Street
Sunninghill
Ascot
SL5 9NQ
United Kingdom

HSE BOOKS

First published 2001

ISBN 0 7176 2040 9

FOREWORD

This document summarises a study undertaken by MSL Engineering Limited for the Health and Safety Executive to determine the effects of pile driving and environmental loading on the fatigue lives of piles in typical minimum facility jacket structures. The study also reviewed the effects of pile driving on the integrity of the pile tip against damage.

The objective of the study was to determine the sensitivity of piles to fatigue with respect to both foundation soils and welding details, and to review the propensity of pile tips built to usual fabrication tolerances or with initial dents to further damage.

CONTENTS

1. SUMMARY

The study reported herein is concerned with two aspects of foundation pile integrity. The first aspect deals with fatigue damage, such damage being the result of pile driving stresses and in-service stresses caused by environmental loads on the structure. The second aspect is a consideration of pile tip integrity i.e. the ability of the pile tip to maintain its circular shape during handling operations and driving.

The first aspect, i.e. fatigue, is examined by analyses conducted on two minimum facility structures, both with two assumed soils profiles. Minimum facility structures have been chosen for this study as it can be expected that the ratio of environmental to gravity loads will be higher for these type of structures than jacket structures with heavy topsides loadings. A monotower structure and a Vierendeel structure were selected.

Pile tip integrity was investigated assuming an initial pile geometry ovalised either in accordance with or outside maximum fabrication tolerances, and a pile dented due to handling or due to hitting a boulder or rock during driving.

The fatigue study showed that fatigue damage of piles due to in-place conditions and driving is significant and in order to achieve acceptable total fatigue lives a HSE "C" curve is required. For the structures considered in the report grinding of girth welds in the fatigue sensitive regions is therefore needed if this detail is to be achieved. Both sand and clay foundation soils were found to be almost equally sensitive in giving rise to pile fatigue damage.

The overall conclusions of the pile tip integrity study are that where the sections remain within usual fabrication tolerances, piles will not experience unstable increases in ovality. Even where the ovality significantly exceeds allowable tolerances, ovality could, at most, double in extent, due to a wedge effect increase in lateral soil pressure. Damage due to high tip loads, caused by handling or installation forces, can occur for tubulars of high D/t ratios and under medium to hard driving conditions, initial damage can increase under a wedge mechanism. Only conditions of significant initial damage are likely to present a problem. For typical driving conditions and normal soils, it has been shown that end tip stresses will remain below yield. However, where end bearing is a very high proportion of total resistance, for example in soft rocks, stresses may reach dynamic yield stress. Damage could then occur if local concentrations of high stress occurs, coupled with reduction in wall thickness due to chamfering.

2. INTRODUCTION

2.1 General

Fatigue damage is of particular concern where members are not accessible for inspection. Therefore it might be expected that fatigue calculations for pile foundations would be highlighted in the usual offshore codes. However, API RP2A[1,2] for instance does not provide any guidance on the procedures for pile fatigue design. Fatigue damage can be caused by loads due to pile driving as well as by in-place loading. It might also be expected that where single piles are used at each leg, such as minimum facility structures, potential damage could be more severe, since there is no re-distribution of loads within a pile group. Therefore, given the increasing use of minimum facility structures, supported by single piles rather than pile groups, and where there is a higher proportion of environmental to gravity loading, there is a need to determine the likely damage suffered by these foundations.

Pile tip damage is an area for which designers do not carry out any explicit calculations, since it is assumed that typical pile geometries will provide robust piles which will not be subject to potential problems. While there is no known incidences of damage to North Sea installations, problems are known to have occurred in other offshore regions. Design codes provide very little guidance on the likely problems to be met in driving conditions where tip integrity is an issue.

HSE has commissioned MSL Engineering to carry out a short study on the subject of pile fatigue and pile tip integrity, the objectives and scope of work for which are given below

2.2 Objectives and Scope of Work

2.2.1 Objectives

The objectives of the study were as follows:

- To establish the propensity for pile fatigue damage during pile installation and under in-place conditions.
- To investigate the fatigue lives of piles used on typical Minimum Structures deployed offshore.
- To establish conditions under which pile tip integrity may be compromised under driving conditions.

2.2.2 Scope of Work

The scope of work, which was carried out, was as follows:

- Undertake data capture activities relating to all information on pile fatigue and pile tip integrity
- Identify approaches to pile driving fatigue and in-place pile fatigue
- Agree with HSE two pile driving scenarios for clay and sand soil profiles
- Agree two minimum facility structures for analysis
- Carry out in-place analysis to determine pile requirements and in-place fatigue analysis to assess fatigue damage for two structures in the two soil types

- Derive methods for determining tip capacity of tubular piles
- Undertake pile tip integrity calculations for typical soil types
- Establish conditions under which integrity may be compromised
- Prepare report covering fatigue and pile tip integrity findings.

3. PILE FATIGUE

3.1 Background

Steel jacket structures are usually supported by a foundation system comprising tubular steel piles. These may be driven through the legs or through sleeves attached to the legs in a pile cluster or arranged around the perimeter of the jackets as skirt piles. Connections between the piles and the sleeves or legs may comprise mechanical or grouted connections, or alternatively via a welded connection at the top of the leg.

Methods for calculating the static strength of the piles are provided in the usual offshore design rules, e.g. API[1,2] and DNV[3], along with alternative procedures for calculating the strength of grouted connections. There are no guidelines available in the existing codes for the treatment of fatigue in relation to piles either during the in-place or driving condition. Thus, despite the well-documented consideration of driving damage to secondary appurtenances such as anodes and hose or pipe connections (e.g. Beryl 'B'[4] monitoring), there are no pile driving fatigue guidelines for the designer. Although there are no documented in-service failures due to fatigue, the inaccessibility of piles and therefore the lack of inspection possibilities, implies that the possibility of fatigue damage should be considered at least as critical as for platform members. Minimum facility structures are probably more vulnerable since tension-compression load cycling in the piles is more likely and therefore fluctuating stress damage could be more onerous.

It is noted, however, that the offshore industry generally approaches the design of piles responsibly, and therefore fatigue checks on the piles are usually conducted. Where these checks indicate low lives, more careful and accurate assessments of pile fatigue life are conducted, including possible defect tolerance by fracture mechanics. Grinding of pile girth welds to improve the S-N curve is not unknown.

Whilst there are no recommendations in the codes, work has been carried out on the effect of pile driving on fatigue lives by British Steel [5,6] (now part of the Corus group). This work concluded that residual stresses are reduced due to the stress shakedown effect of pile driving and hence fatigue performance is improved. Test specimens were subjected to a very onerous impact loading (maximum 44,000 hammer blows), and the fatigue life was improved by a factor of four relative to control specimens. The latest proposals for ISO [7] and the HSE Guidance Notes[8] (now withdrawn) do not recognize this beneficial effect.

Damage occurs as a result of in-place cyclic loads from environmental loading and fluctuating stress waves caused by the driving hammer during the installation phase. It is usual to carry out a spectral analysis of jacket members since the probabilistic nature of the loads and response is more accurately described. This procedure uses harmonic analysis and assumes a linear load response, to allow interpolation between different wave heights. Where non-linear behaviour of soils exists, it may be considered that assumptions of linearity are inaccurate. However, it is found that damage is concentrated in the low wave heights of the spectrum, and therefore linearity assumptions may be adequate. Driving fatigue damage is assessed by a deterministic approach using best estimates of driving resistance, coupled with wave equation analyses, to calculate blowcounts and stress ranges respectively.

Fracture mechanics analysis may be used if it is considered that fatigue damage is very onerous, in an effort to quantify the effect of defects.

3.2 Design Data

3.2.1 Structures

The minimum facilities structures which have been chosen for this study represent generic types of lightweight structures, i.e. maximum lift weight of about 250tonnes, which may be used in the shallower areas of the UK offshore sector. It has been assumed that they are located in the Southern North Sea, where water depths are a maximum of about 40m and wave heights (Hmax) limited to about 14m to 16m. Topsides facilities will be of the order of a maximum of 150 tonnes, and installation could be using a HLV or possibly with a jack-up. A monotower structure with three piles, and a Vierendeel jacket with four piles are considered. Each platform is situated in 34m of water (Mean Sea Level - MSL).

3.2.1.1 Monotower

A computer analysis model of the Monotower structure is shown in Figure 3-1. It comprises of a single column, referred to as a caisson. This pierces the water surface, to support the topsides and shield risers, j-tubes and conductors. The caisson (2.4m diameter) is braced at its base with diagonal bracings, which connect it to three pile sleeves arranged in the form of an equilateral triangle in plan. The pile sleeves are approximately 23m apart and form grouted connections with the 1067mm diameter piles.

3.2.1.2 Vierendeel

The Vierendeel structure, Figure 3-2, comprises four legs (approximately 0.8m diameter and approximately 5m apart), which support the topsides and pierce the water surface. Horizontal bracing members connect each leg to the adjacent leg. There are no diagonal braces connecting the legs of the platform to each other. The base of the platform has a wide square arrangement in plan of 20m x 20m. This is connected to the legs by diagonal bracing and at each corner of the square is a pile sleeve. Again these are attached to the piles via grouted pile-to-sleeve connections. For each platform model the topsides is assumed to support a load of 150 tonnes and the piles are sized at 1067 mm diameter and 38 mm thickness.

3.2.2 Environmental and Hydrodynamic Data

There is an abundance of wave and current data available for the Southern North Sea of the UK sector. Therefore suitable water depth and wave and current data was assumed using data available in-house and typical of this location. For the storm wave a maximum water depth was used, including tidal variations. A scatter diagram for fatigue was adopted from typical data for this region.

Omnidirectional extreme waves for a 50 year return period storm were used for the analysis as shown below:

Table 3.1
Extreme Waves for 50-year storm

Water depth (m)	H_{max} *(m)*	*Period (sec)*		
		T_{min}	T_{cent}	T_{max}
34.0	14.2	10.9	12.5	13.8

The wave spreading factor used for the storm waves was taken as 0.85. A storm wave current was included in the static maximum loading analysis. A constant mean sea water level (MSL) of 34.0m was used for both the Monotower and Vierendeel platforms.

The waves for the spectral fatigue analysis, which describe the probable seastates that the two platforms would be subjected to, were taken from a typical Southern North Sea scatter diagram which has been used previously for minimum facilities jacket design.

Hydrodynamic coefficients were modified to allow for the presence of sacrificial anodes on the structures. A Cd value of 0.7 and a Cm of 2.0 were used for all members.

Marine growth was included on the jacket members. The following profile was used:

Table 3-2
Hydrodynamic coefficients

MSL (m)	Thickness (mm)
Above +2.0	0
+2.0	125
0.0	125
- 6.0	50
Seabed	50

3.2.3 Geotechnical Data

3.2.3.1 General

Two types of soils have been considered, an all sand site and an all clay site. Data has been assumed which are typical of Southern North Sea deposits. A sand site was chosen representing typical moderately hard driving conditions and a clay site, where softer driving conditions would exist and therefore less severe driving fatigue damage would be incurred. Higher mudline bending stresses on the piles under in-place conditions in the softer strata might be expected; a different distribution of pile stresses below mudline at each site would be expected to result in varying damage ratios.

3.2.3.2 Soils Profiles

In the Southern North Sea sands often dominate the stratigraphy. The soils usually comprise sands or over-consolidated to normally consolidated clays at depth. The sands often lie over the clays and are usually dense to very dense at depth. It is common to find clay beds within the sand sites. For design and comparison of the two generic type soils, all sand and all clay design profiles are used to represent the two idealised sites.

The sand site profile is characterised by a CPT profile and a corresponding internal friction angle profile, Figure 3-3. It is assumed that the progression is loose to medium dense sands overlying dense to very dense sand. Minimum q_c varies from 0.1MPa at mudline to 5MPa at 5m below mudline and to 60MPa at 60m depth. Maximum internal friction angle for API pile capacity checks was assumed as 35 deg.

A normally consolidated clay profile has been assumed. The strength, Su, with depth profile is shown in Figure 3-4, where the strength is assumed to vary as twice the penetration depth below mudline. At 50m depths the maximum shear strength is 100kPa.

Profiles of unit weight assumed in the design are shown for the two sites in Figure 3-5.

3.3 Pile Capacity Curves

Axial capacity is assessed from considerations of skin friction and end bearing. For offshore pile design it is usual to follow the recommendations of API [1,2] in determining the capacity, although other methods are currently available, for example the MTD method [9]. The design was carried out according to working stress methods and pile capacity curves were therefore determined for both sites following 20th Edition API RP2A procedures adapted to usual North Sea design methods, as recommended by Lloyd's Register [10].

The sand site capacity curves are shown in Figure 3-6 for piles of diameter 1067mm and 762mm. K values of 0.5 in tension and 0.7 in compression (API 13th Edition[11]) were assumed. Although the latest API allows interface friction angles up to 33deg, maximum values of interface friction angles (δ) of 30 deg were used. These are in line with usual North Sea recommendations[10]. Maximum values of compressive capacity for the 1067mm Dia pile is 6.7MN at 25m and 19.7MN at 50m penetration depths. The corresponding tension values are 2.3MN and 9.5MN. End bearing comprises about 30% of the compressive capacity. In determining these curves an allowance of 1.0m scour has been included.

Clay site capacity curves are shown in Figure 3-7. The c/po method in API 20th Edition was used to calculate shaft friction. End bearing was determined as 9 x Su, where Su is the undrained shear strength. Maximum compressive capacity is 2.5MN at 25.0m penetration depth increasing to 9.2MN at 50.0m penetration. Corresponding tension capacities are only a little lower at 2.0MN and 8.4MN respectively. An allowance for 1.0m scour has again been included.

3.4 Static Analysis

3.4.1 Static Design of Piles

3.4.1.1 Background

A foundation model usually includes a description of the pile axial and lateral soil springs for each pile in a group. This may then be incorporated as a sub-structure in the analytical model which is coupled to the jacket and allows full interaction effects between structure and foundation to be accounted for.

Having determined axial pile loads, shear and head moments from a structure-foundation interaction analysis, the problem is then to determine the optimum pile size and penetration depth. Capacity curves will be available for a range of pile sizes, either determined by the designer or provided by the soils consultant. Using the capacity curves, the required penetration depth is determined. A driveability study is required to confirm that the penetration depth is achievable with the proposed hammer. In terms of efficient use of pile material it would be appropriate to use the smallest diameter suitable for the shear and moment loads, and deepest pile penetration. Installation requirements, however, will usually result in a shallower pile of larger diameter.

Shear stiffness is decided by the p-y curve stiffness. This is dependent on the soil type and strength and is partly a factor of the pile diameter, the unit stiffness negatively correlating with pile diameter.

Pile installation considerations and achievable penetration depth will be governed by the availability of driving hammers and the driving resistance expected at the site. Wall thickness in the top of the pile (mudline thickening) is governed by the static resistance required to resist the applied lateral loads. Overall pile wall thickness considerations partly govern the

pile driveability response, and therefore it is likely that the heavier pile will be easier to install.

Wall thickness design for fatigue is not normally a primary design consideration. Whilst cyclic degradation is not usually checked for UK offshore structures, test results indicate that cyclic degradation may be significant and this could be of particular relevance for minimum structures, particularly where topsides loads are low and leg reactions are resisted by a single pile. A typical flow diagram for this pile design procedure is shown in Figure 3-8.

3.4.1.2 Analytical Model

For the models reported herein, the soil-structure interaction was carried out using an ASAS/SPLINTER[12] analysis, in which the piles and non-linear soil springs are modelled using p-y (lateral springs), t-z (skin-friction springs) and q-z (end bearing springs). The model is sub-structured so that pile head load vectors from the jacket are applied to the pile-soil model and a solution to the pile displacements determined by iteration. The displacement vector is then back-substituted to allow the final jacket forces and displacements to be calculated.

3.4.1.3 Target Penetration

Initially a static analysis was carried out assuming that the jacket was fixed at mudline, and the maximum foundation reactions were determined. Using the results from this analysis, maximum tension and compression loads were identified. To determine target penetrations, the self-weight was added to the static analysis results and a factor of 1.5 applied to give total required capacity. In calculating maximum tension capacity requirements, self-weight was ignored.

Maximum capacity requirements and target penetrations identified using these loads are shown below.

Table 3-3
Target Penetration Requirements

	Monotower Capacity MN	***Monotower Penetration***	***Vierendeel Capacity MN***	***Vierendeel Penetration***
Sand Site	4.0 Compression* 1.0 Tension	23m	3.6 Compression 1.6 Tension*	22m
Clay Site	4.2 Compression* 1.0 Tension	34m	3.7 Compression* 1.6 Tension	32m

* governing condition

3.4.2 Pile-Soil-Interaction Models

3.4.2.1 Lateral Load Deflection

The lateral load deflection curves have been calculated using the recommendations given in API. In sands the curves are calculated according to the O'Neill Murchison[13] method. The required coefficients were determined using the relationship with angle of internal friction, ϕ, shown in API. For clays, the modified Matlock[14] soft clay formulation has been used. Cyclic degradation of the p-y curves has been assumed for both clays and sand.

To determine the curves, spreadsheets were used, with the idealised design soil profiles as input data, including internal friction angles, undrained shear strength, and overburden pressures. The calculated spreadsheet curves were then transferred into input data files for SPLINTER.

In the models it was assumed that shear loads are applied at mudline.

3.4.2.2 Axial Load Deflection

Deflection curves for skin friction (t-z) and end bearing (q-z) in sand and clay were determined in spreadsheets using the API method. Skin friction values (t) were input from the axial capacity calculations for the appropriate penetration depth. End bearing (q) values were determined for the skirt pile assuming full end bearing, as the capacity analysis concluded that the pile acts as plugged.

3.4.2.3 Mudline Stress Checks

In each SPLINTER file the foundation model was created with a single soil type; due to the relatively large pile spacing, it was assumed that there would not be any Mindlin-type interaction between the piles. The pile length determined from the preliminary static model was used in the analysis. The P-Δ option was used to ensure that the secondary moment effects were included within the model.

Wall thickness of the piles are determined by the requirements for resistance to static axial and bending loads during in-place conditions as well as driveability considerations. Mudline stress checks of the steel cross-section to API LRFD were carried out as part of the ASAS member stress checks. At the mudline the maximum utilization (API) for combined axial and bending stresses in the monotower piles are 0.16 for the sand site and 0.32 for the clay site. The drop-off in pile stress from the mudline is shown in Figure 3-9 and Figure 3-10 for the monotower pile in sand and clay respectively. Both bending stress and combined axial and bending stress values are shown. Variation in the direction of the bending stress along the pile is indicated, while the absolute magnitude of maximum combined stress is shown.

Lateral deflections at the skirt pile head for the sand and clay sites are shown in Figure 3-11. At the soft clay site the mudline deflection (117mm) is much larger than at the sand site (27mm).

Whilst not shown, stress and deflection profiles for the Vierendeel piles are similar, although slightly smaller in magnitude because of the lower mudline shear.

3.5 In-Place Fatigue Analysis

3.5.1 Introduction

Methodology

The spectral fatigue approach to the calculation of fatigue is well documented [15]. The main features of the spectral analysis are as follows:

- The spectral fatigue analysis considers the dynamic response of the structure to a range of waves covering a frequency range which includes all sea states contributing to significant fatigue damage.
- Response transfer functions and sea state spectra are used to generate stress spectra according to the power spectral density approach.

- Assuming that the stress histories conform to a Rayleigh distribution, damage is calculated using Miner's Rule.

ASAS was used for the spectral fatigue analysis and to calculate damage. The dynamic response analysis which is used to determine the behaviour of the structure under the forcing transfer functions, is applicable to a linear system only. Therefore, strictly speaking, it is not appropriate to use a non-linear soils model in the analysis. Under the wave loads which cause the maximum damage, it can be argued that the incorporation of the soils model will be adequate, since the soil response will be linear at those loads. However, since it is not possible to interrogate the pile stresses and thus to determine damage using SPLINTER [12], the foundation model has been incorporated by using a linear spring representation of soils, applied to a pile modelled as a structural member.

The aim of the in-place fatigue analysis is to determine the resistance to fatigue, and hence the fatigue lives, of hypothetical girth welded joints down the pile length. To assess the fatigue performance of the pile for in-place conditions, the service life of each platform is assumed to be 30 years; thus to comply with API [1,2], DNV [3], and the proposed ISO [7] codes the target fatigue life for the piles (non-inspectable item) is 10 times that of the platform life, i.e. 300 years.

The analysis of each platform was carried out using a seastate spectrum that is typical for a platform in the Southern North Sea area. This spectral data of significant wave heights, with corresponding periods and occurrences, was used for waves attacking the platforms from all eight (8) compass directions.

3.5.2 Description of Analysis

The first two Eigen modes and natural periods, for each structure, were determined to establish the Dynamic Amplification Factors (DAF) for the waves. Each platform structure was subjected to a range of omnidirectional wave heights and frequencies in the eight compass directions. This was done to establish a relationship between wave height and stress range. These waves are referred to as stress transfer waves.

The final stage of the fatigue analysis, that concerning the response of the structures to loading comprised three (3) stages:

- Identification of foundation loads for pinned supported model at seabed level – to define pile penetrations; the two platforms were subjected to deterministic storm wave loads.
- Spectral fatigue analysis to establish the centre of damage wave – the wave was used to establish the soil-springs for the next stage;
- Spectral fatigue analysis to determine the cumulative damage, and thus the fatigue life of the pile foundations.

The two platforms were subjected to the loads due to self-weight, buoyancy, weight of the topsides and the wave loads from eight wave directions. The base shears and overturning moments were then used to determine the adequate penetration depth, for the chosen pile geometry, required in the clay and sand soils respectively. For the wave loading the wave height and period were omni-directional and are represented by the 50-year return storm wave of height 14.2 m and period 13.8 s (stream function theory).

The foundation reactions at the seabed are shown overleaf.

Table 3-4
Monotower storm load reactions

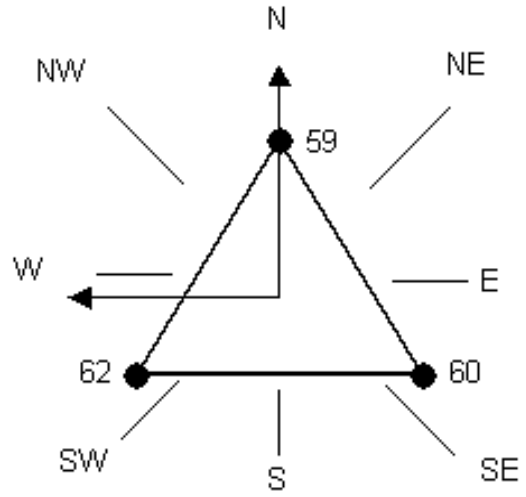

Axial loads on seabed (kN)			
Wave from direction…	Support node at seabed		
	59	60	62
South	-2367	-10.9	-20
South East	-1924	+752	-1228
East	-807	+589	-2191
North East	+331	-394	-2356
North	+809	-1597	-1606
North West	+331	-2347	-404
West	-807	-2182	+580
South West	-1924	-1219	+743

Note: compressive loads are –ve.

Table 3-5
Vierendeel storm load reactions

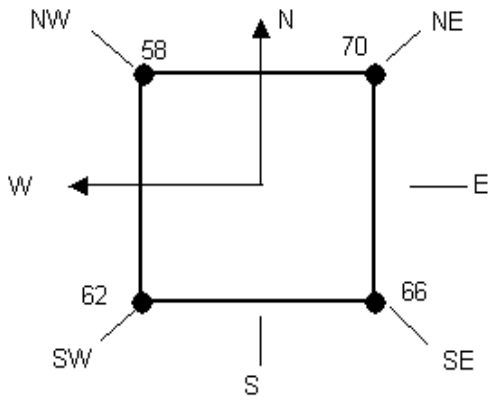

Axial loads on seabed (kN)				
Wave from direction…	Support node at seabed			
	58	62	66	70
South	-1626	+811	+807	-1616
South East	-2077	-399	+1263	-399
East	-1627	-1616	+807	+812
North East	-409	-2067	-403	+1266
North	+803	-1618	-1616	+807
North West	+1258	-404	-2064	-404
West	+803	+807	-1616	-1618
South West	-409	+1266	-403	-2067

Note: compressive loads are –ve.

3.5.3 Calculation of DAFs

For the calculation of the Dynamic Amplification Factors (DAFs), the first step in the calculation was to determine the first natural period for each structure respectively. For spectral fatigue analysis the stress levels are normalised to wave height. Therefore stream function waves with wave frequencies between 0.025 Hz and 0.605 Hz were enhanced with DAFs so that the maximum stress levels induced by these waves would provide the basis of the spectral analysis.

The Dynamic Amplification Factors are based on the steady state harmonic loading calculated for each wave. If the applied frequency of the wave is ω, the natural frequency of the structure is ω_n and the critical damping ratio ξ is 5%, then the DAFs are calculated using the formula below:

$$DAF = [\{1-(\omega/\omega_n)^2\}^2 + (2.\xi.\omega/\omega_n)^2]^{-½}$$

3.5.4 Centre of Damage Wave

The spectral fatigue analysis was performed, with soil-pile interaction behaviour described by p-y and t-z curves, to determine the wave that produced the maximum cumulative yearly fatigue damage (the centre of damage wave), in the two structures respectively. Fatigue damage was calculated on the following basis.

Stress range transfer functions were determined for the eight (8) wave directions using stream function waves with wave frequencies between 0.025 Hz and 0.605 Hz. The wave height (H)-wave period relationship (T) was determined on the basis of a 1/20 steepness between the wave height and wavelength (L), and the relationship: $L=1.56\ T^2$. The resultant stresses were normalised to wave height. The seastate, which is a series of spectral wave sequences, was defined by a JONSWAP spectrum. Loads were calculated using Morison's equation and the induced stresses were calculated for the spectrum using the stress transfer functions, which were enhanced by the DAFs previously calculated.

The damage waves for the Monotower and Vierendeel are shown in Table 3-6 below and graphically in Figure 3-12 and Figure 3-13 respectively. Note that in accordance with HSE [8] a maximum trough-to-crest height of $1.86H_s$, and an associated period of $3.58H^{0.5}$, has been used to calculate the maximum wave height H_{max}, the zero crossing period T_z and maximum period.

Table 3-6
Centre of damage wave

Structure	***Centre of Damage Wave***				***1st Natural period (seconds)***
	H_s (m)	T_z (s)	H_{max} (m)	T_{max} (s)	
Monotower	1.75	4.73	3.26	6.46	2.18
Vierendeel	1.75	4.73	3.26	6.46	1.97

3.5.5 Linearised Soil Springs

Each structure was analysed using a quasi-static analysis with environmental loading provided by the centre of damage waves. The damage wave analysis on the platforms was run in conjunction with a soil-pile interaction analysis to determine the forces in the soil and therefore to determine appropriate linear soil springs for the spectral fatigue analysis. The soil springs represented the stiffness of the soil along the length of the piles. These were positioned at 1 metre intervals near and immediately beneath the seabed; and at deeper levels at 2 metre intervals along the pile length.

A modified spectral fatigue analysis was undertaken with the piles modelled explicitly and the soil stiffness represented by linear springs. This was to enable the cumulative damage to be calculated along the pile length, with the appropriate soil response.

3.5.6 Estimate of SCFs

Stress Concentration Factors (SCFs) for the piles were calculated in accordance with the method described by Connelly and Zettlemoyer[16] . The SCF at a girth weld due to local radial misalignment, e, of the pipe or tubular sections is given by:

$$SCF = 1.0 + 2.6 \cdot \frac{e}{t_{thin}} \cdot \left[\frac{1}{1 + 0.7 \cdot \left(\frac{t_{thick}}{t_{thin}} \right)^{1.4}} \right]$$

where t_{thin} and t_{thick} are the thickness of the thinner and thicker pipe respectively. The local misalignment e is a function of local out-of-roundness, OOR, such that:

$$e = OOR + \frac{t_{thick} - t_{thin}}{2} \qquad OOR_{max} = \frac{OD_{max} - OD_{min}}{2}$$

where OD is the outside diameter of the tubular pile. These formulas are the basis for the 1.35 value used as an SCF in the analysis.

3.5.7 Calculation of Fatigue lives

The following S-N curves, in accordance with the HSE [8] guidelines, were used:

- Curve F2 - butt weld made from both sides, but with step changes in thickness i.e. for the case of these piles: anomalies in the diameter. The welds are not ground flush.
- Curve C - butt weld overfill is ground flush with the surface, internally and externally, and the weld is proved free of defects by non-destructive examination.

Reference to the F2 and C curves enabled the permissible number of cycles N, at each stress range S, to be determined. The fatigue life was calculated using Miner's rule. For a joint subjected to a number of repetitions, n_i of a given stress range produced by the seastate; the ratio of n_i to the number of permissible cycles, N_i , at that stress range, gives the damage ratio. Thus the cumulative damage ratio is given by:

$$\frac{n_1}{N_1} + \frac{n_2}{N_2} + \frac{n_3}{N_3} + \frac{n_4}{N_4} + ... = \sum \frac{n}{N} < 1.0$$

Fatigue damage is calculated on an annual basis, and therefore total in-service life, assuming no prior damage, is obtained by taking the reciprocal of the annual damage.

The fatigue lives for the Monotower and Vierendeel foundations, based on the two S-N curves, are given below:

Table 3-7
Fatigue lives in years for Monotower piles in clay, 34m penetration

Depth below seabed (m)	*HSE S-N curve C*	*HSE S-N curve F2*
3	5745	97
4	62807	671
5	90348	950
6	23000	303
7	9130	144
8	4379	75
9	2254	45
10	1531	34
11	1271	29.7
12	1235	29.2
13	1369	31.6

Table 3-8
Fatigue lives for Monotower piles in sand, 23m penetration

Depth below seabed (m)	*HSE S-N curve C*	*HSE S-N curve F2*
3	59509	683
4	15292	199
5	3563	64
6	1502	33.7
7	1309	30.6
8	1823	39.4
9	3667	67
10	10161	149

Table 3-9
Fatigue lives Vierendeel piles in clay, 32m penetration

Depth below seabed (meters)	*HSE S-N curve C*	*HSE S-N curve F2*
3	176850	2032
4	$>10^6$	14976
5	$>10^6$	270854
6	$>10^6$	52146
7	986803	8752
8	282911	2967
9	129209	1535
10	80766	1044
11	63553	860
12	59917	822
13	65672	887

Table 3-10
Fatigue lives for Vierendeel piles in sand, 22m penetration

Depth below seabed (meters)	*HSE S-N curve C*	*HSE S-N curve F2*
3	$>10^6$	158999
4	$>10^6$	10870
5	234935	2529
6	84747	1083
7	69285	921
8	95912	1206
9	198250	2217
10	571987	5520

These results are shown graphically in Figure 3-14 through to Figure 3-17.

In comparison with the Vierendeel structure, the lower lives attributed to the Monotower can be explained by the smaller number of piles provided. This results in higher loads and stresses, and therefore the damage ratio increases.

The fatigue performance of the piles depends on the location below the mudline, reflecting the bending stress distribution. At mudline where the piles in clay are more highly stressed, the clay life is lower than the sand life. Further down the pile, this is reversed, and the lives of piles in sand are lower. The Vierendeel piles show a different stress distribution, and the sand lives are generally lower.

To determine total fatigue damage, the spectral in-place analysis result was added to the damage calculated from a consideration of driving stresses (Section 3.6).

3.6 Pile Driving Fatigue

3.6.1 General

The analysis of pile driving includes a method for combining the expected resistance to installation with the characteristics of the hammer-pile dynamic system.

Soils resistance to driving (SRD) may be determined using a variety of methods, depending on the soils conditions and the preference of the designer. These have usually been derived based on back analysis of driving records, and therefore are dependent on the parameter values assumed. Use of a preferred method therefore assumes the adoption of certain parameter values.

Analysis of the pile-hammer driving system is usually carried out using a wave-equation analysis based on the original method developed by Smith [17]. Results of this analysis are presented as hammer blowcounts against soils resistance. Blowcounts are usually limited to 250 per 0.25m penetration depth.

Results from the soils resistance and hammer model analysis procedure are usually presented as profiles of blowcount with depth. A graphical description of this process is shown in Figure 3-18.

3.6.2 Pile SRD Methods

Methods commonly used to determine resistance to driving for North Sea sands and clays are:

- Toolan & Fox Method [18]
- Steven's Method [19]
- Semple & Gemeinhardt [20]
- Alm & Hamre [21]
- Proprietary Methods: e.g. Heerema [22].

A range of resistance is usually determined to provide upper and lower bound to the expected response of the soils. An upper bound profile would be expected to provide the most pessimistic hammer blowcount behaviour. If the measured response is less than the lower bound limit, then the assumptions made to determine the soil parameters might need to be examined and pile capacity, which also depends on the assumed soil parameters, might then be modified.

The behaviour of the pile during driving may be as a plugged, or un-plugged response. The size of the pile may have a significant effect on the response. Smaller diameter pipes, such as conductors, may respond in a plugged response, whereas larger piles, will behave as unplugged (cored). Quite often the minimum of the calculated response is assumed, as in the Toolan & Fox method. However, some of the methods (eg Stevens) recommend the use of plugged behaviour based on back-analysis.

The Toolan and Fox method has been calibrated against North Sea driving conditions and is generally considered to give conservative, that is, high SRD values. This, in turn, will lead to higher damage and a conservative estimate of fatigue lives. Therefore this method has been used for driveability predictions.

In the Toolan & Fox method, driving resistance is determined using an upper and lower bound resistance. In sands measured qc values are used to provide end bearing (base area/annulus area x $0.6q_c$) and skin friction (qc/300) using the limits given in API (for skin friction). The design SRD value is taken as the minimum of plugged and coring response. Remoulded shear strength, calculated using published correlations between liquidity index and remoulded strength, is used to determine the resistance in clays.

For a lower bound resistance, the tip resistance may be calculated using say $0.3q_c$ and the shaft friction has been determined using half the upper bound value i.e. $q_c/600$.

3.6.3 Wave Equation Models

Wave equation models analyse the effect of the hammer induced dynamic wave as it passes through the pile-soil system. The pile model is formed of a discrete number of elements, connected by springs, to which a compressive stress wave is applied. The characteristics of the model include the "quake" and damping coefficients. "Quake" or set represents the maximum permanent displacement which the soil will undergo under the shock wave. Damping represents loss of energy within the soil system and can therefore have a significant effect on the response of the system.

In the original paper by Smith[17] , values were assigned as follows to these parameters:

- Side Damping Clay: 0.65sec/m Sand: 0.164sec/m
- Tip Damping Clay: 0.033sec/m Sand: 0.492sec/m
- Quake 0.00254m

The results of the analysis are sensitive to these assumed values, particularly side damping values. In general the procedure for driveability assessment should be viewed as a recipe, and for any of the suggested methods, it is usual to use the recommended parameters, unless back analysed data is available.

For this study wave equation analysis was carried out using the GLRWEAP[23] program. This package is used widely in the industry for the analysis of pile driving, and is based on the original WEAP and WEAP87 programs, developed at the University of Colorado and backed by the Case School of Engineering at Case Western Reserve University. It has been supported by the Federal Highways Agency in the United States and its use is well documented in the public arena.

3.6.4 Driveability Results

3.6.4.1 Introduction

It has been initially assumed that piles will be installed using either an IHC S200 hammer (sand) or an IHC S90 hammer (clay) in underwater driving mode, without a follower. However, additional calculations were carried out for the IHC S90 hammer for the Monotower at the sand site to investigate the sensitivity of the fatigue results to hammer size (see Section 3.6.5).

Soils resistance to driving (SRD) was assessed using the Toolan & Fox method described previously. This (Toolan & Fox) method has been calibrated against North Sea driving experience, and it is generally considered to give conservative SRD values.

Remoulded shear strength, was used to determine the resistance in clays. If the data are available this is usually calculated using correlations between liquidity indices and Cr. For this study it has been assumed that the remoulded strength ranges between 0.5Su (upper bound) and 0.33Su (lower bound).

3.6.4.2 SRD Range

The results of the pile SRD calculations in sand is shown in Figure 3-19. In sands at 23m (i.e. the Monotower target penetration) the upper bound SRD is 7.9MN and the lower bound value is 3.9MN. AT 22.0m (the Vierendeel target depth) these values reduce to 7.3MN and 3.6MN. The Toolan & Fox response is "plugged" for both upper and lower bound values.

In clay the SRD range is shown in Figure 3-20. At 33m, (average of Monotower and Vierendeel target depths) the maximum SRD is 2.4MN. The lower bound value is 1.5MN.

In calculating the SRDs for both skirt and leg piles, it has been assumed that there will be no delays during driving of sufficient duration to allow set-up to take place. If this occurs, then the SRD in the clays could increase significantly, thus increasing the driving blowcount. It is also recognized that sand resistance increases with time and thus set-up effects could also occur. With the short piles and relatively easy driving conditions at these idealised sites, it is unlikely that problems would take place.

3.6.4.3 Hammer and dynamic soil data

The dynamic soil parameters recommended by Smith were used in the analysis. Data for the IHC hammers were assumed as below.

Hammer:	IHC S200	IHC S90
Hammer Weight:	35 tonne in air	9.2 tonne in air
Hammer Weight in Water:	25 tonne	5.5 tonne in water
Rated Hammer Energy:	200kN-m	90kN-m
Ram Weight	97.9kN	45kN
Maximum Efficiency	95%	95%
Maximum ENTHRU Energy	184kN-m	82kN-m

Performance curves, showing the variation of blowcount with Ru (static soil resistance), are shown in Figures 3-21 and 3-22 for piles in clay and sand, respectively. In generating these curves, a tip resistance of 20% has been assumed in sand and 7% in clay. The hammer data and relevant soil damping and quake parameters shown above have been used.

3.6.4.4 Results of Driveability Analysis

The results of the driveability analysis in sand are shown in Table 3-11 for the Toolan & Fox derived SRD. Maximum energy levels of 55% were used:

Table 3-11
Driveability Analysis Results: Sand Site

Structure/ Pile	*Penetration Depth*	*SRD*	*Upper Bound Blowcount*	*Lower Bound Blowcount*
Vierendeel 1067 x 38	22.0m	7.3MN Upper Bd 3.6MN Lower Bd	38Blows/0.25m	28Blows/0.25m
Monotower 1067 x 38	23.0m	7.9MN Upper Bd 3.9MN Lower Bd	41Blows/0.25m	30 Blows/0.25m

Since the criterion of driving refusal is usually about 250 blow/0.25m on continuous driving, the analysis shows that the monotower piles, with an upper bound 41blows/0.25m, can be installed to the target penetration. If the lower bound SRD is met, then blowcounts reduce to 28 blows/0.25m. Driving the shallower Vierendeel leg piles is easier and leads to a maximum blowcount of 38 blows/0.25m.

The results for the clay site are shown in Table 3-12.

Table 3-12
Driveability Analysis Results: Clay Site

Structure/ Pile	*Penetration Depth*	*SRD*	*Upper Bound Blowcount*	*Lower Bound Blowcount*
Vierendeel/ 1067 x 38	32.0m	2.2MN Upper Bd 1.4MN Lower Bd	35Blows/0.25m	26Blows/0.25m
Monotower/ 1067 x 38	34.0m	2.5MN Upper Bd 1.65MN Lower Bd	39Blows/0.25m	29 Blows/0.25m

The results show that the IHC S90 hammer can readily install the piles in clay. Upper bound resistance leads to 39 blows/0.25m and lower bound resistance gives a maximum blowcount of 29 blows/0.25m.

3.6.5 Fatigue Driving Damage

Driving damage was calculated form the results of the wave equation analysis and the SRD profiles discussed above. The procedure for calculating driving damage (Figure 3-18) included the following steps:

- Using the Wave Equation results, determine profiles of blowcount with depth and stress range with depth.
- Choose appropriate SCFs and S-N curves to calculate fatigue damage.
- Using number of blows and stress range data calculate driving damage due to each increment of depth. Apply Miner's Rule to sum incremental damage and obtain the total damage due to driving the pile.

The blowcount depth profiles calculated using the SRD and wave equation models for both sand and clay sites are shown in Figure 3-23 and Figure 3-24 respectively. The range for upper and lower bound resistance is shown. Corresponding profiles of stress range are shown in Figure 3-25 and Figure 3-26. In determining damage it was assumed that the upper bound resistance would apply. This is probably conservative as it is unlikely that the upper bound

values would apply throughout the depth profile. A less onerous profile could be selected using say median best estimate values.

The selection of a suitable SCFs has been described previously. A maximum SCF of 1.35 was applied to allow for tolerance step changes between cans. At a weld bead location, it is assumed that there is no stress raiser due to geometry effects.

Appropriate S-N curves are dependent on the weld detail. The most onerous S-N curve is the F2 curve, which assumes one-sided butt welding with no backing strip. The C curve may be applied to two sided butt welding accompanied by grinding flush. Damage corresponding to weld bead details has been calculated by using the E curve. The resulting damage ratios are tabulated below.

Table 3-13
Driving Fatigue Damage

Hammer	*Penetration Depth*	*Structure*	*Soil Type*	*Fatigue Damage*		
				E Curve Weld Bead	*F2 Curve Butt Weld*	*C Curve Butt Weld*
IHC S200	23m	Monotower	Sand	0.0133	0.0804	0.0136
IHC S200	22m	Vierendeel	Sand	0.0126	0.0740	0.0123
IHC S90	34m	Monotower	Clay	0.0193	0.1140	0.0202
IHC S90	32m	Vierendeel	Clay	0.0180	0.1050	0.0190
IHC S90	23m	Monotower	Sand	-	0.0345	0.0050

A comparison of the first and last rows in Table 3-13 indicates the role of hammer size on driving fatigue damage. The damage is reduced by a factor of over two when the IHC S200 hammer is replaced by the IHC S90 hammer. However, as seen in the next section, driving fatigue damage has only a small effect on the remaining in-service life and therefore the latter is rather insensitive to choice of hammer size.

3.7 Remaining Fatigue Life after Driving

To calculate the total fatigue damage in a pile, the maximum in-place fatigue damage and the driving damage may be summed to give a total damage ratio. However, it is often more useful to know the available life remaining after driving damage is accounted for. This is determined as:

$$\text{Remaining fatigue life} = (1-d_r)/d_i$$

where d_r = driving damage
d_i = annual in-place damage

The results for damage ratios and available (remaining) fatigue lives immediately after driving are shown in the tables below.

Table 3-14
Fatigue lives and ratios for the C curve

Structure, soil type	*Fatigue life with no driving damage (years)*	*Annual in-place fatigue damage ratio*	*Driving fatigue damage ratio*	*Remaining fatigue life after driving (years)*
Monotower in clay	1235	0.810×10^{-3}	0.0202	1210
Monotower in sand	1309	0.764×10^{-3}	0.0136	1291
Vierendeel in clay	59917	0.017×10^{-3}	0.0190	58778
Vierendeel in sand	69285	0.014×10^{-3}	0.0123	68433

Table 3-15
Fatigue lives and ratios for the F2 curve

Structure, soil type	*Fatigue life with no driving damage (years)*	*Annual in-place fatigue damage ratio*	*Driving fatigue damage ratio*	*Remaining fatigue life after driving (years)*
Monotower in clay	29.2	34.2×10^{-3}	0.1140	25.9
Monotower in sand	30.6	32.7×10^{-3}	0.0804	28.1
Vierendeel in clay	822	1.22×10^{-3}	0.1050	736
Vierendeel in sand	921	1.09×10^{-3}	0.0740	853

3.8 Conclusions

Although pile fatigue is not explicitly addressed in existing design codes, potential damage to piles due to in-place conditions and driving may be a significant concern, particularly when the environmental loading is a high proportion of gravity loading.

The conclusions from the minimum facilities structures study considered above are as follows:

(1) Fatigue damage of piles due to in-place conditions and driving is significant. Although the in-place stress utilisation of the piles in this study are low, the environmental fatigue damage is relatively high.
(2) In order to achieve an acceptable remaining fatigue life (10 x service life, ie. 300 years) a HSE "C" curve is required for the piles of the monotower structure. Grinding of girth welds in the fatigue sensitive regions is therefore needed if this detail is to be achieved.
(3) An acceptable fatigue life for the Vierendeel structure piles is obtained with the F2 curve and hence no weld grinding is required for these piles.
(4) Driving fatigue damage is sensitive to calculated driving resistance. Upper bound values were used for this study. Use of lower bound values or median "best estimate" values would reduce driving damage.

This study included structures where single foundation piles were placed under each leg, and therefore bending stresses were high. Pile cluster arrangements may result in a smaller proportion of in-place damage; however, driving damage could be greater, particularly where deeper piles are installed. It has been assumed in the study that there are no thickness transitions near the most heavily stressed regions at the mudline and SCFs were therefore based only on tolerance differences in the adjacent fabrication can walls. If thickness transitions were included, the SCFs would be more onerous, and therefore fatigue lives would be lower. Therefore transitions should be avoided near the mudline regions of high stress in order to ensure that fatigue damage in these welds is minimised.

Shakedown of residual stresses due to pile driving has been shown to be beneficial in reducing residual tensile stresses and therefore improving fatigue performance. It has not been possible to quantify these effects within this study.

4. PILE TIP INTEGRITY

4.1 Background

During installation, pile tips and pile shells may be subjected to high stresses from pile driving forces and soil reactions. Although informal guide rules are observed on the choice of D/t ratios in the UK North Sea, no recommendations are provided on the analysis of these forces to ensure that the integrity of the pile or pile tip is not impaired. In the case of particularly hard driving, pile shoes may be proposed, although this is generally for the purpose of reducing internal skin friction, and therefore reducing driving resistance.

Whilst no damage to pile tips has been reported in the North Sea, damage has occurred in other regions of the world where limestones or calcarenites are present. In the calcareous soft rocks of the Arabian Gulf, and the Gulf of Guinea, damage has been reported [24]. However, in these cases the tip damage appeared to be local buckling. The only reported case of pile collapse is in the calcareous sands of the Australian North West Shelf [25].

Whilst any damage may remain undetected unless the pile has to be excavated for a secondary insert, damage could make driving more difficult and could reduce pile capacity.

4.2 Geometry of Piles and Driving Shoes

According to API[1,2], pile geometry slenderness as indicated by the D/t ratio may be as high as 60, without reducing the inelastic buckling (yield) strength. In the same document, minimum wall thickness criteria suggest that the D/t ratio may range from 46.9 to 78.6 for the normal pile sizes in use offshore. In practice most designers would not be happy to employ a D/t greater than 40, and it is common to see the use of D/t ratios as low as 24 and sometimes as low as 20.

Local pile tip thickening (usually referred to as a "driving shoe") is employed to improve driveability, to provide reinforcement against local hard spots such as boulders and to reduce tip stresses. During the 70s and 80s many piles installed in the North Sea were provided with shoes, e.g. as in the Heather, Ninian, Magnus, Eider and West Sole platforms. The shoe usually incorporates an internal wall thickening (internal shoe) which reduces the internal skin friction and hence reduces the overall resistance to driving. The shoe may reduce the plugged end bearing capacity of the pile.

Generally the shoe consists of a length of pile at the tip which is increased in thickness by up to say 50% of the pile wall; the length of tip thickening varies but should be, according to earlier editions of API[26] , a minimum of one diameter in length. This recommendation has not been generally observed (in the North Sea) and it has been usual practice to use a shoe up to about 1500mm in length and with a thickening of less than 20mm; however, this thickening has been exceeded as for instance on the Heather project, where hard driving in clays with shear strength of 600kPa was expected. On the Magnus project, which incorporated piles driven in stiff clay for between 75 and 85m penetration, a shoe thickening of 17.5mm over a length of 1400mm was used.

The reduction in internal skin friction during driving is dependent on the decrease in effective contact stress against the pile wall, caused by the difference in diameter of the soil plug extruded through the shoe and the pile internal diameter. To account for this extrusion and subsequent dilation reductions of 50% to 75% on the internal friction are commonly used whilst to preserve the capacity of the pile it must be ensured that the plug, which has been extruded and remoulded through the shoe, regains sufficient internal adhesion to support the plugged end

bearing force. It should be noted that some operators do not permit the use of shoes in sand strata due to the possibility of reduced capacity.

Confirmation of the reduction in driving resistance was provided by the West Sole pile load tests [27], which were performed on 0.762m diameter piles with and without driving shoes. Comparison of the test-driving results showed a large reduction in internal friction for the piles with thick shoes. The amount of radial strain undergone by the soil plug to contact the pile inside wall appears to be an important parameter in determining the magnitude in reduction in inside friction and on the West Sole test piles this radial straining amounted to about 5%.

Appendix A provides references to the use of shoes for tubular piles in offshore platforms or in test piles driven offshore at platform locations. Some of the test piles shoes have high radial stiffness (minimum D/T 12.7) whilst shoes used in platform piles vary in geometry from a D/T of about 27 (Magnus, Maui) to a minimum D/T of 16.9 (Heather).

4.3 Mechanisms of Pile Tip Buckling and Collapse

4.3.1 General

There is no methodology in the public domain for examining the possibility for pile tip collapse. By making reference to classical mechanics and published work on pipeline buckling, several potential mechanisms of tip buckling and pile collapse during pile installation may be postulated as follows:

- Pile tip local buckling (crimping) due to high tip stresses.
- Classical ring or shell buckling under lateral pressure.
- Ovalisation of initially imperfect tube under lateral pressure.
- Enlargement of initially dented pile, under the action of lateral soil pressures.
- Propagation buckling of damaged pile.

Combinations of some of the above mechanisms could also occur, as for instance, the presence of high axial stress with bending stresses due to lateral pressure ovalisation. Whilst it is generally accepted that column buckling modes are not relevant due to lateral soil support, yielding may occur at the tip leading to crimping. During pile driving other overall instability considerations may be significant, for example pile flutter. This could lead to wander of the pile and may induce large bending moments. For normal offshore pile geometry, it will be shown that this is not a critical factor.

4.3.2 Pile Tip Buckling

This is a local buckling phenomenon. The classical [28] elastic axial buckling stress is given by:

$$\sigma_{cr} = 2E(t/D)/(3(1-\nu^2))^{0.5}$$

where: E = Young's Modulus for steel
ν = Poisson's Ratio
t = Tubular wall thickness
D = Tubular average diameter

To allow for imperfections this is reduced in API [1,2] so that the maximum stress is given as:

$$F_{xe} = 2C_xE(t/D) \text{ where } C_x = 0.3$$

Usually this is well above the yield stress for a pile and inelastic local buckling applies:

$$F_{xc} = f_y \text{ (yield stress)}, \text{ for } D/t < 60$$

Pile driving in sand or clay would not usually result in the pile tip stress reaching this value, since a significant part of the driving energy is absorbed in shaft friction and the tip resistance will not generate yield stresses. However, in rocks, particularly if the overlying material does not generate sufficient shaft friction, large stresses could be reached. Non-uniformity of the strata or local hard points could exaggerate this effect.

4.3.3 Ring Buckling

The original classical solution for a perfect ring subjected to radial (fluid pressure) loading was provided by Bresse [29] and later by Levy [30]. The critical pressure is given as:

$$p_e = 3EI/(D/2)^3$$

where: p_e = Critical Bresse pressure
I = Section Inertia ($t^3/12$)

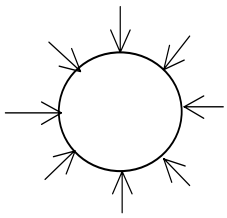

It should be noted that the classical elastic buckling pressure is not dependent on the initial ovality. For a cylinder subjected to a fluid pressure loading, the ring buckling expression given above is usually modified to allow for the shell effect by dividing by $(1-\nu^2)$. This modification was conservatively ignored for this study.

4.3.4 Ovalisation Under Lateral Pressure

Most offshore tubulars and piles will contain initial out-of-circularity imperfections due to normal fabrication tolerances. Timoshenko and Gere [31] provide a solution for the effect of ovality imperfections as follows:

$$w = w_o /(1- p/p_e)$$

where: w_o = initial ovalising imperfection
w = increased imperfection under pressure
p = applied pressure
p_e = critical Bresse pressure

In this the initial imperfection represents the deviation from the nominal perfect circle.

If the ovality is present along with a small fabrication out-of -roundness or "flatness", then the section becomes more flexible. Using an approach due to de Winter et al [40] it can be shown that:

$$w = w_o /(1- p/p_e) + c/4(p_e /p - 1)$$

where c is the flatness of the tubular.

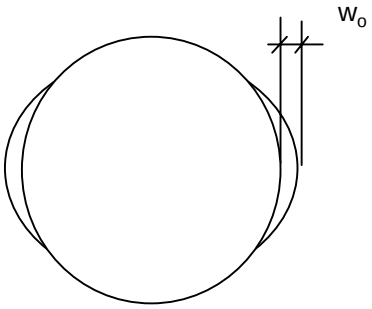

Ovalised Cylinder

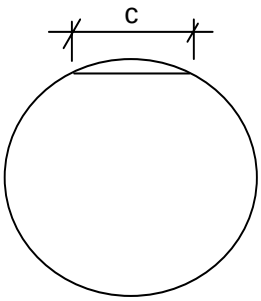

Flatness

The buckling pressure for most tubulars will result in membrane and bending stresses well in excess of yield. Yield collapse pressure then becomes the critical criterion. Timoshenko first published a solution for this collapse mode [31]. A formula for this critical pressure has been formulated as follows by de Winter [32]:

$$(p/p_p) + (p/p_p).(p_e/(p_e-p).6\beta_O\, R/t) - 1 = 0$$

where p = collapse pressure
p_p = hoop yield pressure ($= f_y t/R$)
p_e = critical Bresse pressure
β_o = ovalisation angle = w_o /R
R = tubular radius
t = wall thickness

4.3.5 Denting Damage and Enlargement

Due to its significance for the offshore industry, damage and energy absorption of jacket bracing members and pipelines have been investigated extensively. Methods for calculating dent damage have been provided by Ellinas & Walker [33]. For simply supported tubulars, the load to cause damage is given as:

$$Q_{ss} = KM_p \sqrt{(\delta/D)}$$

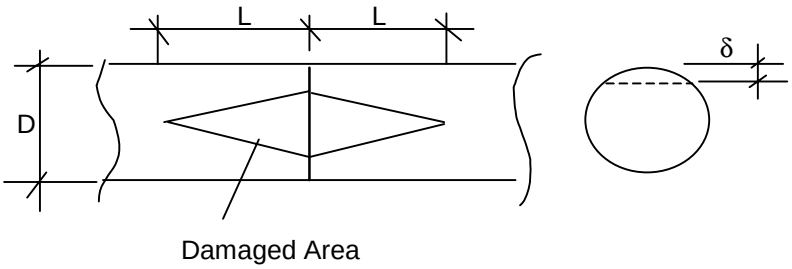

Plan and Section on Damaged Tubular

K is an empirical constant which has been found to be 150.0 for a load applied to a brace member under end supported conditions. $M_p = f_y t^2/4$ is the plastic moment resistance of the tubular wall, where fy is the yield stress and t is the wall thickness. D is the mean diameter and δ is the dent depth.

Substituting the expression for M_p, the denting load is then given as:

$$Q_{ss} = 37.5 f_y t^2 \sqrt{(\delta / D)}$$

By simple yield line theory considerations for a load applied to a cantilevered end of a pile, it can be shown that the maximum load will be given as:

$$Q_{tip} = 37.5 f_y t^2 / 8 \sqrt{(\delta / D)}$$
$$= 4.65 f_y t^2 \sqrt{(\delta / D)}$$

For a typical value of $\sqrt{(\delta / D)}$ of 0.1 used in the Ellinas & Walker work, then:

$$Q_{tip} = 1.2 f_y t^2$$

It should be noted that this analysis is based on a theoretical comparison with the Ellinas & Walker brace member damage, and would require to be confirmed experimentally.

If a pile tip has pre-existing damage, e.g. due to handling operations, it will be shown that subsequent loading during driving could lead to enlargement of this initial damage. For any increase in load, ΔQ_i, the increased dent, δ_i, can be calculated from the original dent size, δ_o, and load, Q_o, as:

$$\delta_I = \delta o / (1 - 2\Delta Q_i / Q_o)$$

This is analogous to the Timoshenko ovalisation mechanism, where the initial dent size, δ_o, replaces the ovalisation parameter, w_o, and $2\Delta Q_i/Q_o$ replaces p/p_e.

4.3.6 Pile Flutter

Pile flutter, and the possible curvature of the pile, has been considered by Burgess [34]. Large deviations could cause large curvature, and therefore high bending stresses could occur. He showed that for shaft friction T, the critical geometry, when bending of the pile is likely to happen, is given by:

$$L^3/(EI). \quad T < 40.7$$

where T = shaft friction /length (assumed uniform)
EI = Bending Stiffness

For typical offshore tubular piles, it will usually be found that this criterion is satisfied and therefore pile wander and associated curvature need not be considered further.

4.3.7 Propagation Buckling

It has been observed that once a buckle has been initiated in a pipeline, it may travel for a considerable distance before being arrested. Critical pressures for propagation buckling phenomenon in a pipeline once a buckle commences was first addressed by Palmer [35]. It is assumed that that the pipeline will be subjected to a uniform pressure regime and if the pressure reduces, the propagation process will cease.

Formulae for calculation of propagation pressures are given in various references [36,37,38]. The formulae have been derived both from theoretical considerations and empirically from experimental testing observations, and assume a constant pressure regime as noted above. The propagation pressure will generally be lower than the critical buckling pressure calculated according to classical mechanics formulae.

A comparison of critical collapse pressures and an empirical formulation for propagation buckling (due to Kyriakides and Babcock[36]) is shown in Figure 4-1 for a pile of diameter 2438mm and a range of pile geometries. It is clear that the collapse pressures, even for a high D/t of 60.0, are comfortably in excess of in-situ soil stresses ('at-rest' soil pressures). Whilst propagation pressures are lower than the classical buckling pressures, they appear to be generally higher than the probable in-situ soil stresses (at rest pressures), except for very deep penetrations. For a D/t of 60.0, the propagation buckling pressure is 0.5 MPa, which could exist at a minimum depth of about 100m with a soil having an at rest coefficient Ko of 0.5, and an average vertical soil pressure of 1.0MPa (due to an average unit weight of 10kN/m3). Most soils would have a maximum 'at-rest' coefficient of 0.5 at this depth, and hence the propensity for propagation of a buckle is probably minimal. However, although a trigger mechanism would be needed to initiate buckling, it would seem prudent to avoid use of piles with high D/t at deep penetration depth.

4.4 Model Studies

4.4.1 Introduction

It has been seen above that a pile fabricated without imperfections will be adequate to resist lateral soil pressures, since these are generally lower than critical buckling pressures at normal pile penetration depths. However, when built to offshore fabrication tolerances, and including ovality or out-of-circularity, then if a mechanism exists to increase lateral pressure as penetration progresses, the magnifying effect shown in the Timoshenko & Gere formula could result in larger deformations. With existing dent damage there is a similar magnifying effect, which could result in extension of the damage with increased pile penetration.

It is assumed that initial damage or ovalisation exists in the pile. The general mechanism for extending this damage is a wedge or ratchet mechanism, whereby the geometry of the pile results in a wedge action on the soil, and consequent lateral soil pressures. With increasing penetration the pressures progressively increase the extent of the damage or initial ovalisation.

In the following, typical pile geometries are considered for various soils to determine the propensity for pile tip damage or pile wall collapse using the ovalising and denting mechanisms considered above. For damage of the piles to occur, it is obvious that the relative stiffness of piles and soil will be a significant parameter. For instance if the relative soil stiffness is very low it is unlikely that progressive damage can take place.

4.4.2 Damage Scenarios

A pile tip could be damaged, with the formation of a dent, during handling or installation. Subsequent loading during driving could lead to enlargement of this dent. The mechanisms leading to pile tip collapse may be summarized as follows:

(1) Initialising of dent at or near pile tip.
(2) Cycling/ load stepping to increase the dent progressively. There will be a small increase in denting on each cycle, so that eventually, unacceptable deformations may build up.

The scenario leading to damage could be any of a number of events during the installation process or during handling. For instance, stabbing the pile into the sleeve and subsequent

loading under self weight and environmental forces may be sufficient to cause denting forces, particularly if the pile is slender. Even lifting operations can damage the ends of piles. If a pile is dropped during handling, the consequent end reaction will normally be sufficient to exceed the critical denting load.

Stick-up loads caused by releasing the pile load during stabbing into the pile sleeve are compared with denting loads in Figure 4-2. For higher D/t pile ratios, it is possible to generate stick-up loads for long piles which are sufficient to cause significant denting. During pile driving, localized hard spots or boulders could give rise to eccentricity of tip reaction, which could be balanced by lateral tip loads of magnitude sufficient to dent the pile wall. This would only occur if the overlying soils were very soft, allowing most of the driving energy to be transferred into the tip.

4.4.3 Fabrication Tolerances

For piles fabricated according to the normal UK Engineering Equipment and Material Users Association [39] guidelines (now withdrawn), tolerances are defined for ovality (out-of-circularity), out-of-roundness, and straightness. For typical pile sizes, this leads to the following tabulated allowable values of ovality and out-of-roundness. Out of straightness for piles is defined as 12mm in any 12m length.

Table 4-1
Fabrication Tolerances to EEMUA

Pile Size	***Ovality (EEMUA)***	***Ovality (Timoshenko) wo***	***Out-of-Roundness λ***	***Flatness c***
Dia x wt (mm x mm)	mm	mm	mm	mm
762 x 25	6	1.5	1.5	68.1
1067 x 38	6	1.5	2	95.4
1524 x 50	11.5	3	4	136.3
2134 x 80	15	3.75	4.2	190.8
2438 x 90	15	3.75	4.9	218.0

The EEMUA definition of ovality as used in the table above is Dmax-Dmin. The classical Timoshenko (wo) definition of ovality is (Dmax –Dmin) /4. Out-of-roundness (λ) and flatness (c) are defined as follows:

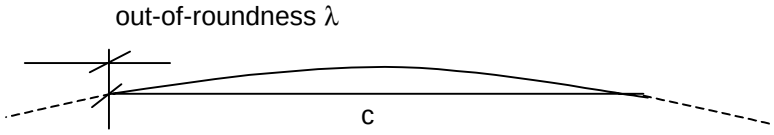

Flatness in the table is calculated as $2\sqrt{(\lambda D)}$ where D is pile diameter and λ is measured out-of-circularity.

4.4.4 Ovalisation Model

As a pile penetrates the soils, soil pressure will be generated against the pile walls due to the at-rest condition. If the pile cores the soils so that the soils inside remain at the same elevation as outside, the internal soils will generate a similar at-rest pressure, and therefore the net pressure will be negligible.

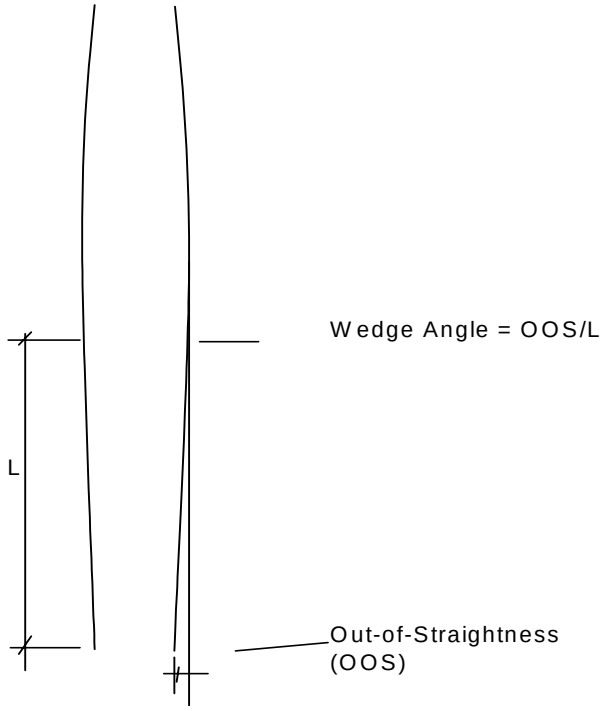

However, if it is assumed that the shape of the pile, fabricated to usual offshore requirements, will result in out-of-straightness, a wedging action can thereby be generated. This will lead to displacement of the soil laterally and resulting soil pressure on the pile will lead to an increase in ovalisation.

A spreadsheet model has been used to generate the response of the pile. The relevant stiffnesses used in the model are the lateral soil stiffness, and the ovalised pile stiffness. The tangent stiffness of the soil is calculated using the p-y characteristic curve for the soil. Sands are modelled using the O'Neill-Murchison method. Clays are modelled using the soft clay formulation in API. Static forms of the curves are used.

For sand, the stiffness is given as:

$$dp/dy = kx\mathrm{Sech}^2(kx/(APu))$$

where: p = lateral pile load
k = initial sand stiffness
x = penetration depth
P_u = ultimate load capacity of sand
A = constant

In clays the p-y curve is a piecewise linear curve, and the stiffness is calculated as:

$$dp/dy = \Delta p/\Delta y = (p_{n+1} - p_n)/(y_{n+1} - y_n)$$

The pile stiffness may be considered uncoupled into a hoop stiffness and an ovality stiffness. Hoop stiffness is calculated in the normal way as:

$$K_{hoop} = Et/R^2$$

The Ovality stiffness is calculated from the Timoshenko formula as:

$$dp/dy = K_{oval} = p_e/w_o\,(1\text{-}p/p_e)^2$$

For any increment in lateral soil displacement, caused by wedge action, the pressure increase is:

$$dp = K_s du/(1 + k1^{-1} + k2^{-1})$$

where $k1 = K_{hoop}/K_s$; $k2 = K_{oval}/K_s$
du = soil displacement
K_s = soil stiffness

Spreadsheets have been assembled to assess the ovality effect in very dense sands and clay, for a typically large offshore pile, 2438mm diameter. Results shown in Figure 4-3 and Figure 4-4, depict the change in a large initial ovality with penetration into very dense sand. It is assumed that the maximum length of the "wedge effect" is 6.0m. Maximum wedge angle of .005 has been used with an initial ovality of 2.1% (50mm). These are very high values which are outside the normal tolerances. Ovalisation increases, to a maximum of about 3.2% from the initial 2.1% but does not become critical. When a fabrication flatness of 200mm is included, the ovalisation increase remains less than 3.5%.

As shown in Table 4-1, the likely fabrication ovality is less than 5mm. Using an initial ovality of 0.2% (5mm), maximum increase is to about 0.7% (17mm) when penetrating a very dense sand or a hard clay. Figure 4-5 shows the growth in ovality for a very dense sand; although not depicted, the hard clay condition is very similar. For the latter analyses a wedge angle of 0.002 has been used which is representative of fabrication details.

As discussed previously, if the pile cores there is no net at rest pressures. A plugged condition has also been considered, in which it is assumed that there is no internal resistance and the net at rest pressure is 0.25MPa corresponding to 50m penetration depth. This pressure is added to the wedge action. Maximum ovality is about 3.3% for a very dense sand when an initial ovality of 2.1% (50mm) is included (Figure 4-6).

From the above results, it appears that increasing ovality is limited by the assumed wedge angle, until an equilibrium condition is reached at the limiting maximum wedge depth, regardless of the pile geometry. If the wedge action were not limited by the assumed fabrication geometry, greater deformation would be caused although the system is eventually governed by the combined soil-ovality stiffness and the imposed wedge displacements. Increasing penetration depth, although leading to increased soil stiffness, does not result in a significant increase in ovality, due to the same wedge geometry limitations.

A condition in which a pile is plugged so that it experiences at-rest soil pressures, but no wedge action exists is shown in Fig 4-7. Penetration to 100m depth is considered with an at rest coefficient of 0.5. With an initial ovality of 2%, maximum enlargement is only to 2.3%, for D/t of 60.0. It can be concluded that ovalisation is not a significant problem for the plugged condition.

4.4.5 Model for Dent Enlargement

It has been shown that accidental handling loads may be sufficient to lead to significant denting damage. Dents can grow in an analogous manner to ovalisation. A model for dent enlargement has been incorporated in a spreadsheet. It is assumed that the dent geometry follows the form given in Ellinas and Walker [33] where the length of the dent (L) is 3.5D. Wedge action is caused by the penetration of the dent geometry, whereby as the pile passes any given soil horizon, the soil is displaced and thereby loads the pile according to its displacement stiffness.

Tangent stiffness of the soil is calculated as described above for the ovalized cylinder.

Stiffness of the dented cylinder is calculated from the Ellinas & Walker formula:

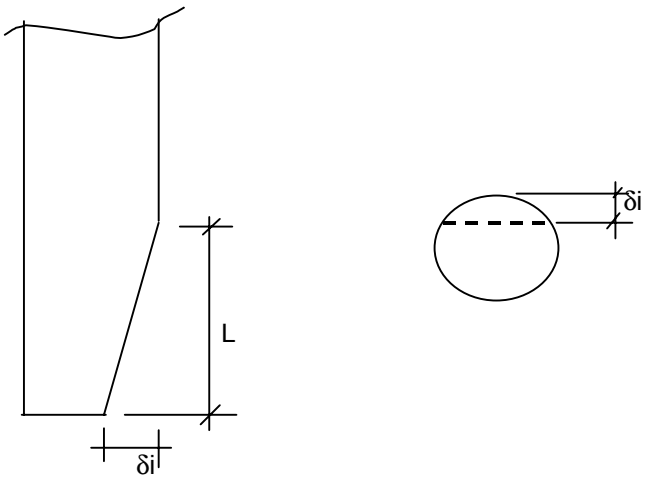

$$dQ/d(\delta i) = (KM_p)^2 / 2QD$$

Where δi is the dent depth and the other terms are as defined previously.

For any incremental lateral displacement, du, the soil and cylinder loading are calculated as:

$$dQ = K_s.du.k_1/(1+k_1),$$

where $k_1 = K_{pile}/K_s$

Total pressure on the dented pile is then calculated by summing the pressure increments. An allowance is included in the calculations for the distribution of the load (in contrast to the Ellinas & Walker line load). It has been assumed that the piles will penetrate through overlying soft material before penetrating the hard soils. The results of this procedure are given in Figure 4-8 to Figure 4-10 for very dense sand and very hard clay strata. It has been assumed the dense sands and clay commence at a depth of 50m below mudline. Initial depth of damage of 2% (50mm) and 4% (100mm) are considered in a pile of diameter 2438mm. The most extreme dent depth of 4% represents almost100mm deep denting for a pile of diameter 2438mm and a "flattening " of almost 1000mm. This is severe damage which would require a large damage load as shown in Figure 4-2.

The enlargement of the deeper initial dents in very dense sand is very similar irrespective of the pile geometry (D/t) , rising from 4% to almost 50% for the very high D/t of 60. If the initial dent is 50mm (some 2%,) the increase is from 2% to 18% for the thickness of strata shown, which is assumed for, the calculations as some 30m. In very hard clay, the effects on a pile of D/t of 60 is shown as it is not possible to realize significant damage increase with a pile having a D/t of 24. It has been assumed that the extent of the wedge action is over a length of 3.5D.

4.4.6 Soil and Pile Stiffnesses

It was suggested previously that a significant parameter in determining the response of the pile-soil system is the relative pile and soil stiffness. These stiffnesses are compared in Figure 4-11 to Figure 4-14 for dense and medium dense sand and very hard clays, for the extreme pile geometries, D/t of 24, and D/t of 60. Dented pile stiffness and ovalised pile stiffnesses are shown. Comparing the soil and pile stiffnesses the following trends are apparent:

- For a low D/t (24), the ovalised pile stiffness is considerably greater than the sands and clay initial stiffness;
- with a high D/t (60), pile stiffness is of the same order of magnitude as the sands; however it is still significantly greater than the clay stiffness;
- the dented pile stiffness is lower than the initial soil stiffness for both sand and clays, irrespective of undamaged pile D/t.

Therefore the soils do not possess sufficient stiffness to significantly deform the ovalised piles for the range of wedge action displacements considered. However, the dented cylinders are much softer and thus the wedge ratchet action can build up larger lateral forces. These figures reinforce the previous results which indicate that damaged tubulars are susceptible to further deformation.

4.4.7 Driving Stresses

It has been proposed that crimping damage at the tip due to high axial stresses may result from very hard driving conditions. Driving stresses at the tip of the pile will depend on the total resistance, the proportion resisted in end bearing as well as the impacting hammer energy. Wave equation analysis can provide the distribution of dynamic stresses along the pile length due to the impacting hammer energy on the pile head.

Using GLRWEAP a number of conditions have been investigated where the pile geometry has been varied along with the proportion of end bearing resistance. It has been assumed that an IHC S2300 hammer is used for driving a pile of diameter 2438mm (96in), of constant wall thickness. D/t has been varied from 24 to 60, and the piles are driven to the refusal criteria. Figure 4- 15 shows how resulting tip stresses at refusal vary with pile geometry and end resistance. As expected maximum stresses develop when the proportion of shaft resistance is minimized, and stresses increase with D/t. When the driving energy is completely resisted at the pile tip, tip stresses vary from 300MPa to 420MPa. Using a more usual 20% tip resistance the range is reduced to between 49MPa and 58MPa.

Although the highest stress determined above (420MPa) is well in excess of the static yield stress (assumed as 330MPa for 45mm thick material), the dynamic yield stress is much higher. Using the Cowper & Symonds [40] relationship:

$$f_y \text{ (dynamic)}/f_y \text{ (static)} = 1 + (\dot{\varepsilon}/C)^{1/n}$$

where $\dot{\varepsilon}$ = strain rate
C = 40.4sec^{-1}
n = 5

Then the dynamic yield stress may be 40% greater than the static stress for a typical wave travel time of 1ms. The yield stress, even for the most onerous case would not be exceeded by the axial tip stress.

It is normal to provide a chamfer on pile tips to enhance the "cookie cutter" action. Typically the tip may be reduced to 50% of its nominal thickness. Under this geometry, the pile tip would exceed yield in the most extreme condition considered above (99% end resistance). For the less extreme case of 80% end resistance, the maximum stress would be 390MPa, which is less than the limiting dynamic yield stress of 450MPa. These calculations ignore any non-uniform resistance which could magnify the stress locally where yield could be exceeded. Bending stresses due to the ovalising effects considered previously are also ignored. The combination of these contributions, under the most unfavourable conditions, could result in yielding. Therefore where driving is expected to meet a very hard end resistance, say in soft rock, and overlying sediments are weak so that shaft resistance is low, the possibility of tip yielding should be investigated.

4.5 Conclusions

Although damage to pile tips has not been reported in the North Sea, damage has occurred in other regions of the world, where calcareous sediments are present. Local pile tip thickening (usually referred to as a "driving shoe") is sometimes employed to improve driveability, to provide reinforcement against local hard spots such as boulders and to reduce tip stresses.

To account for pile distress during installation, various mechanisms have been proposed which could lead to pile collapse, and simplified models have been considered to investigate the likelihood of damage to pile tips during driving. Conditions wherein existing damage may be extended and the propensity for increased deformation of sections ovalised under fabrication conditions have been included in the models. The possibility of tip buckling due to high end bearing conditions has also been determined.

It has been shown that classical buckling and collapse pressures are much greater than possible in-situ stresses. Propagation buckling which has been observed in pipelines is unlikely to be a significant problem, since the threshold pressures are not present until at least100m depth, even for high D/t ratios. Furthermore an initiating buckling event is needed to trigger such a phenomenon.

In order to follow the response of ovalised or damaged piles to increased penetration and a build up of lateral pressures, spreadsheet models have been assembled. The mechanism leading to increased lateral pressure is postulated to be a wedge effect due to the out-of-straightness of the piles or due to existing damage. Conclusions from these models are as follows:

(1) Ovalised sections, where the sections remain within usual fabrication tolerances, will not experience unstable increases in ovality. Where the ovality significantly exceeds allowable tolerances, ovality could double in extent, due to a wedge effect increase in lateral soil pressure.
(2) Damage due to high tip loads, caused by handling or installation forces can occur for all tubulars. It is likely to be more severe for piles of high D/t ratios.

(3) Under medium to hard driving conditions, initial damage can increase under a wedge mechanism. Only conditions of significant initial damage are likely to present a problem.

For typical driving conditions and normal soils, it has been shown that end tip stresses will remain below yield. However, where end bearing is a very high proportion of total resistance, for example in soft rocks, stresses may reach dynamic yield stress. Damage could then occur if local concentrations of high stress occurs, coupled with reduction in wall thickness due to chamfering.

5. RECOMMENDATIONS

The study on pile fatigue has shown that fatigue damage in minimum facility foundations may be significant and improved weld details are needed to ensure that target fatigue lives are achieved. There are no codified recommendations on determining pile fatigue damage. Although calculations show that pile driving increases the total damage, previous work done in the 1980s indicates that pile hammering can be beneficial in reducing residual tensile and compressive stresses.

Therefore the proposed ISO document[41] should include recommendations on pile fatigue. Further work is required to confirm the beneficial effects of stress shakedown which has been indicated in earlier research.

Pile tip damage is not likely to be a significant problem for North Sea jackets, where piles of high D/t ratio are not normally used. Existing ovality due to the fabrication process will not be enlarged to a significant extent such that instability or over-stressing ensues. Where damage to pile tips exists due to previous handling accidents, an assessment should be made of the likely extension of this damage due to pile driving. To ensure that unacceptable deformations do not occur, limits on tolerable damage before driving operations commence should be specified. Denting loads have been determined by comparison with work done on jacket brace members since there exists no public domain data on the effects of lateral tip loads on piles. Axial tip stresses in North Sea soils will normally be low and will not affect the integrity of the pile tip. The possible effects of pile tip damage in high end resistance strata such as soft rock should be highlighted in proposed ISO codes.

REFERENCES

(1) American Petroleum Institute. "API RP 2A. Recommended Practice for Planning Design and Constructing Fixed Offshore Platforms. Load and Resistance Factor Design", 1st Edition 1993.

(2) American Petroleum Institute. "API RP 2A. Recommended Practice for Planning Design and Constructing Fixed Offshore Platforms. Working Stress Design (WSD)", 20th Edition 1993.

(3) Det Norske Veritas. "Classification Notes No 30.4 Foundations", February 1992.

(4) Thompson, G R, Seaman, J W and James, R L. "Monitoring of Beryl 'B' Platform Response to Pile Driving", OTC Paper No 4879, May 1985.

(5) British Steel Technical Research Organisation "The Effect of Pile Driving on the Fatigue Life and Dynamic Yield behaviour of Tubular Piles: Results of Stage 3 Work and Proposals for Stage 4", Ref. EM/RSC/S7323/5/1/88/E, June 1988.

(6) British Steel Technical Research Organisation "Observations on the Effect of Driving Stresses on the Fatigue Life of Tubular Steel Piles", Ref. SL/EM/RSC/S01171/1/1/89/E, October 1989.

(7) International Standards Organisation. "ISO 13819-1 Petroleum and Natural Gas Industries. Pt l: Offshore Structures General Requirements".

(8) Health and Safety Executive. "Offshore Installations: Guidance on Design Construction and Certification", 4th Edition, 1990. (Now withdrawn).

(9) Jardine, J F and Chow, F C. "New Design Method for Offshore Piles", MTD Publication 96/103.

(10) Hobbs, R. "A Review of the Design and Certification of Offshore Piles, with Reference to Recent Pile Load Tests" in Offshore Site Investigation and Foundation Behaviour, SUT 1993.

(11) American Petroleum Institute. "API RP 2A Recommended Practice for Planning Design and Constructing Fixed Offshore Platforms", 13th Edition 1982.

(12) ASAS /SPLINTER. "Soil –Pile-Interaction Program". Version H11, Update 2, May 1996.

(13) O'Neill, M W and Murchison, J M. "An Evaluation of p-y Relationships in Sand", Report to API, May 1983.

(14) Matlock, H. "Correlations for Design of Laterally Loaded Piles in Soft Clay", OTC Paper No 1204, 1970.

(15) Vughts, J H and Kinra, R K. "Probalistic Analysis of Fixed Offshore Structures" OTC Paper No 2608 May 1976.

(16) Connelly, I M and Zettlemoyer, N. "Stress Concentration at Girth Welds of Tubulars with Axial Wall Misalignment", in Tubular Structures V, 1993m (Ed) M G Coutie and G Davies, Pub E & F N Spon, London.

(17) Smith, E A L. "Pile Driving Analysis by the Wave Equation", ASCE Vol 127, 1962.

(18) Toolan, F E & Fox, D A. "Geotechnical Planning of Piled foundations for Offshore Platforms". Proc Institution of Civil Engineers Part 1, May 1977, Paper No 7996.

(19) Stevens, R S, Wiltsie, A W and Turton, H T. "Evaluating Pile Driveability for Hard Clay, Very Dense Sand, and Rock". Offshore Technical Conference, 1982, OTC Paper No 4205.

(20) Semple, R M and Gemeinhardt, J P. "Stress History Approach to Analysis of Soil Resistance to Pile Driving" OTC, Houston, Vol 1 pp 165 – 172, 1981, Heerema.

(21) Alm, T and Hamre, L. "Soil Model for Driveability Predictions." Offshore Technology Conference, Houston, Paper No OTC 8835, May 1998.

(22) Heerema, E P. "Dynamic Point resistance in clay for Pile Driveability Analysis", Ground Engineering, September 1981.

(23) GLRWEAP. "Wave Equation Analysis of Pile Driving", Goble Rausche Likins and Associates Inc, 1998.

(24) Puech, A, Poulet, D and Boisard, P. "A procedure to Evaluate Driveability in the Difficult Soil Conditions of the Southern Part of the Gulf of Guinea", OTC 6237.

(25) Offshore Engineer, February 1993.

(26) American Petroleum Institute. "API RP 2A. Recommended Practice for Planning Design and Constructing Fixed Offshore Platforms. Working Stress Design (WSD)", 19th Edition, 1987.

(27) Clarke, J, Rigden, W J and Senner, D W. "Re-interpretation of the West Sole Platform 'WC' Pile Load Tests", Geotechnique, September 1985.

(28) Brush, D O and Almroth, B O. "Buckling of Bars Plates and Shells", McGraw Hill, 1975.

(29) Bresse, M. Cours de Mecanique Appliquee, 1866.

(30) Levy, M J. Math Pure Applied (Liouville), Ser 3, Vol 10, p5, 1884.

(31) Timoshenko, S and Gere, J M. "Theory of Elastic Stability", McGraw Hill, London, 1961.

(32) De Winter, P E, Stark, J W B and Witteveen, J. "Collapse Behaviour of Submarine Pipelines in Shell Structures Stability and Strength", ed R Narayanan, Elsevier, 1985.

(33) Ellinas, C P and Walker, A C. "Effects of Damage on Offshore Tubular Members", IABSE Colloquim on Ship Collision with Bridges and Offshore Structures, Copenhagen, May 1983.

(34) Burgess, I W. "The Stability of Slender Piles during Driving", Geotechnique, Vol 26, No 2, 1976.

(35) Palmer, A. "Buckle Propagation in Submarine Pipelines", Nature, Vol 254, No 5495, March 6, 1975.

(36) Kyriakades, S and Babcock, C D. "Experimental Determination of the Propagation Pressure of Circular Pipes", Journal of Pressure Vessel Technology, ASME, Vol 193, No 11, 1981.

(37) Wierzbicki, T and Bhat, S U. "On the Initiation and Propagation of Buckles in Pipelines" Report No 85-2 Dept of Ocean Engineering, MIT, Feb 1985.

(38) Det Norske Veritas. "Rules for Submarine Pipeline Systems. Appendix B Buckling Calculations, Section B2 Propagation Buckling", 1981.

(39) EEMUA. "Fabrication Specification". The Engineering Equipment and Material Users Association.

(40) Cowper, G R and Symonds, P S. "Strain Hardening and Strain Rate Effects in The Impact Loading of Cantilever Beams" Technical Report No 28, Brown University Rhode Island, 1957.

(41) International Standards Organisation. "ISO 13819-2. Petroleum and Natural Gas Industries – Offshore Structures – Part 2: Fixed Steel Structures". Committee Draft D, Document Reference ISO/TC67/SC7 N222, May 1999.

FIGURES

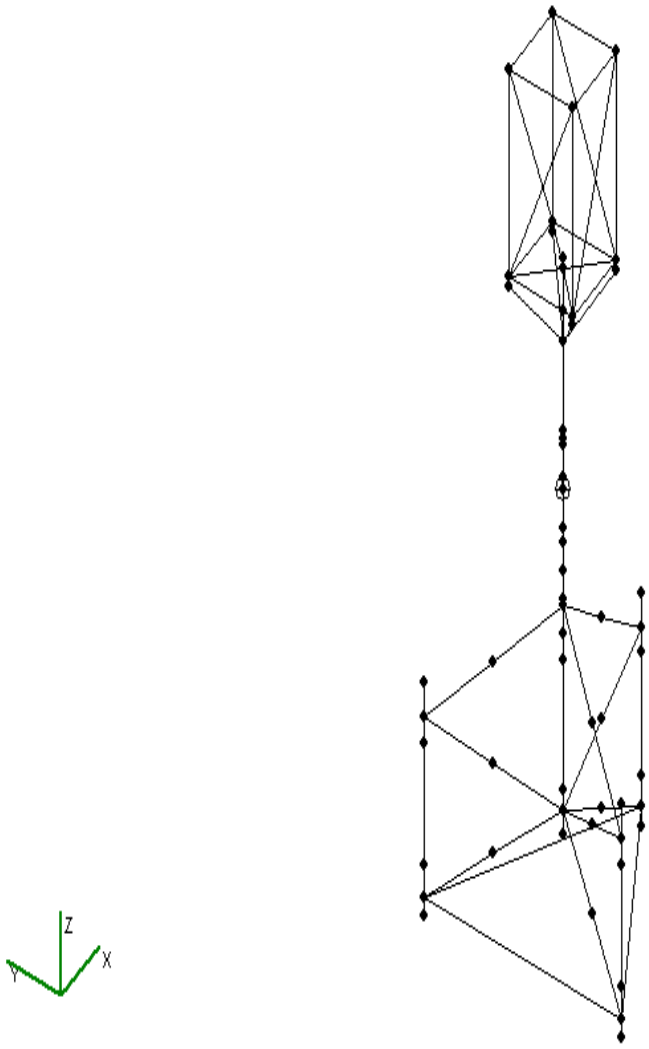

Figure 3-1
Computer Model of Monotower Structure

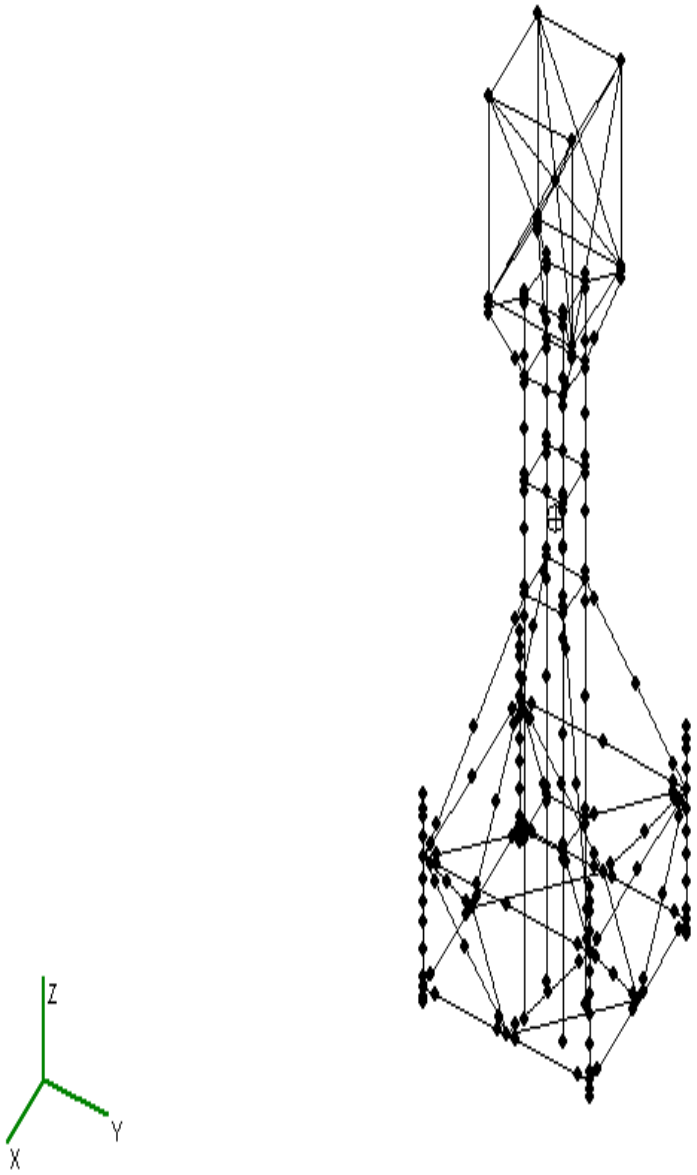

Figure 3-2
Computer Model of Vierendeel Structure

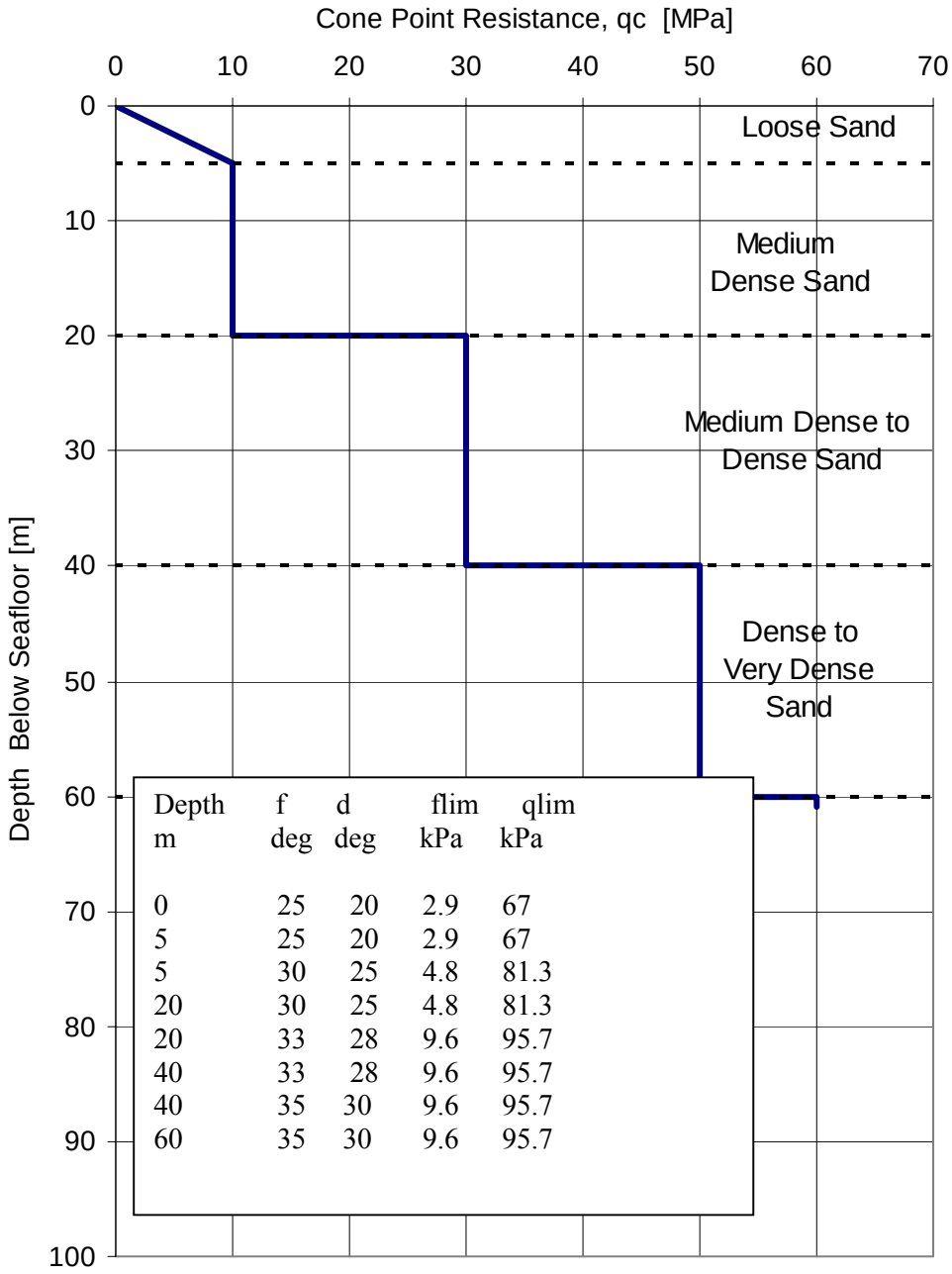

Figure 3-3
Strength Parameters Profile, Sand Site

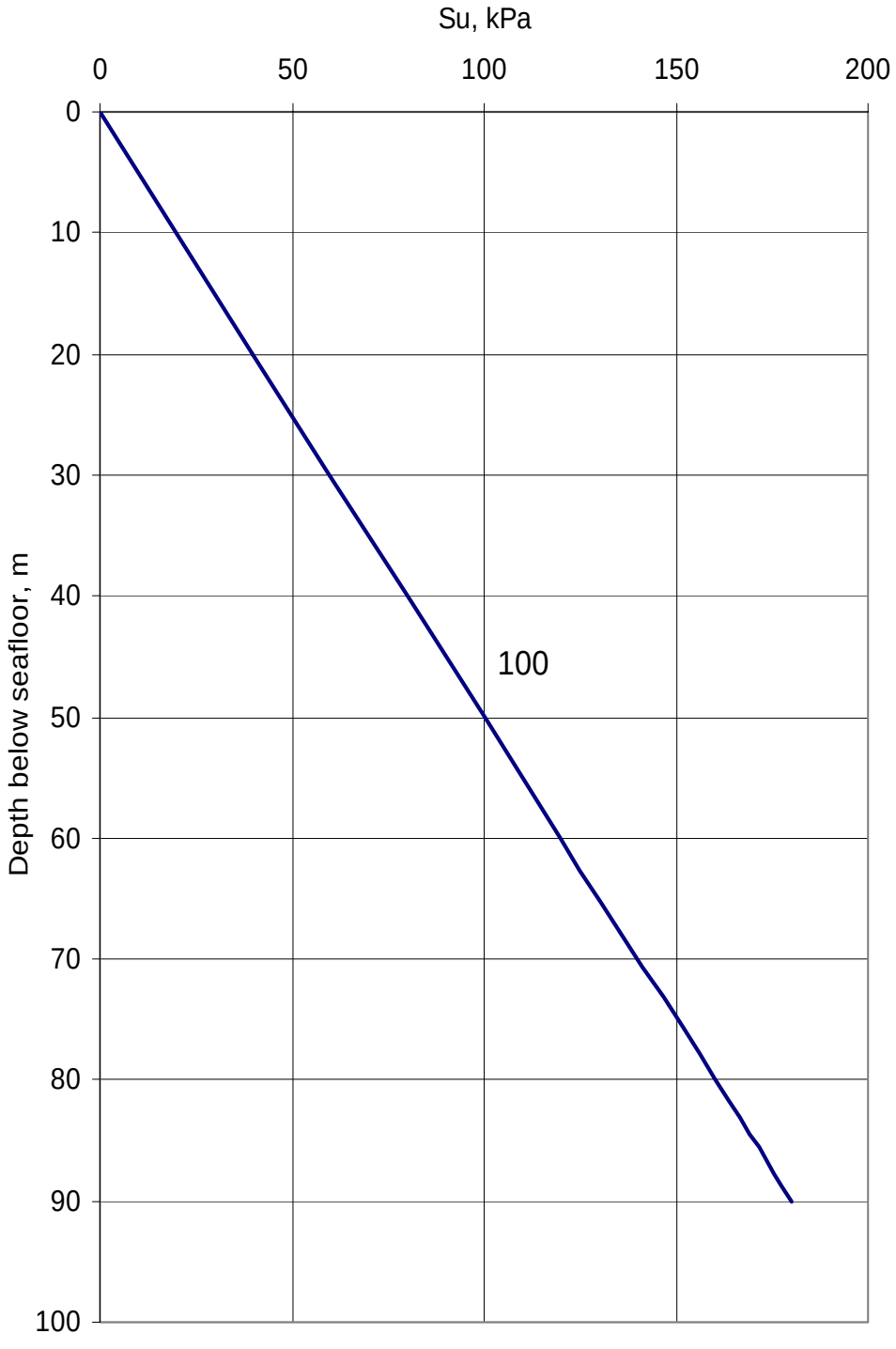

Figure 3-4
Su Profile, Clay Site

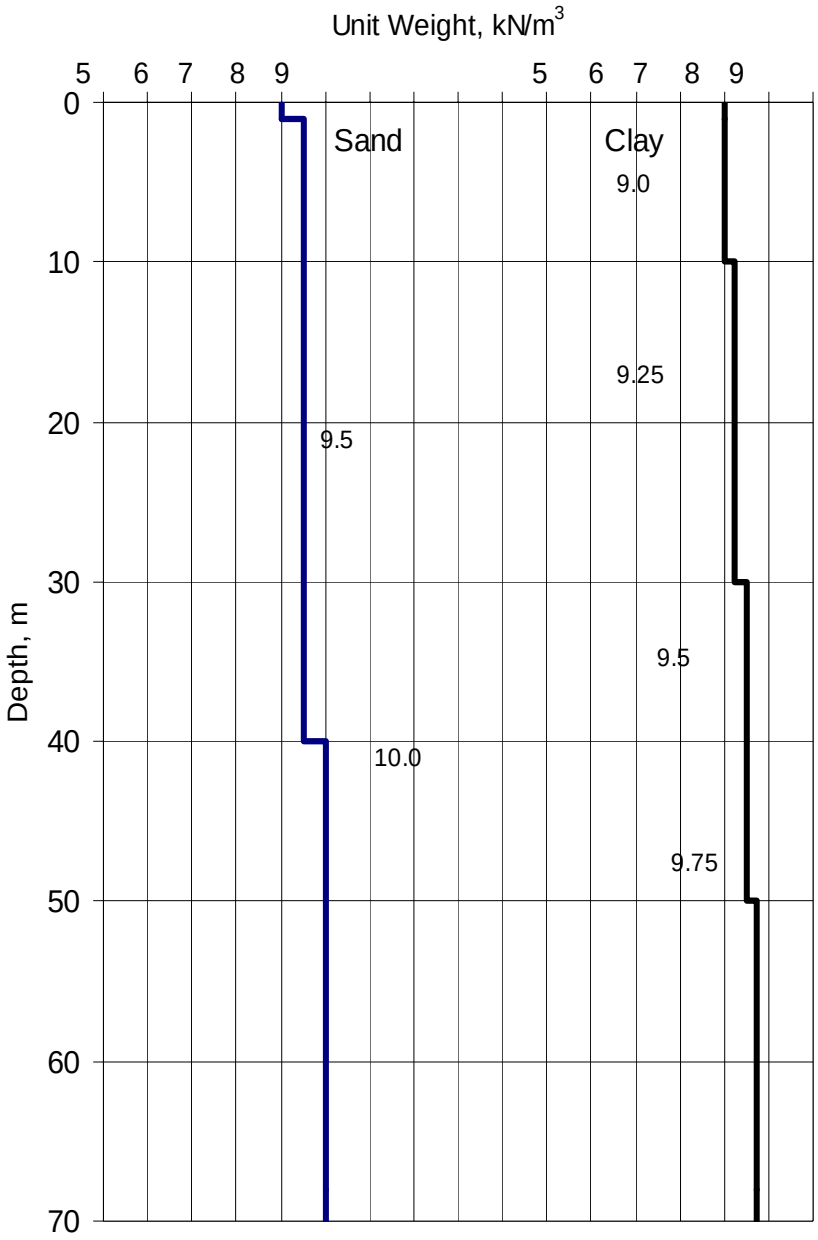

Figure 3-5
Submerged Weight Profile, Clay Site

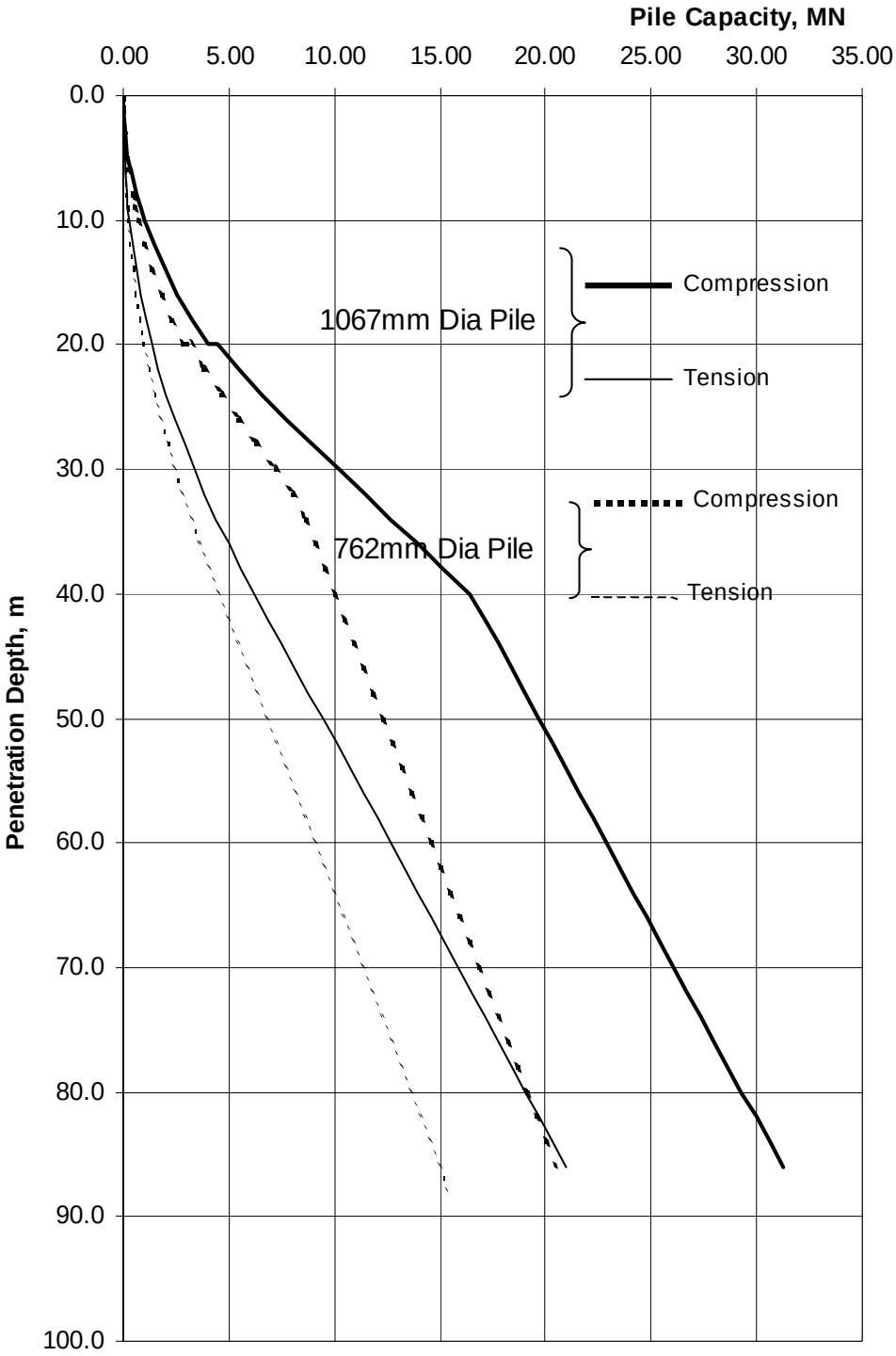

Figure 3-6
API Pile Capacity, Sand Site

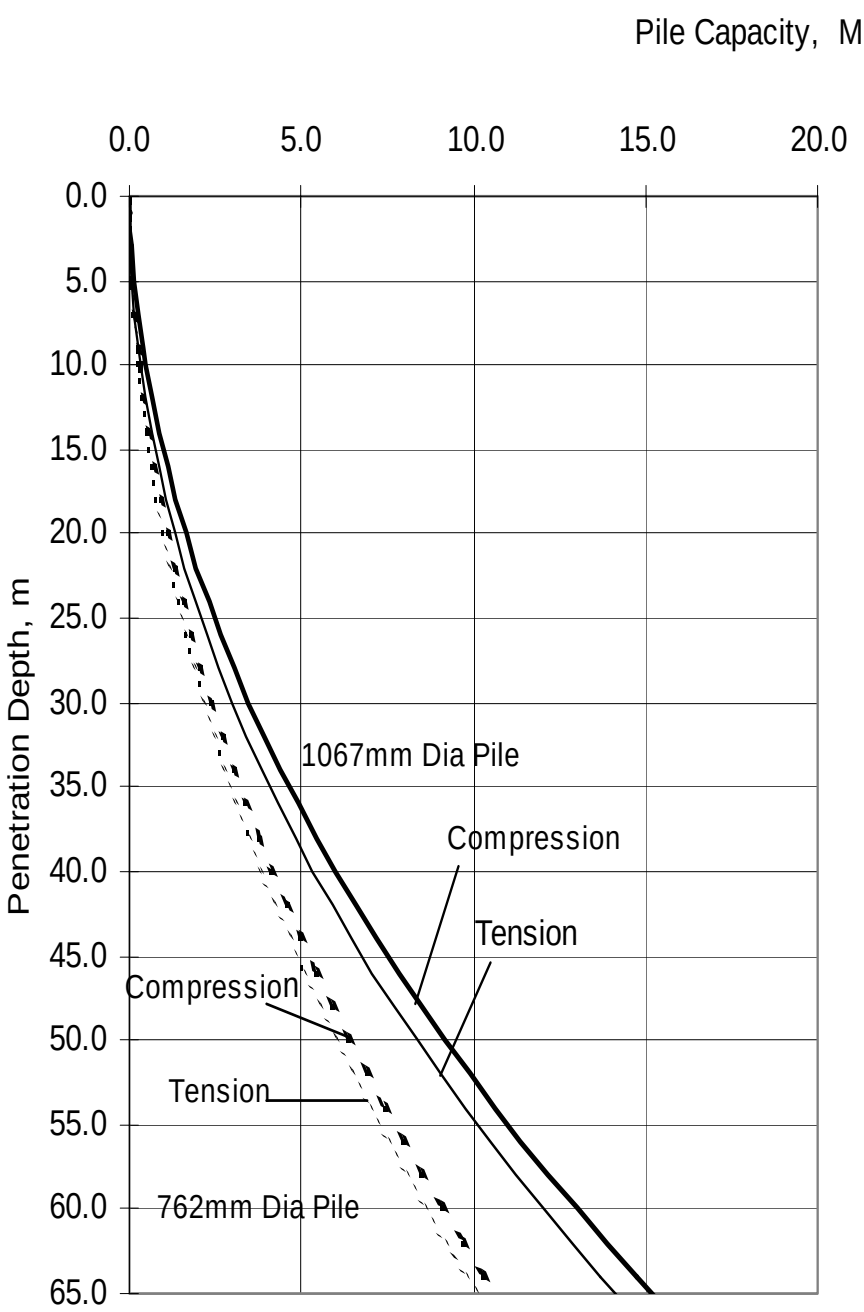

Figure 3-7
API Pile Capacity, Clay Site

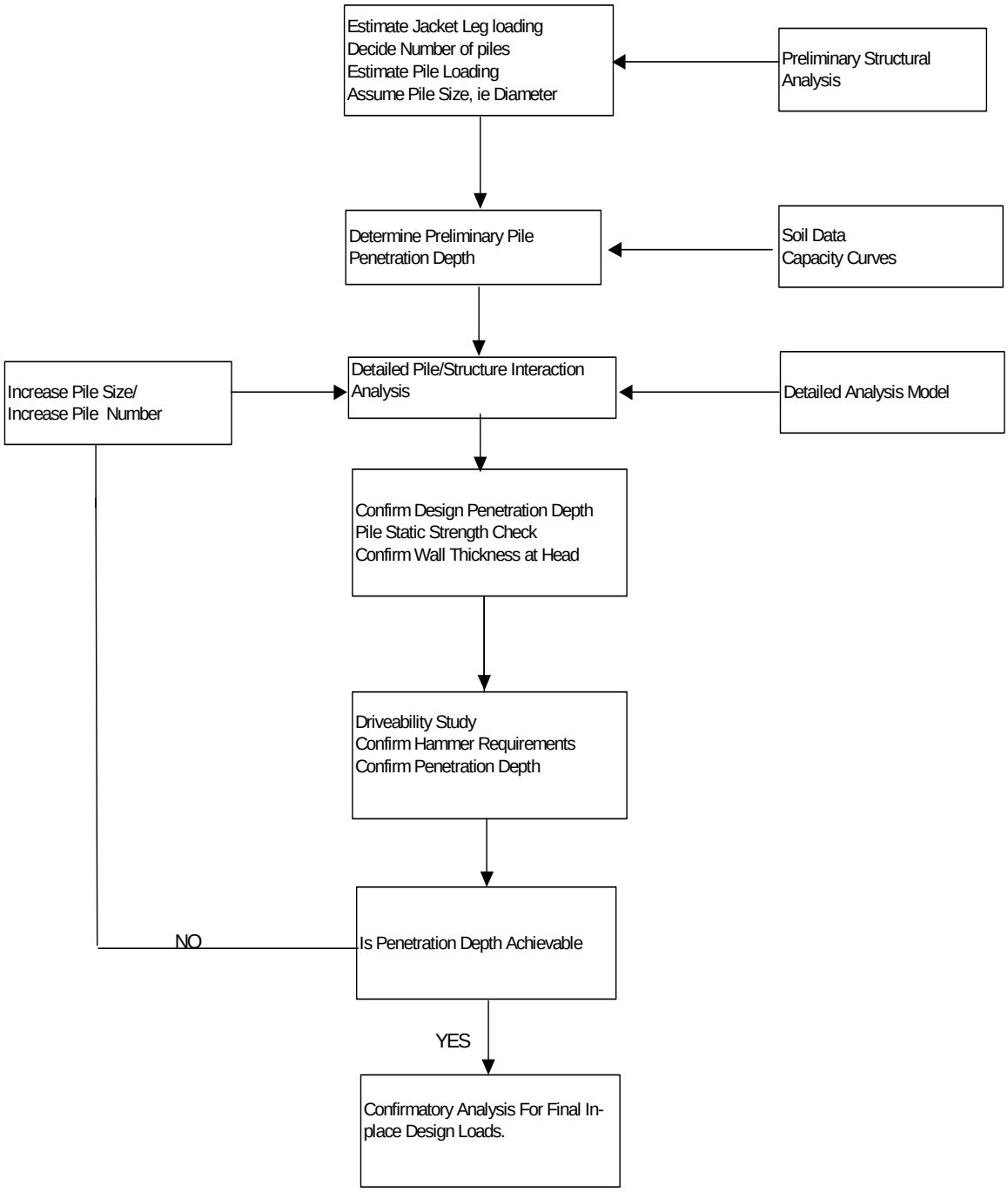

Figure 3-8
Pile Design Decision Tree

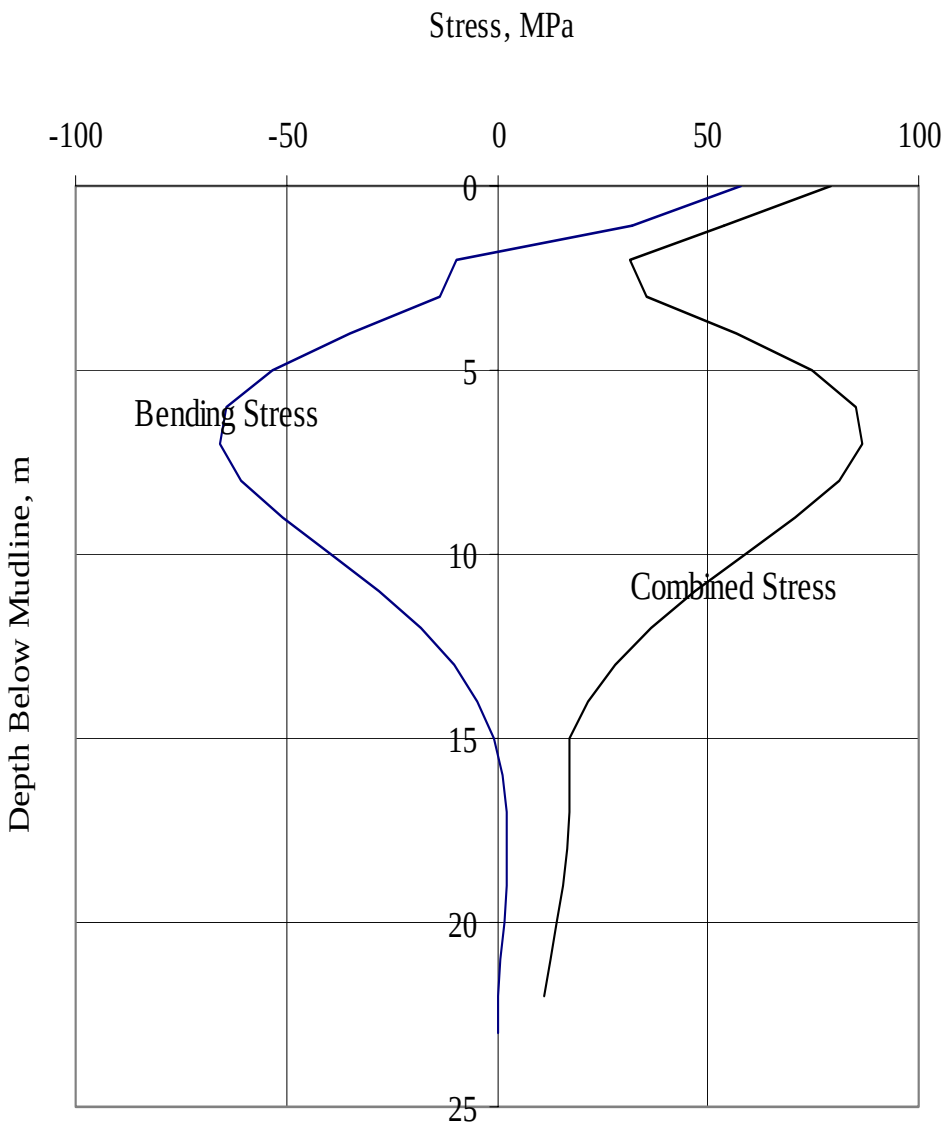

Figure 3-9
Monotower Pile Stress Profile, Sand Site

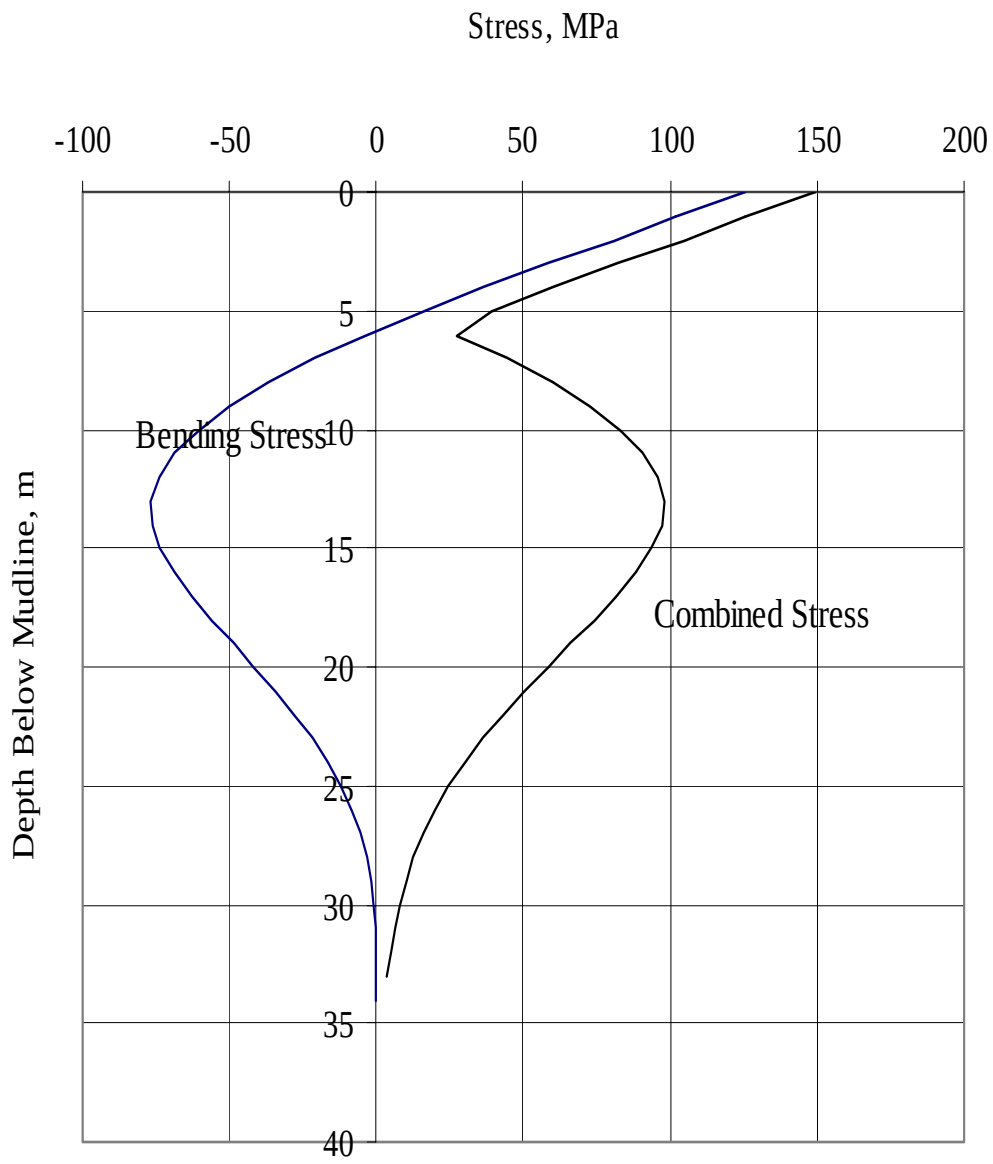

Figure 3-10
Monotower Pile Stress Profile, Clay Site

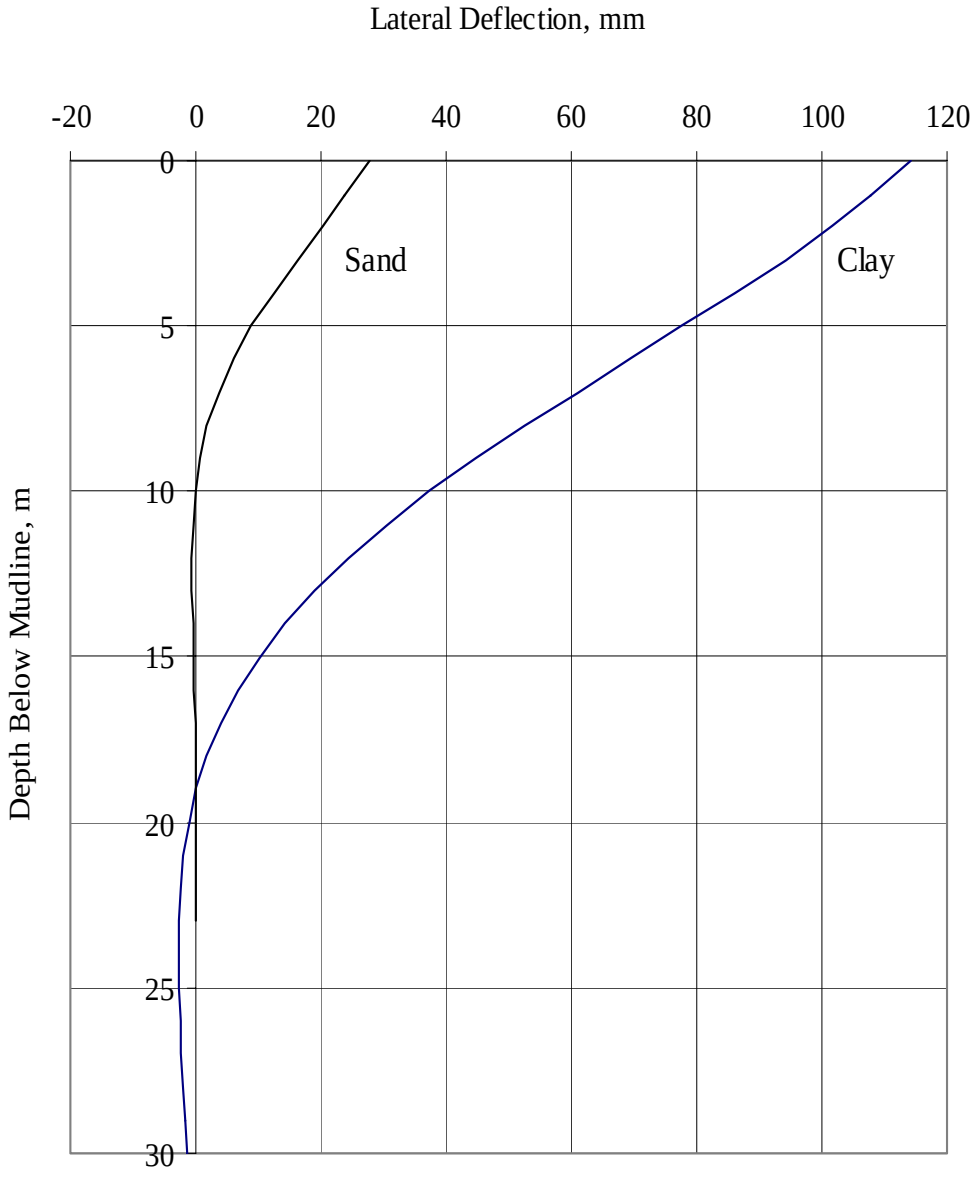

Figure 3-11
Monotower Pile Deflection Profiles

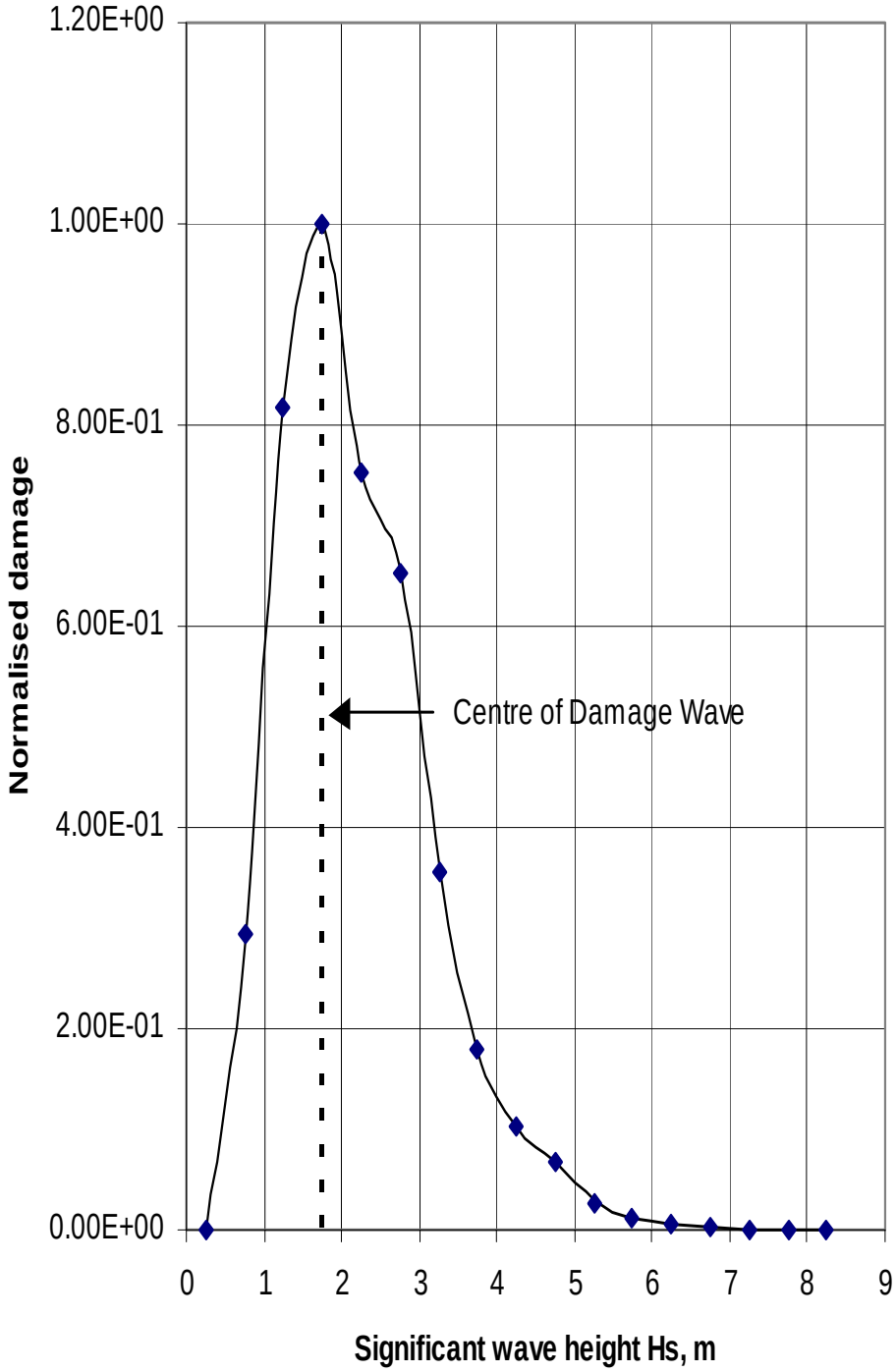

Figure 3-12
Spread of Damage with Wave Height, Monotower

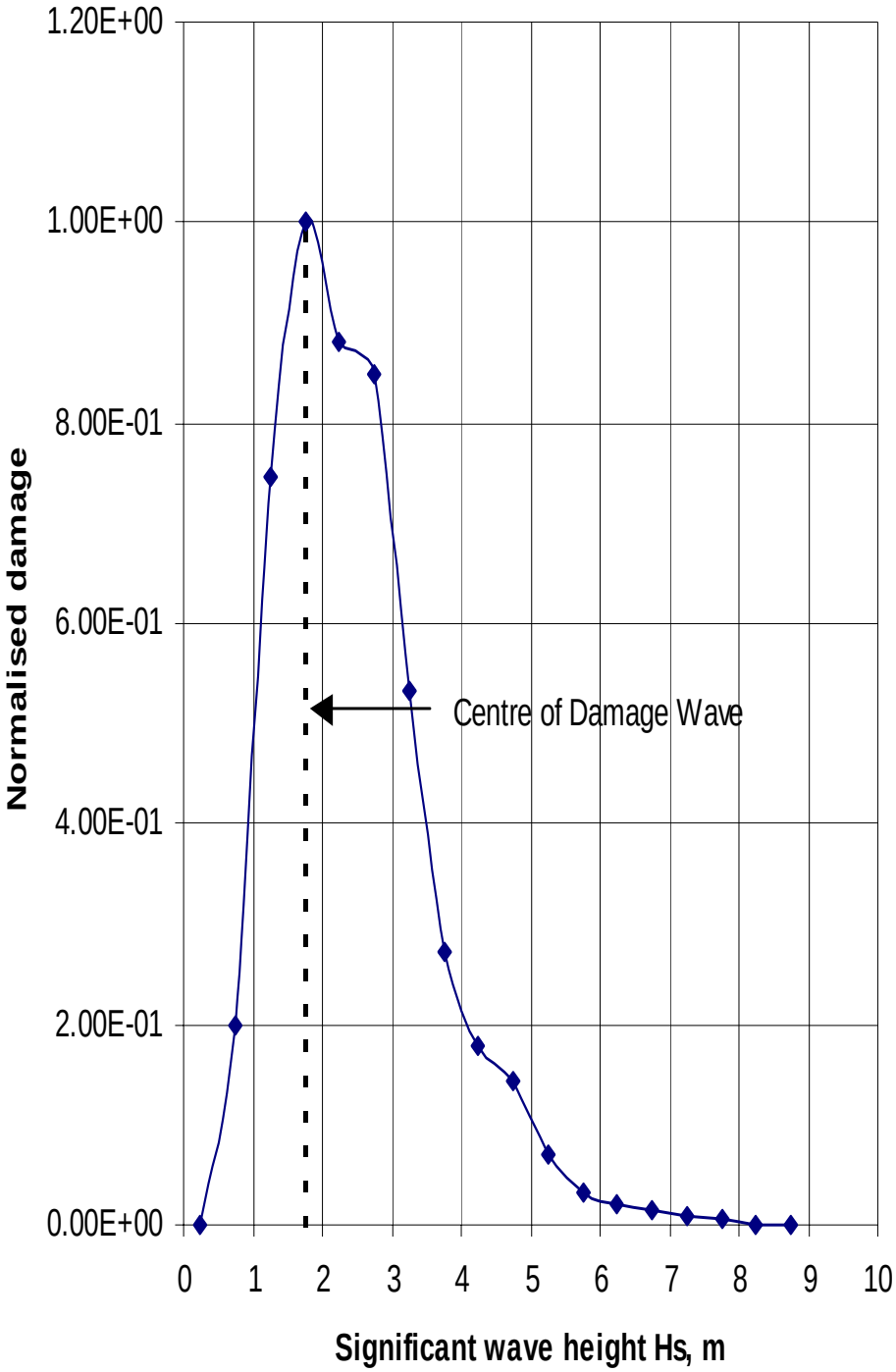

Figure 3-13
Spread of Damage with Wave Height, Vierendeel

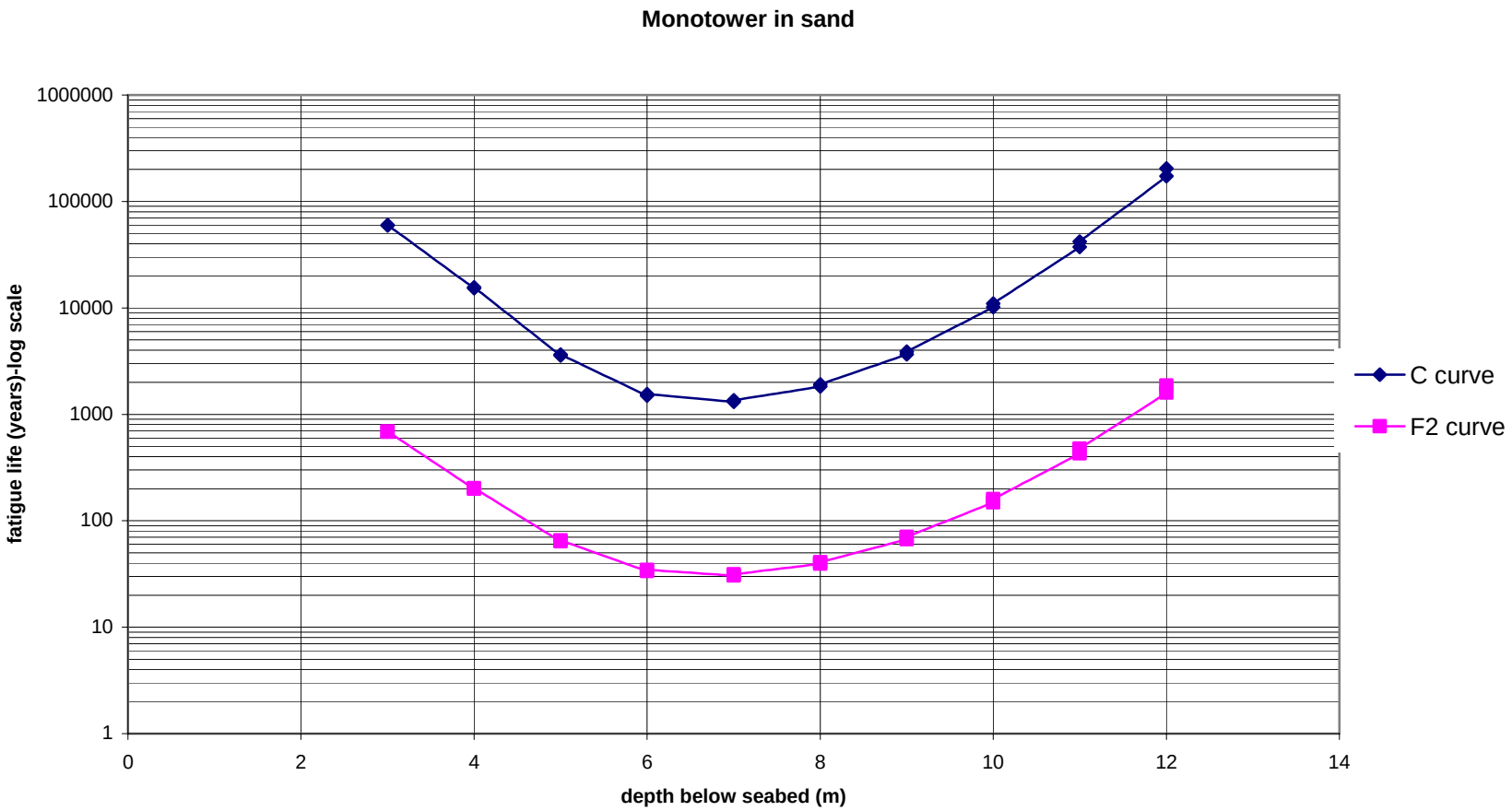

Figure 3-14
Fatigue Life Profile Monotower Piles in Sand

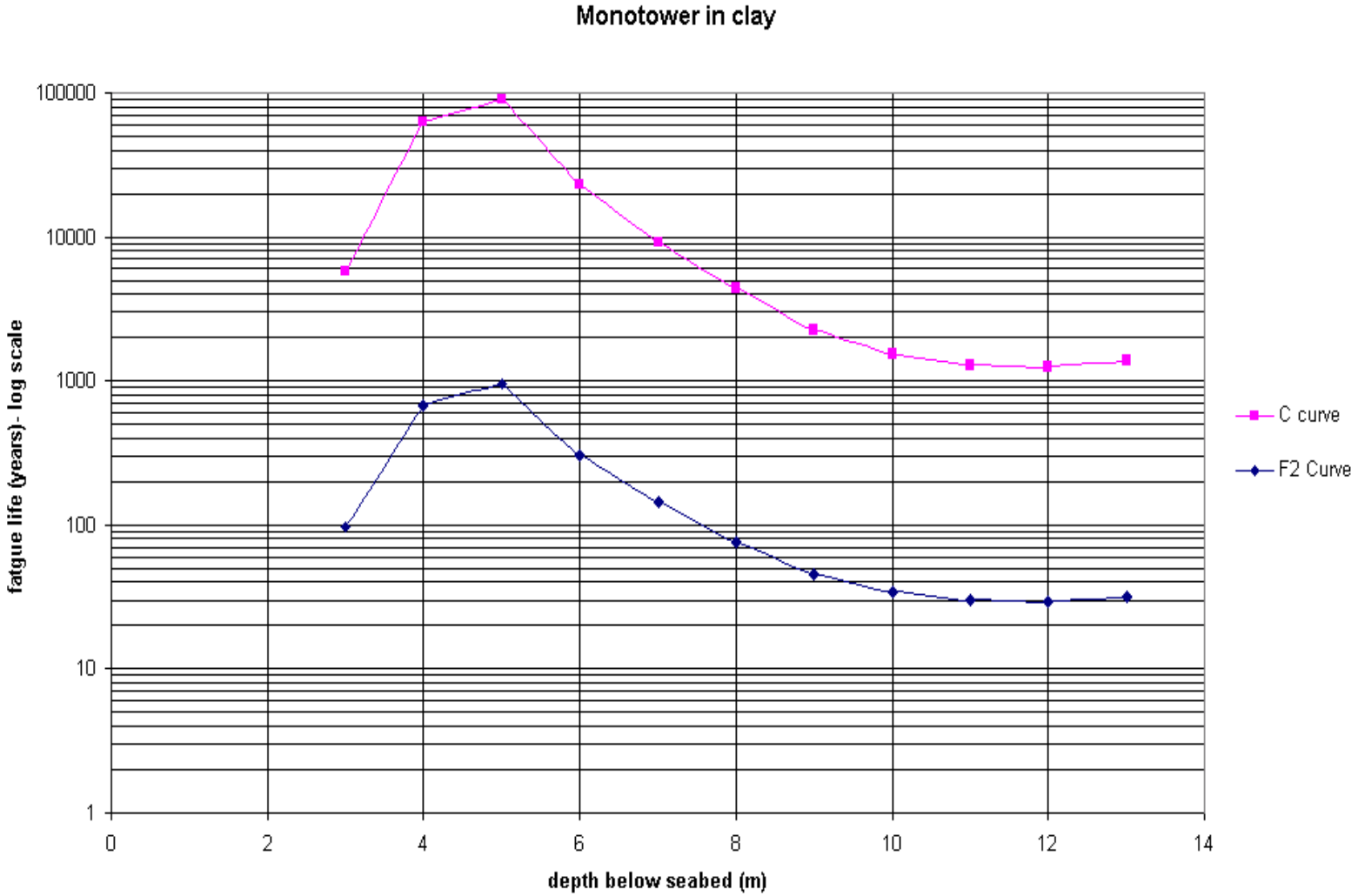

Figure 3-15
Fatigue Life Profile Monotower Piles in Clay

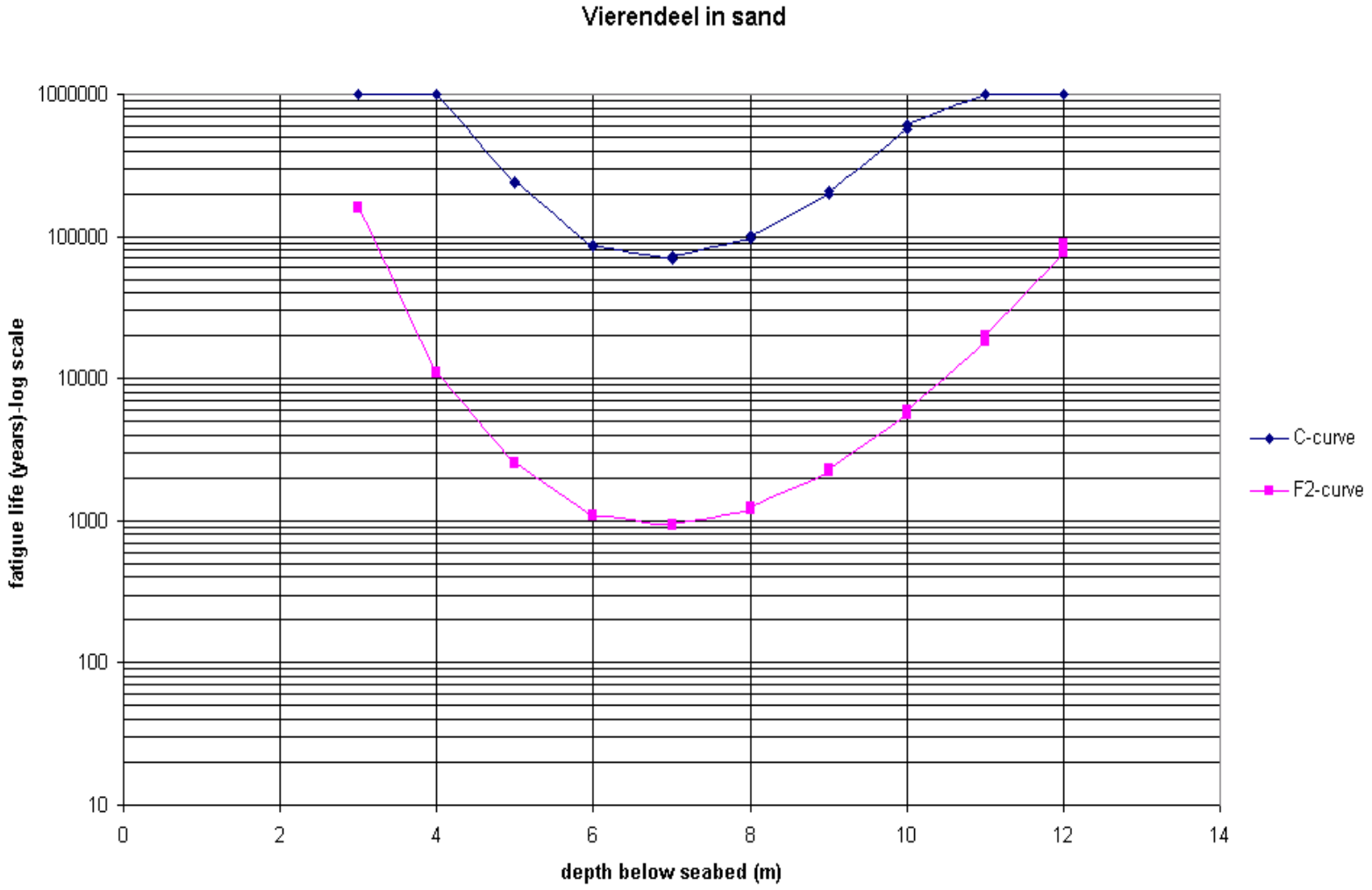

Figure 3-16
Fatigue Life Profile Vierendeel Piles in Sand

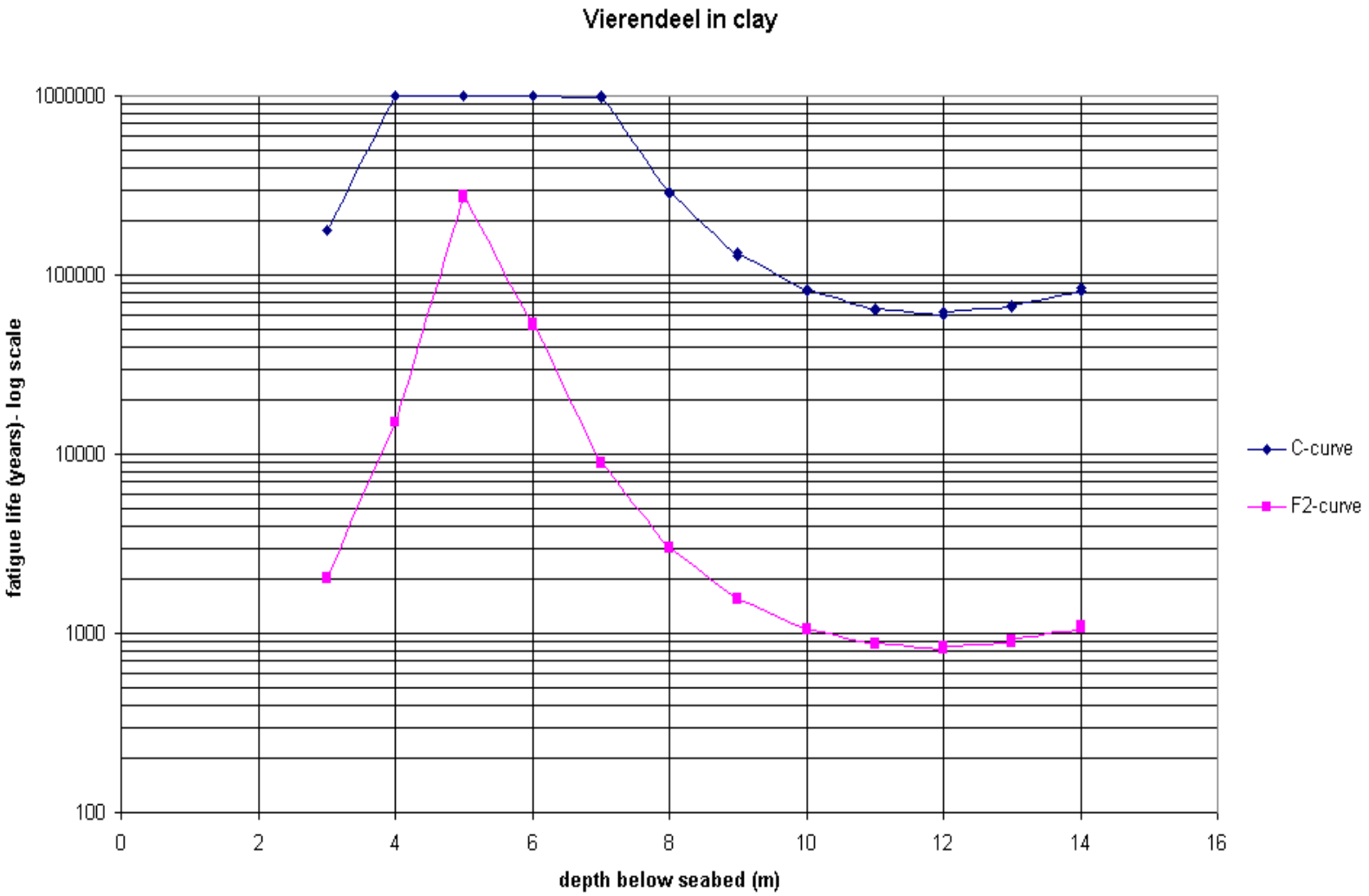

Figure 3-17
Fatigue Life Profile Vierendeel Piles in Clay Sand

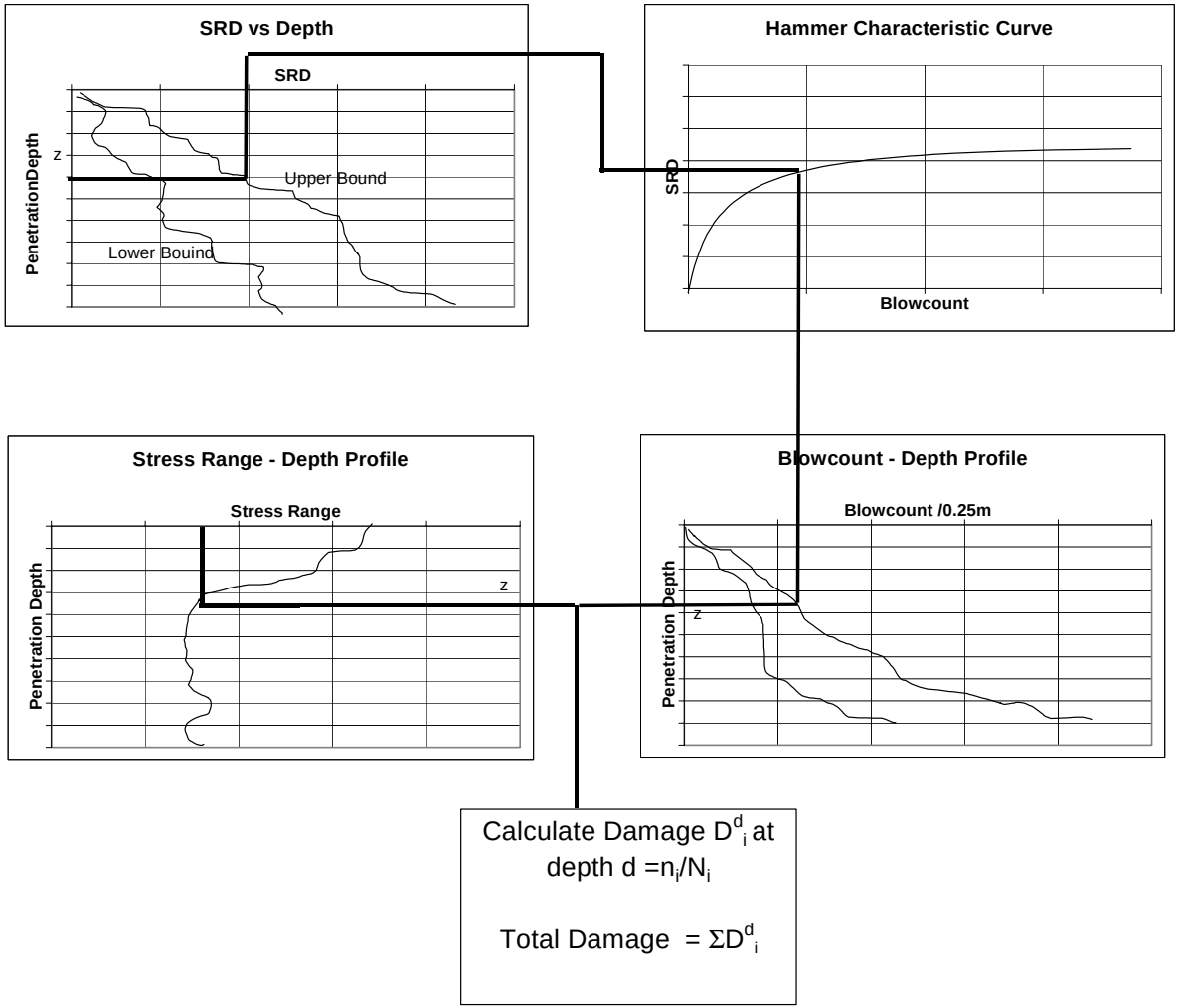

Figure 3-18
Calculation of Driving Damage

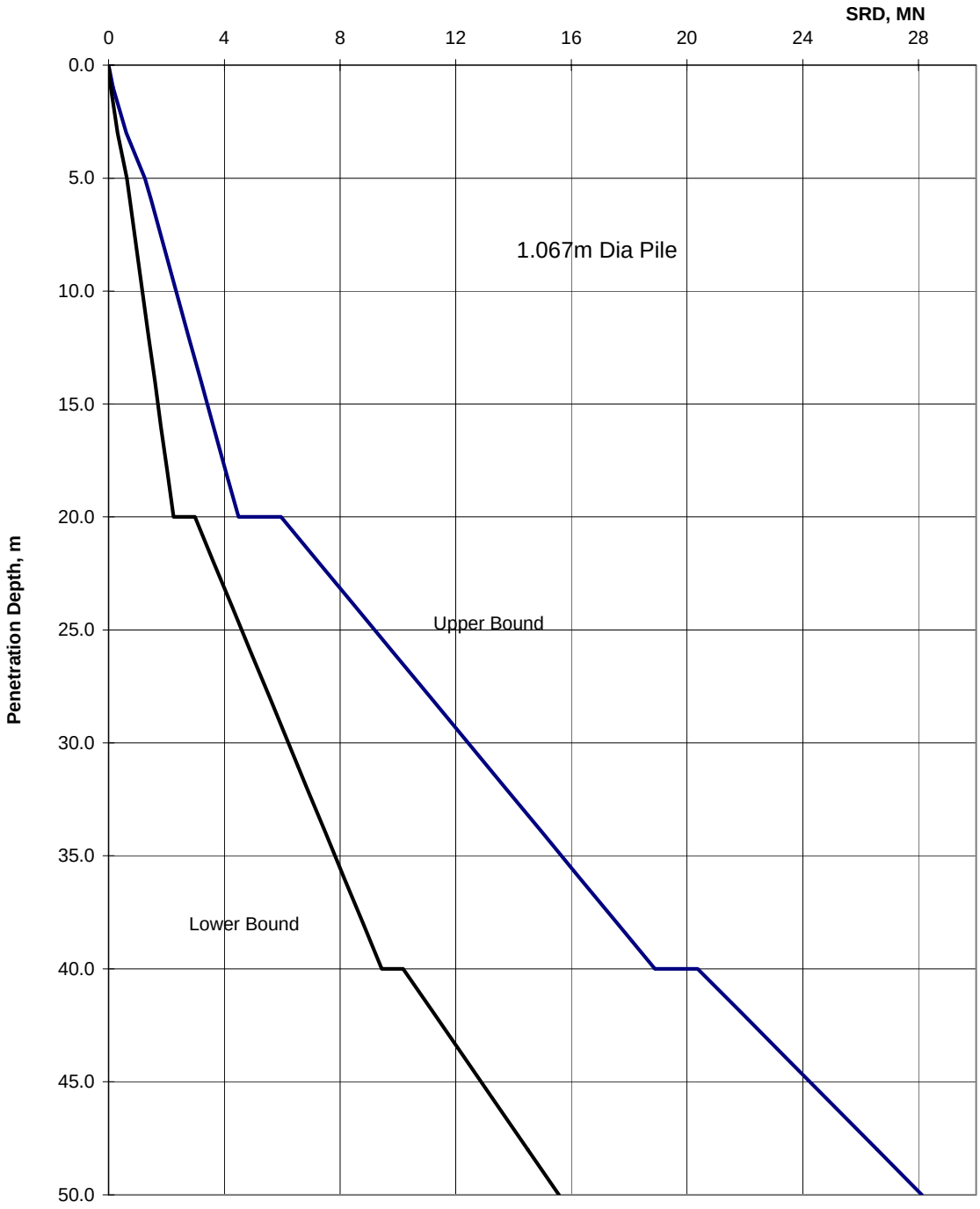

Figure 3-19
SRD Profile Sand Site

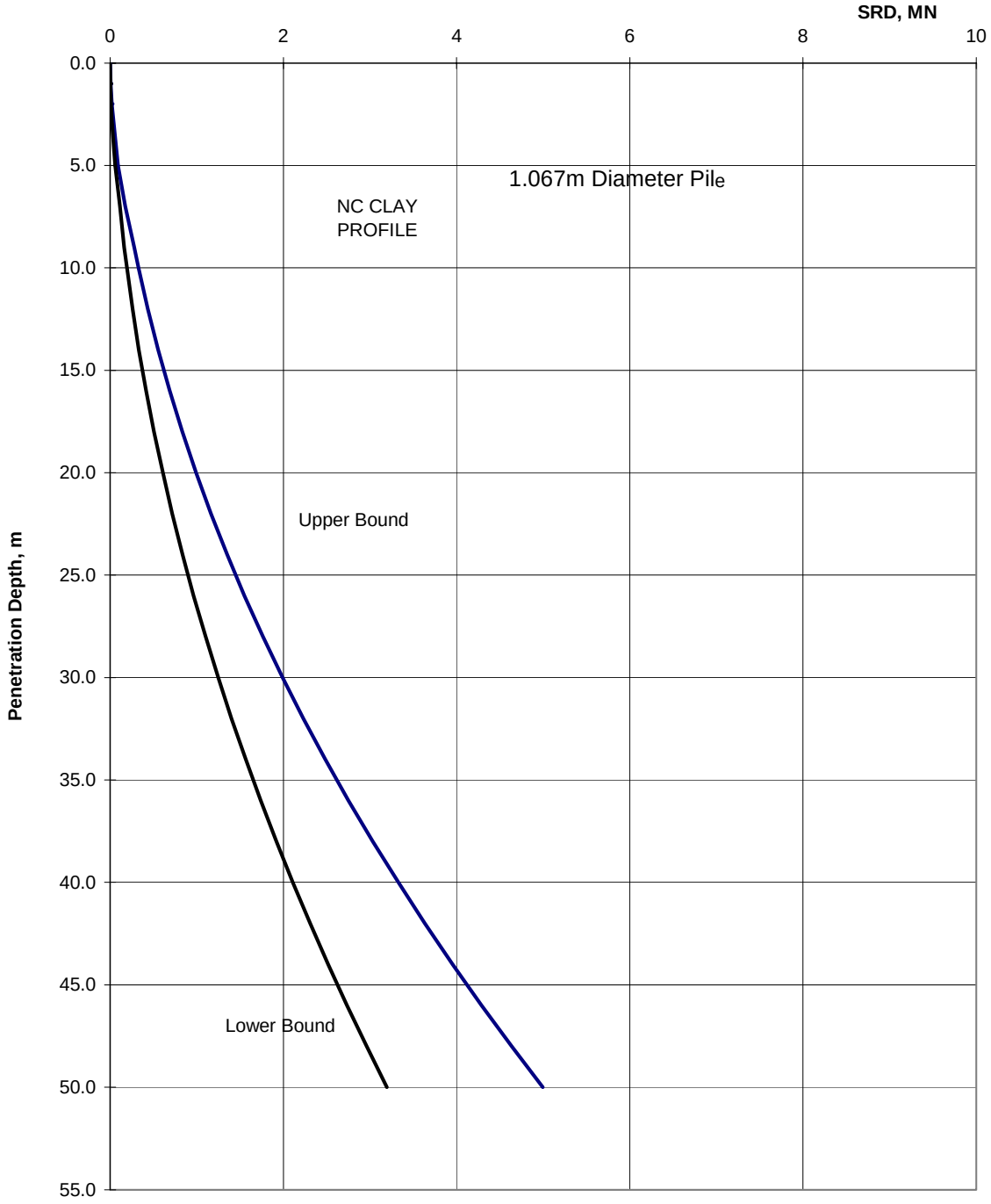

Figure 3-20
SRD Profile Clay Profile

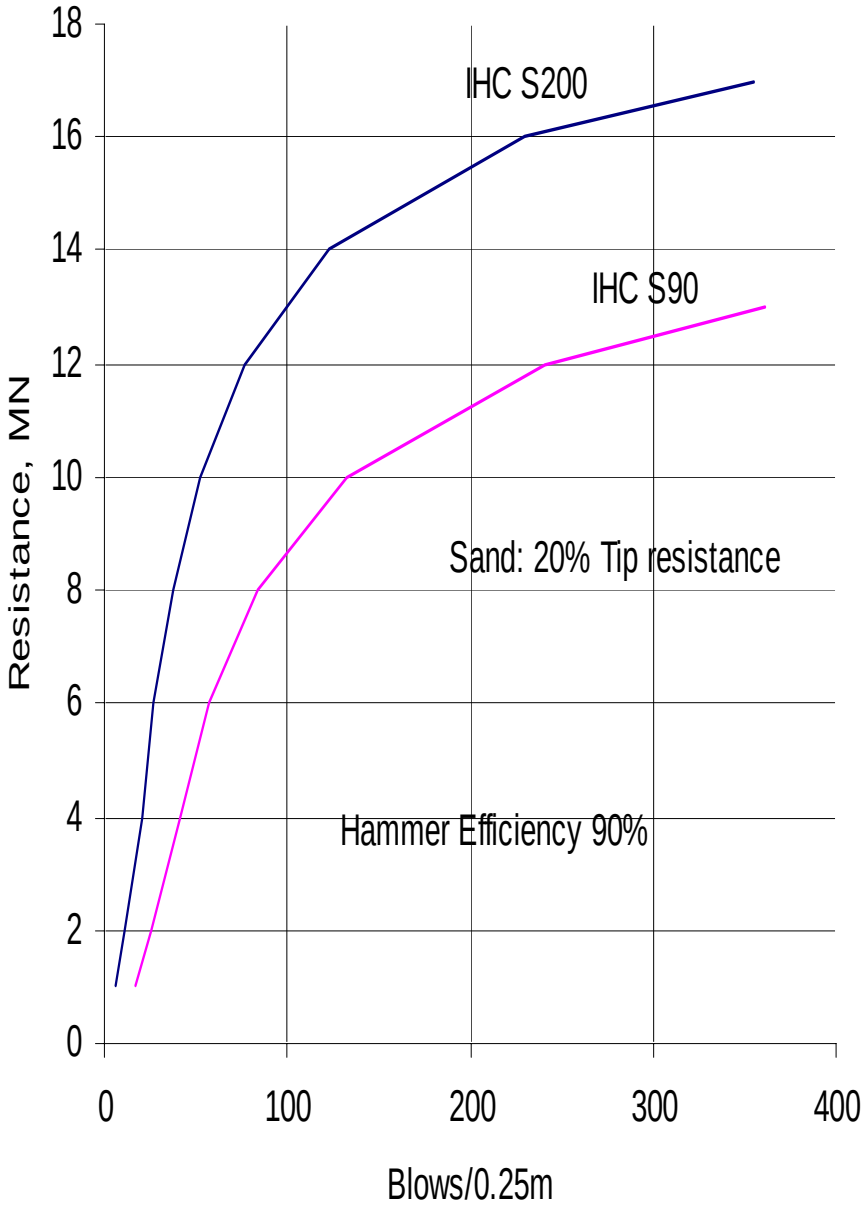

Figure 3-21
Hammer Performance Curves, Sand Site

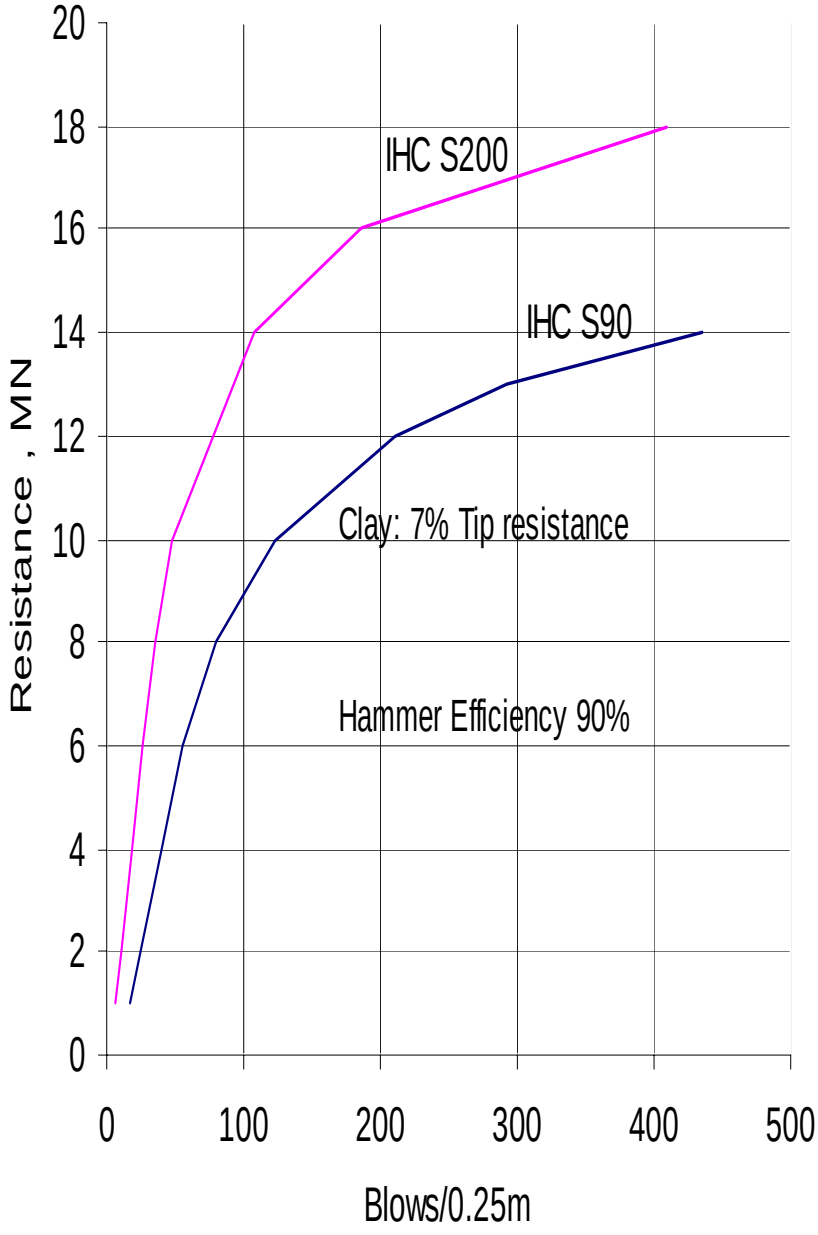

Figure 3-22
Hammer Performance Curves, Clay Site

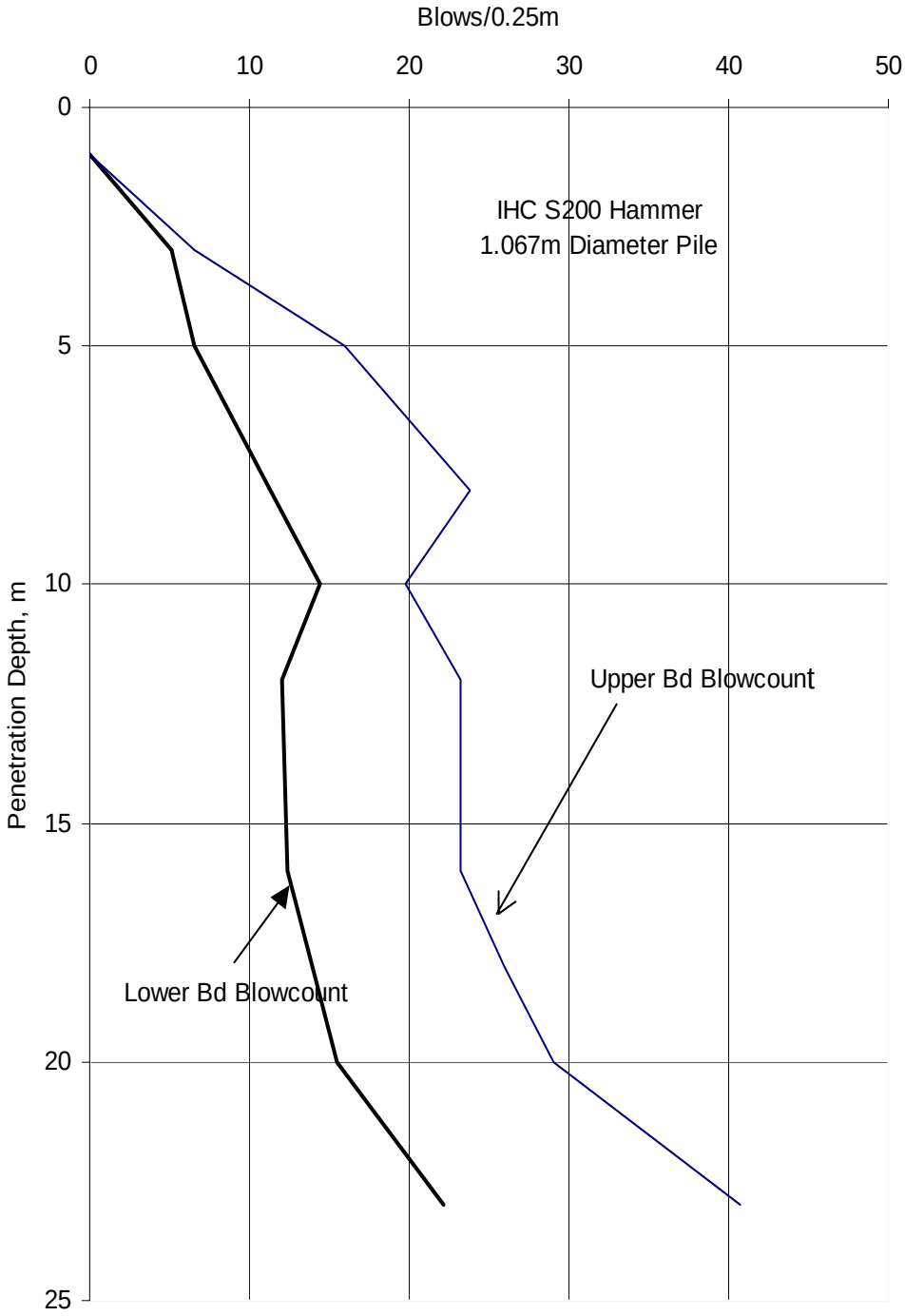

Figure 3-23
Monotower Pile Blowcount Profile, Sand Site

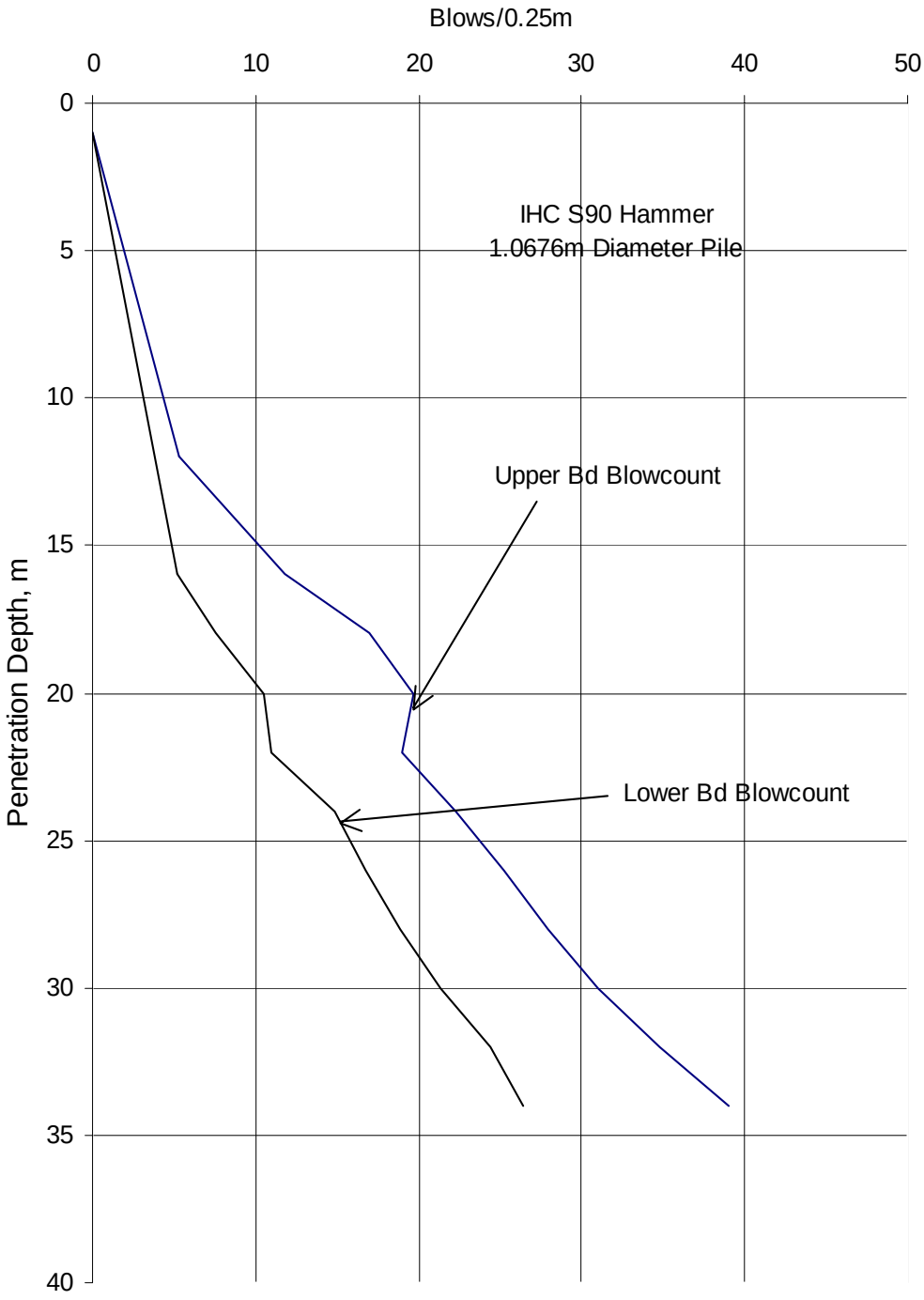

Figure 3-24
Monotower Pile Blowcount Profile, Clay Site

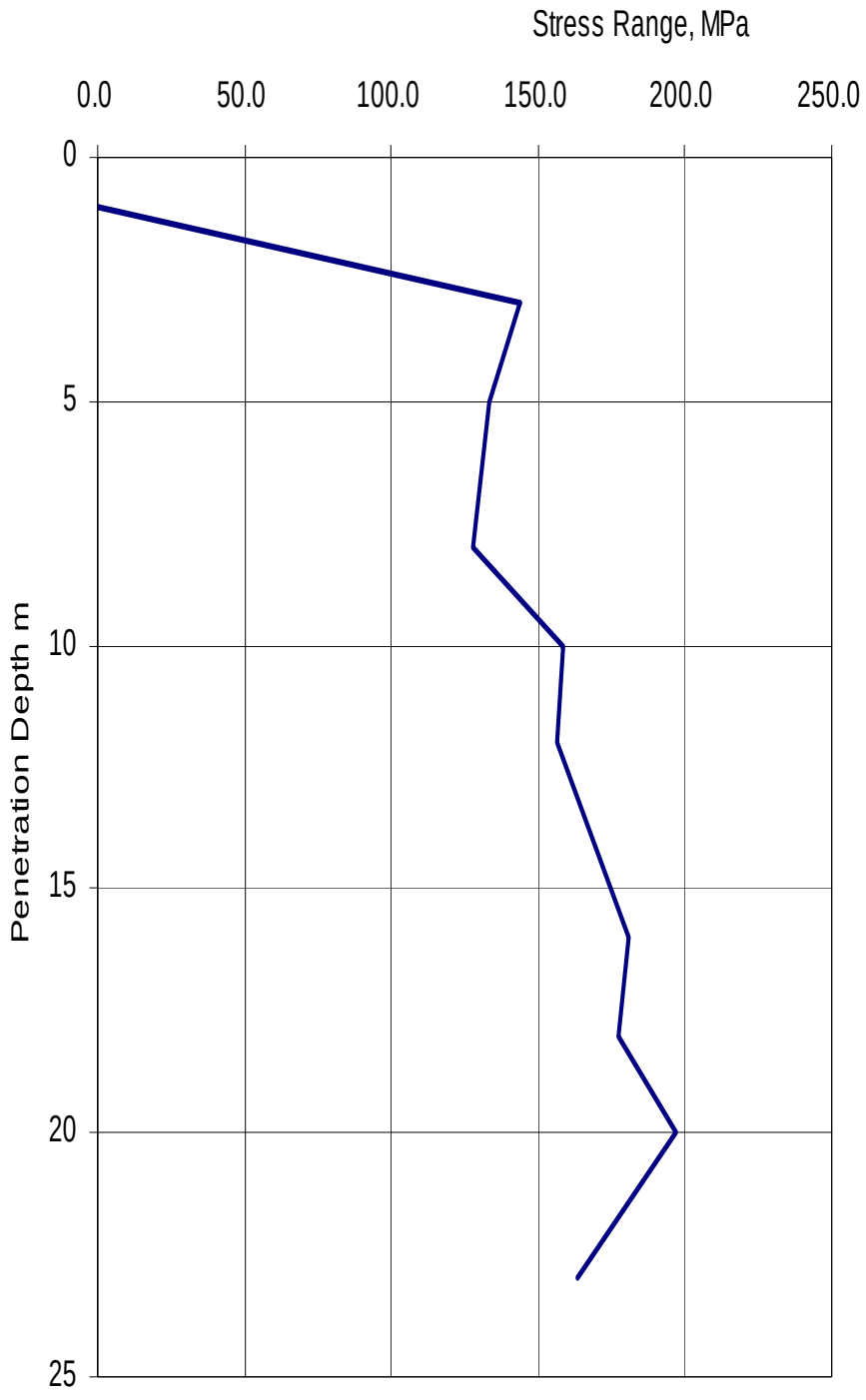

Figure 3-25
Monotower Pile Stress Range Profile, Sand Site

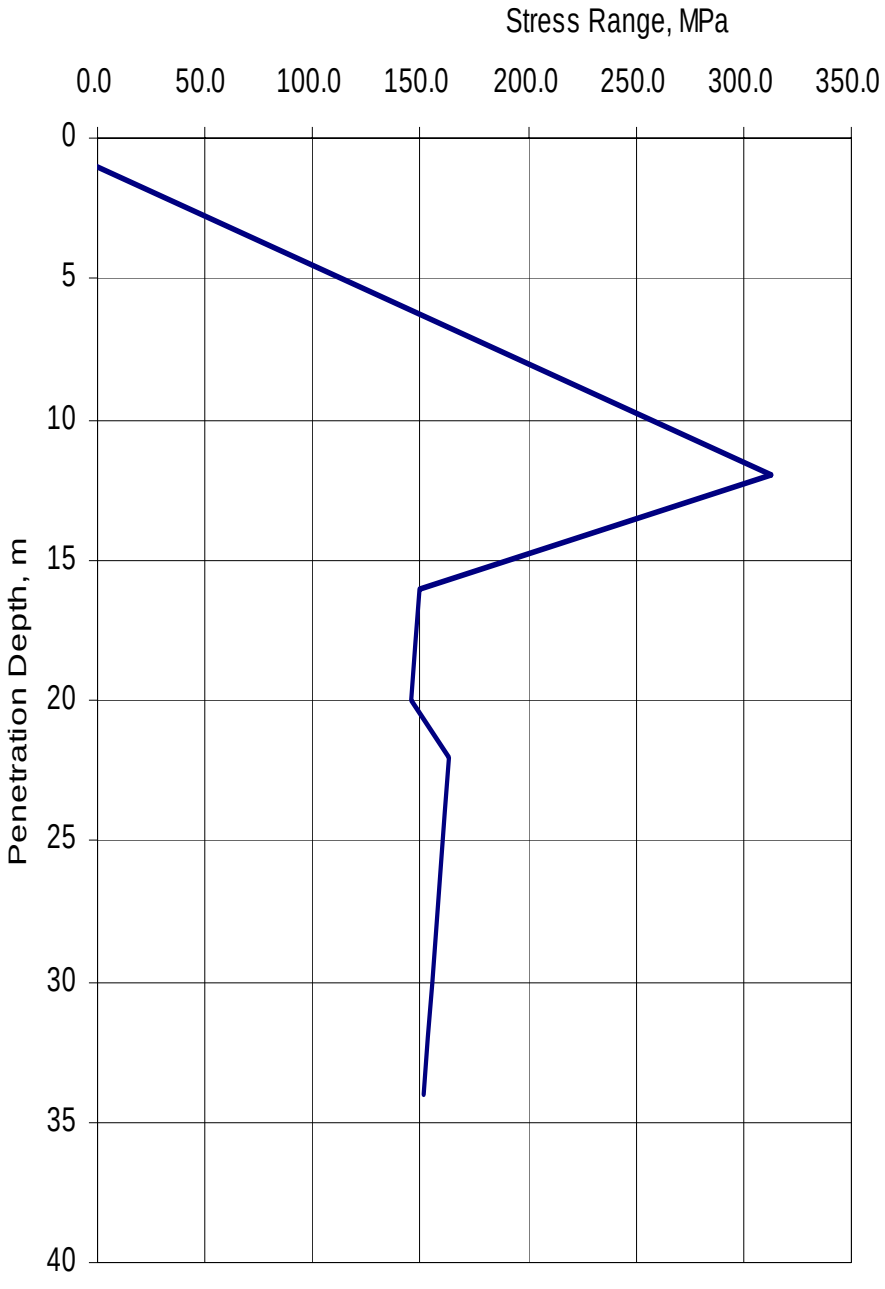

Figure 3-26
Monotower Pile Stress Range Profile, Clay Site

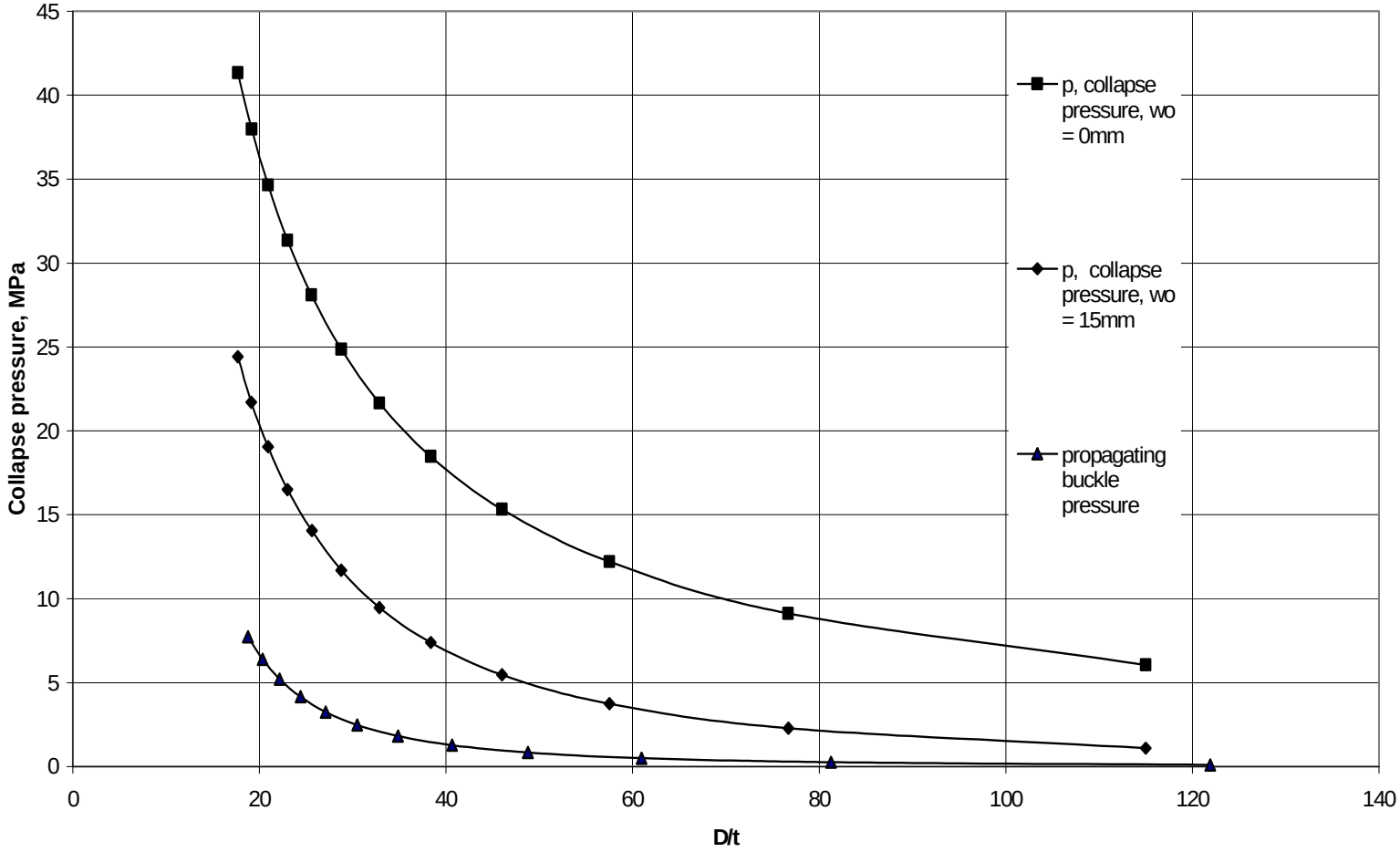

Figure 4-1
Collapse Pressures and Propagation Pressures for Tubulars

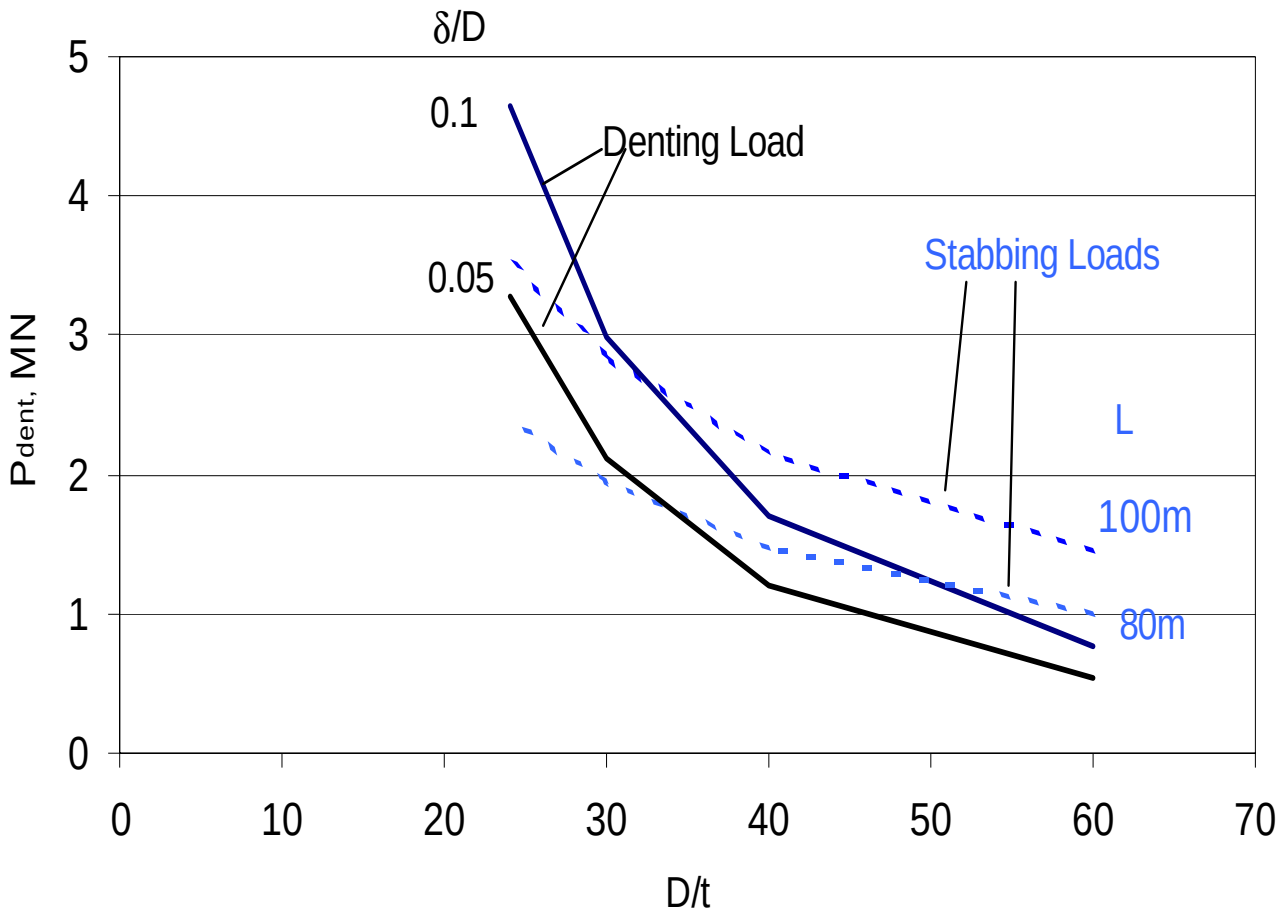

Figure 4-2
Comparison of Denting Loads and Pile Stabbing Loads

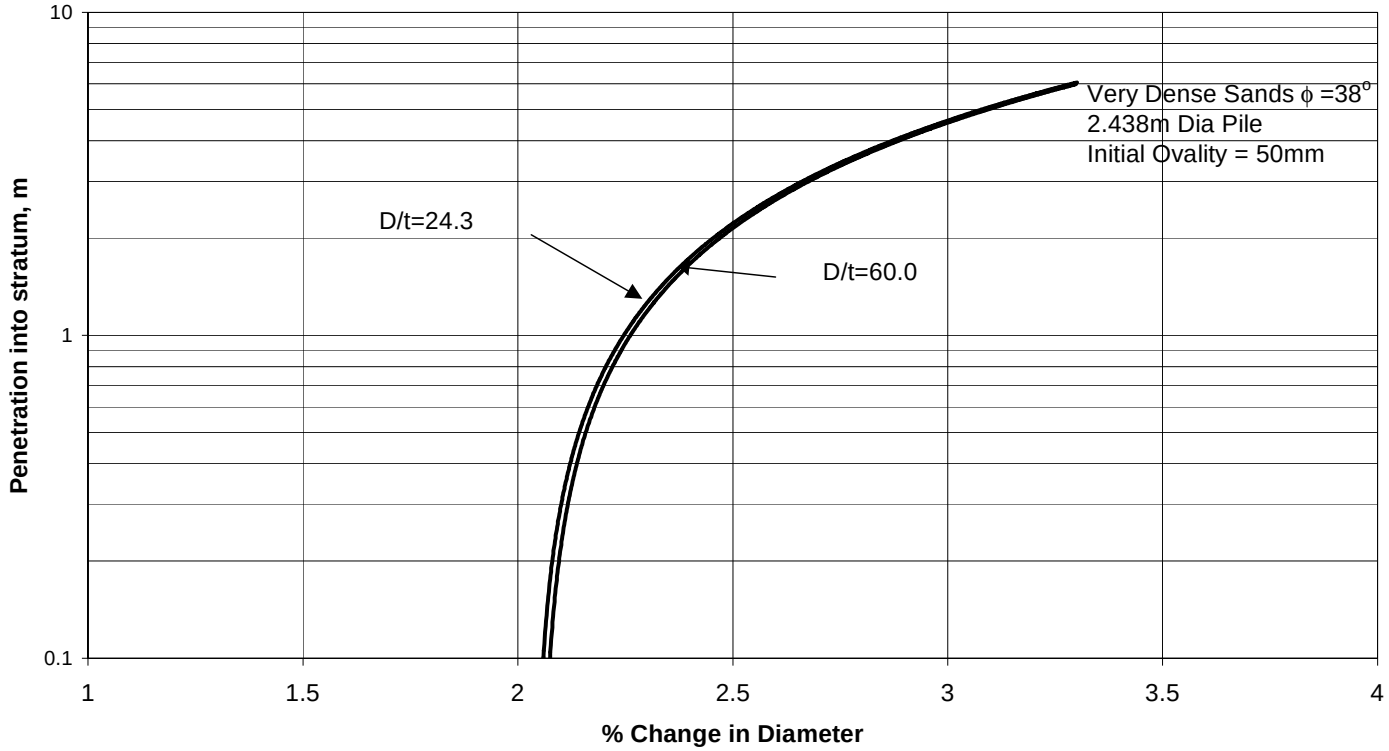

Figure 4-3
Effect of Pile Penetration of Very Dense Sands Initial Ovality 50mm

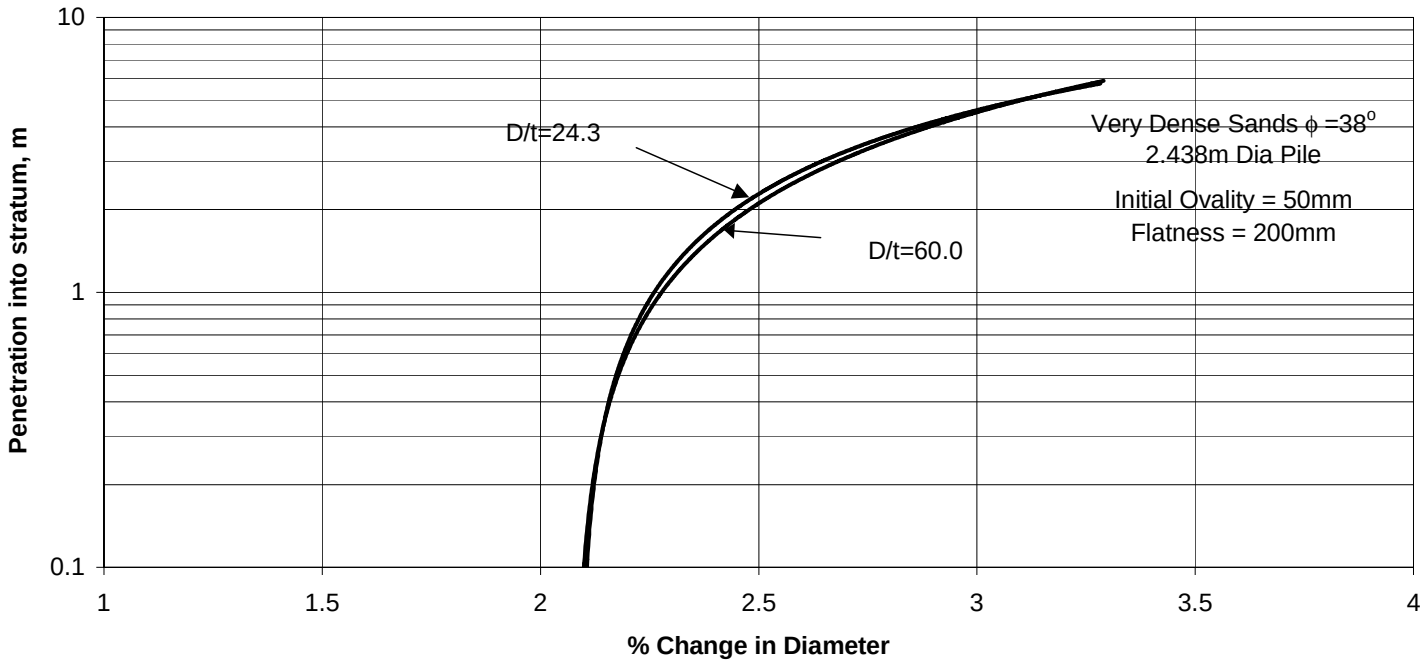

Figure 4-4
Effect of Pile Penetration of Very Dense Sands Initial Ovality 50mm and Flatness 200mm

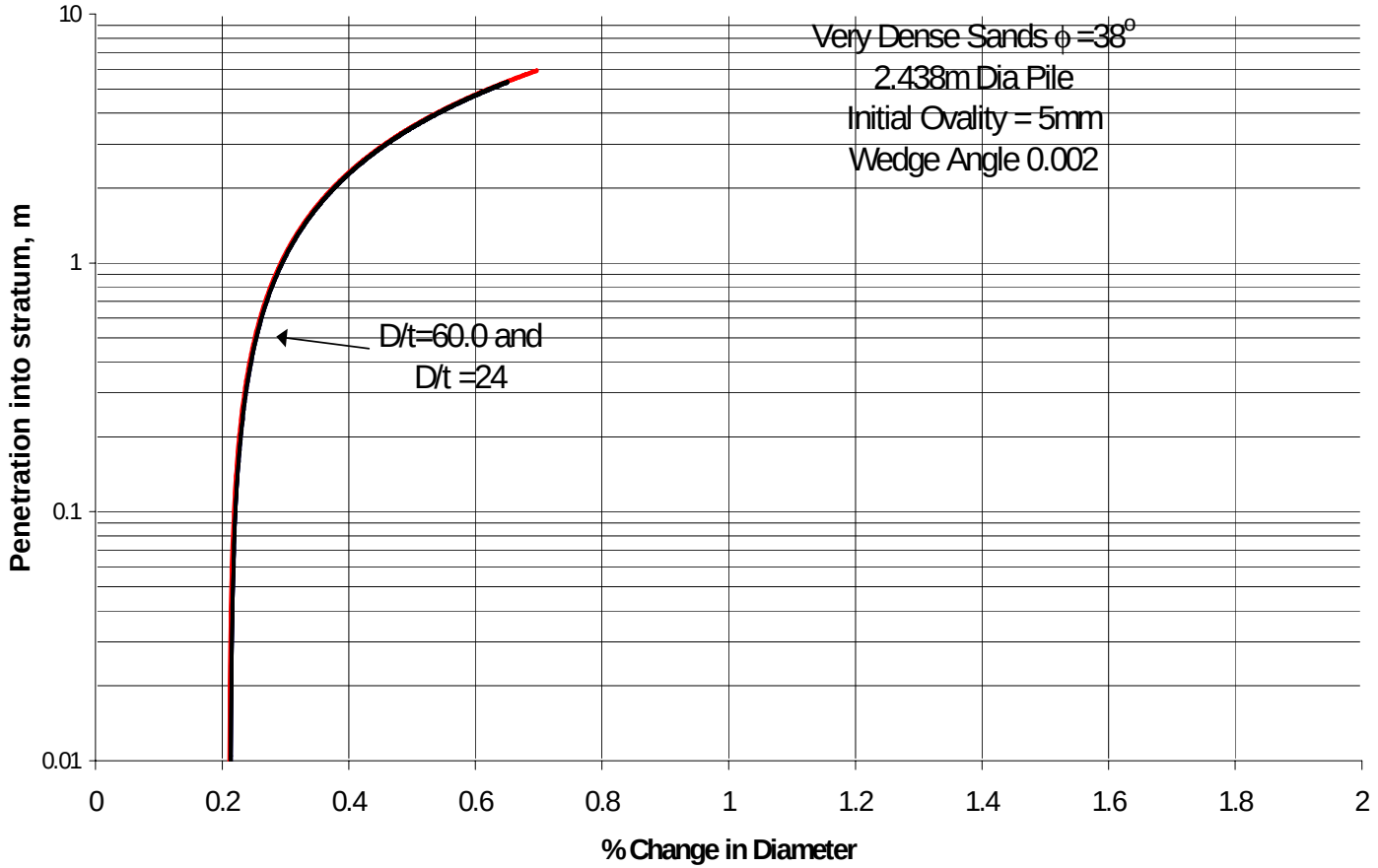

Figure 4-5
Effect of Pile Penetration of Very Dense Sands Initial Ovality 5mm

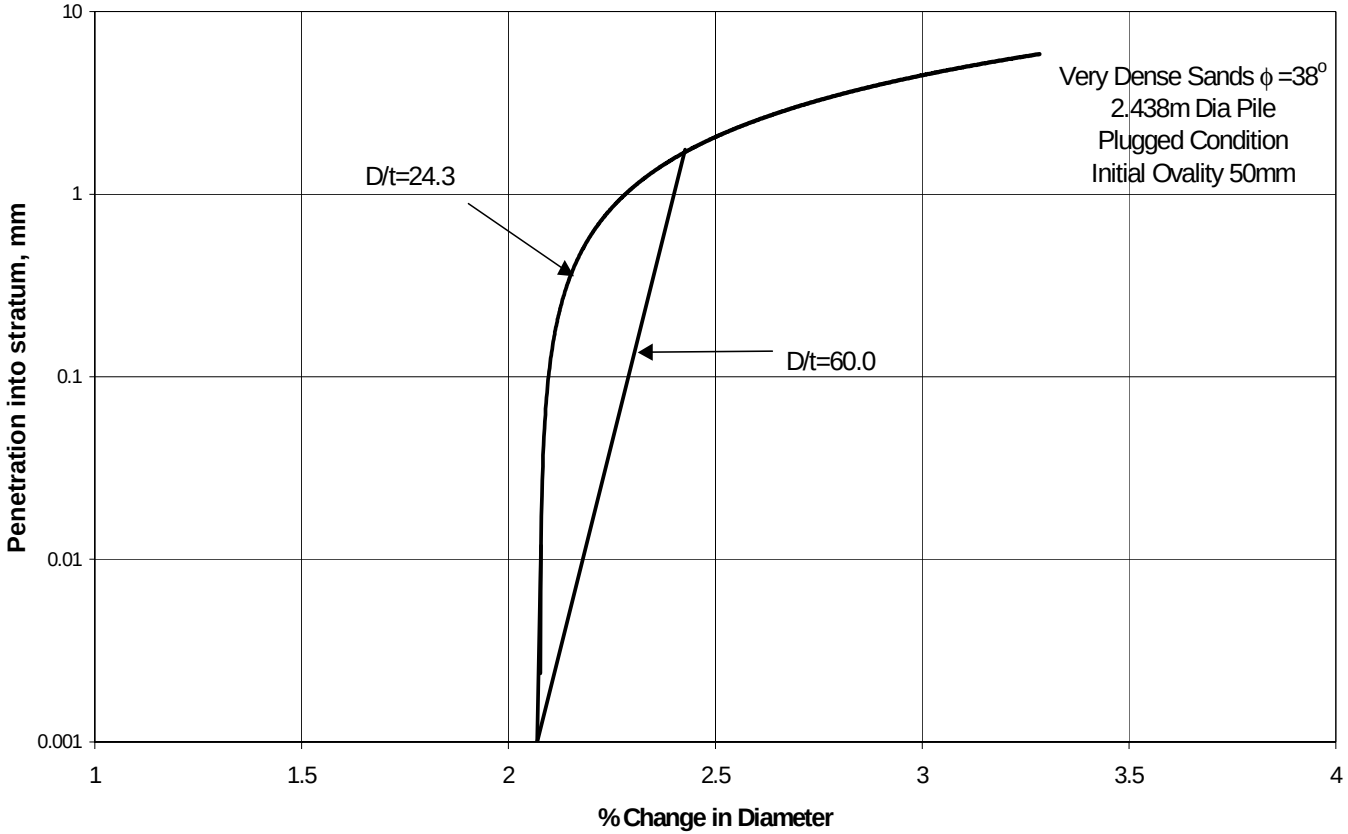

Figure 4-6
Effect of Plugged Pile Penetration of Very Dense Sands Initial Ovality 50mm

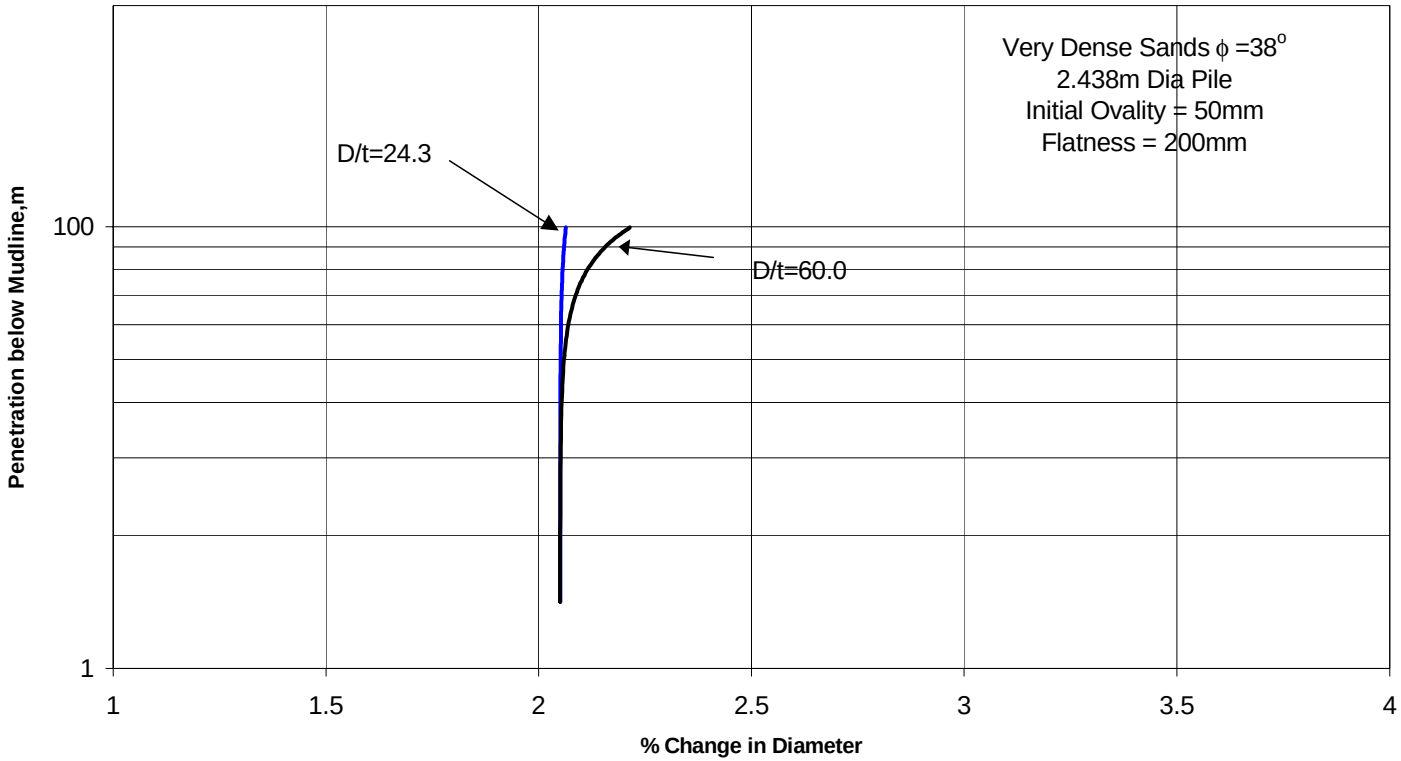

Figure 4-7
Effect of At-Rest Pressures on Plugged Pile

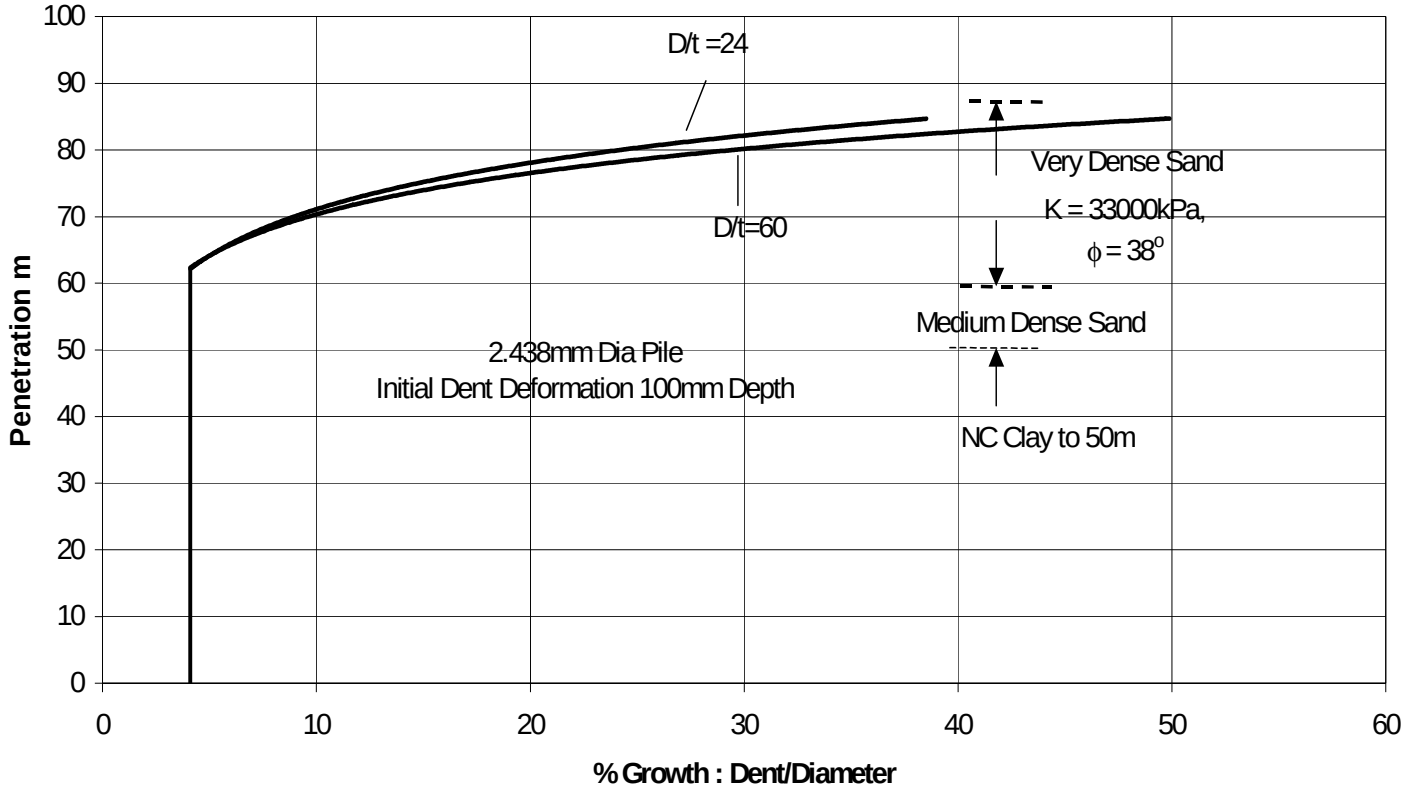

Figure 4-8
Increase in Initial Dent of 100mm with Penetration into Very Dense Sand

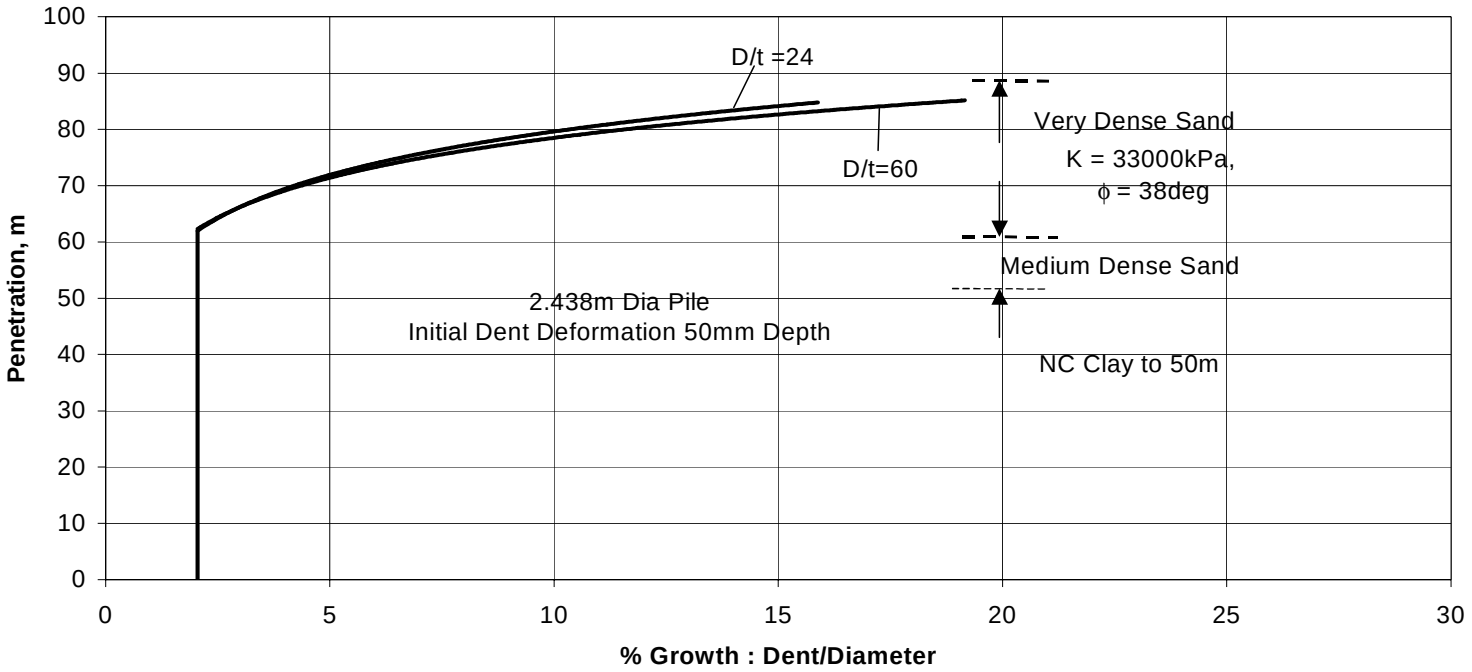

Figure 4-9
Increase in Initial Dent of 50mm with Penetration into Very Dense Sand

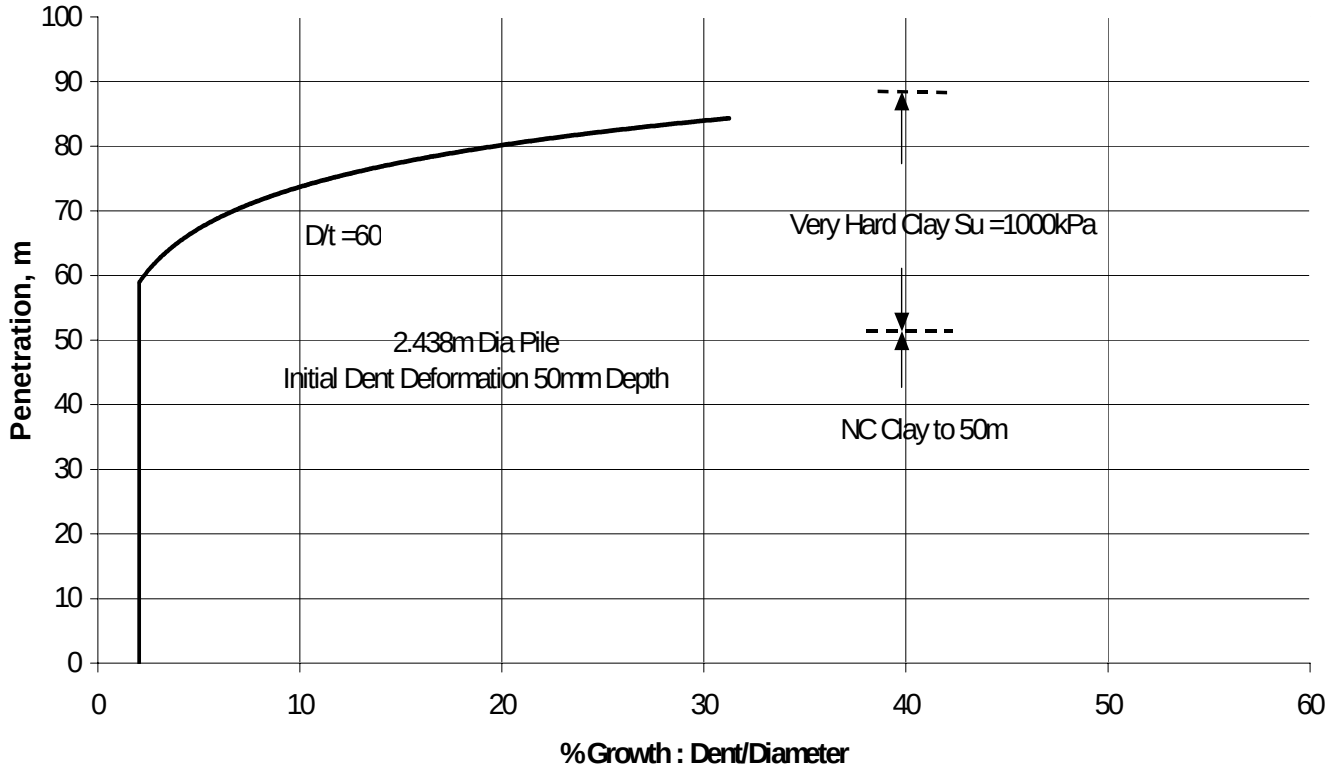

Figure 4-10
Increase in Initial Dent of 50mm with Penetration into Very Hard Clay

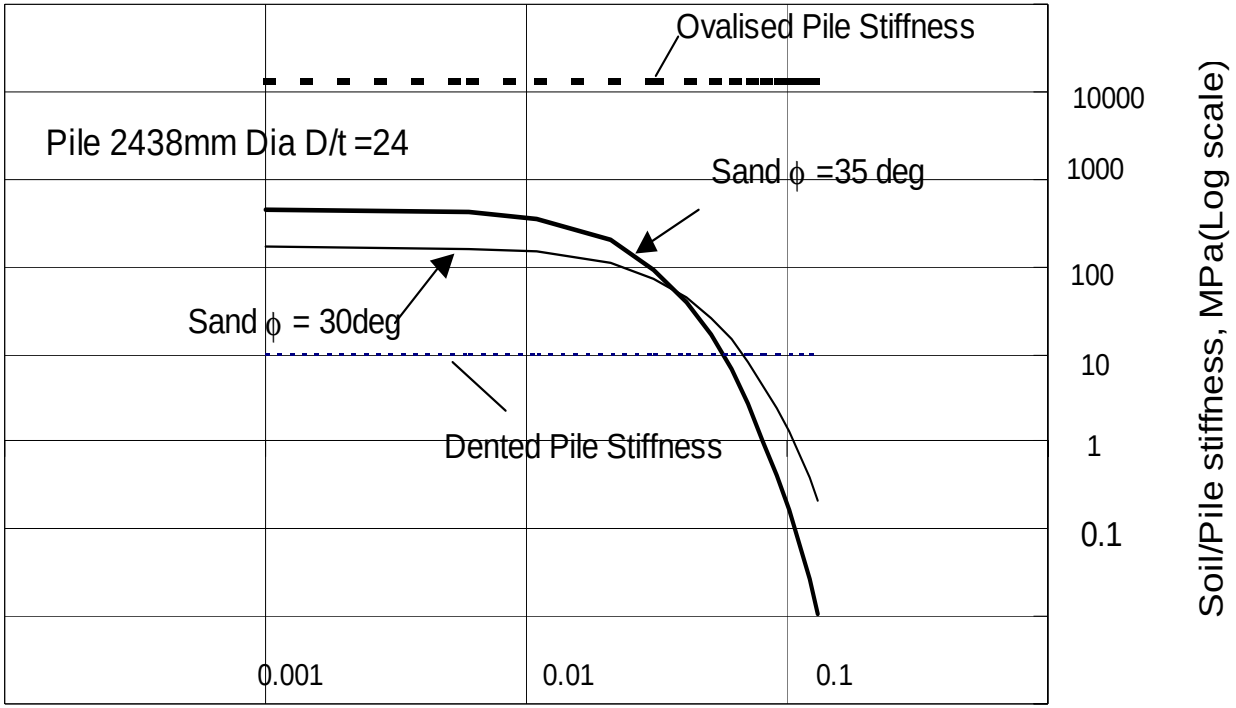

Figure 4-11
Comparison of Pile and Sand Stiffness D/t = 24

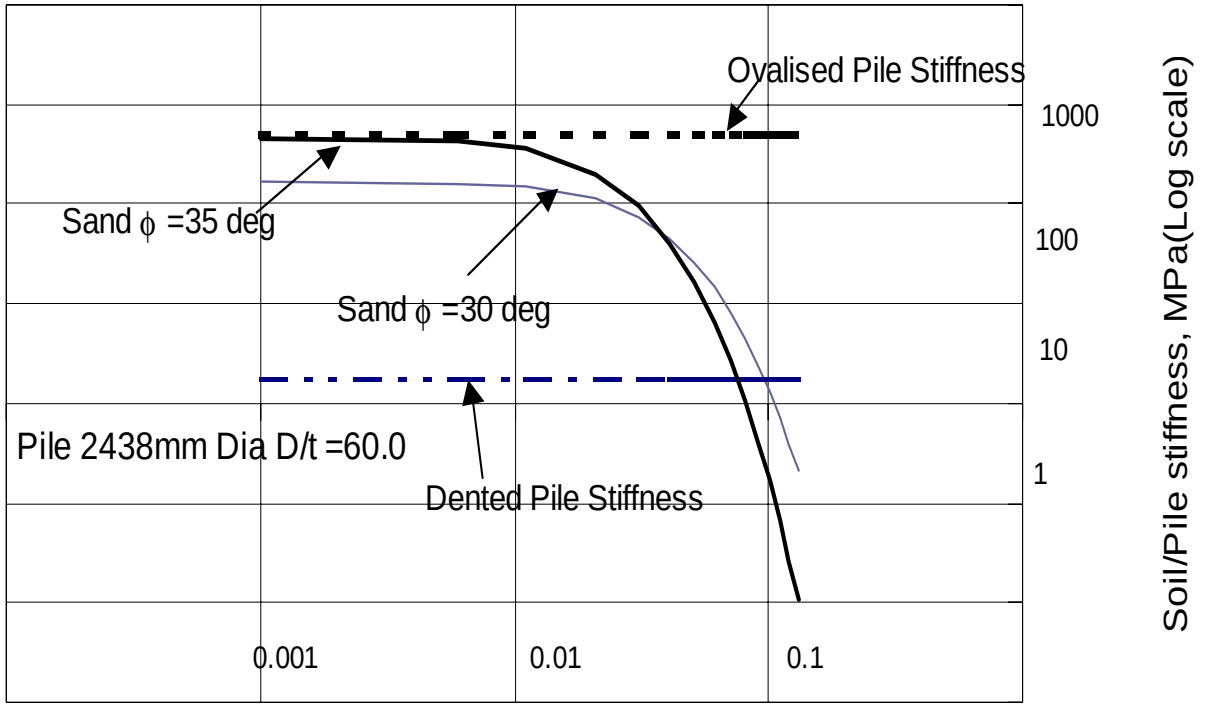

Figure 4-12
Comparison of Pile and Sand Stiffness D/t = 60

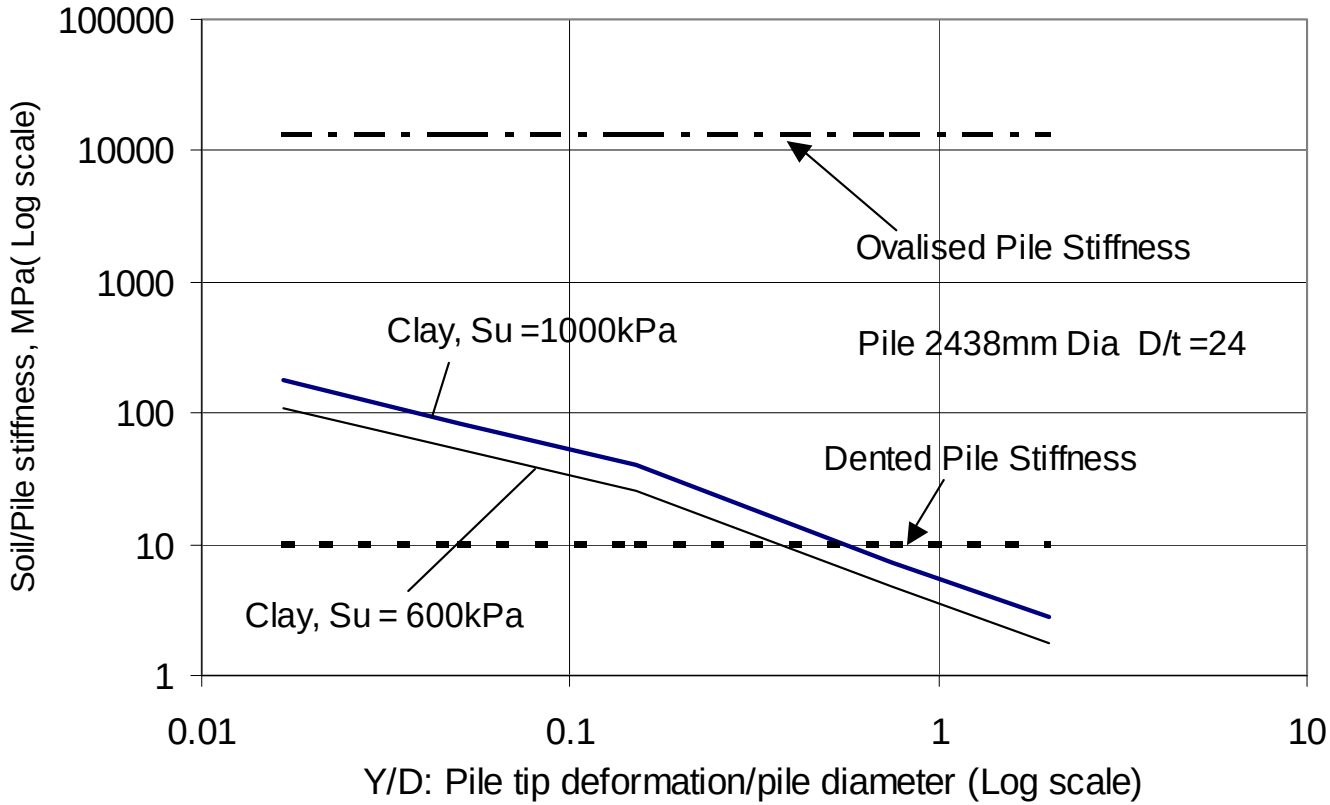

Figure 4-13
Comparison of Pile and Clay Stiffness D/t = 24

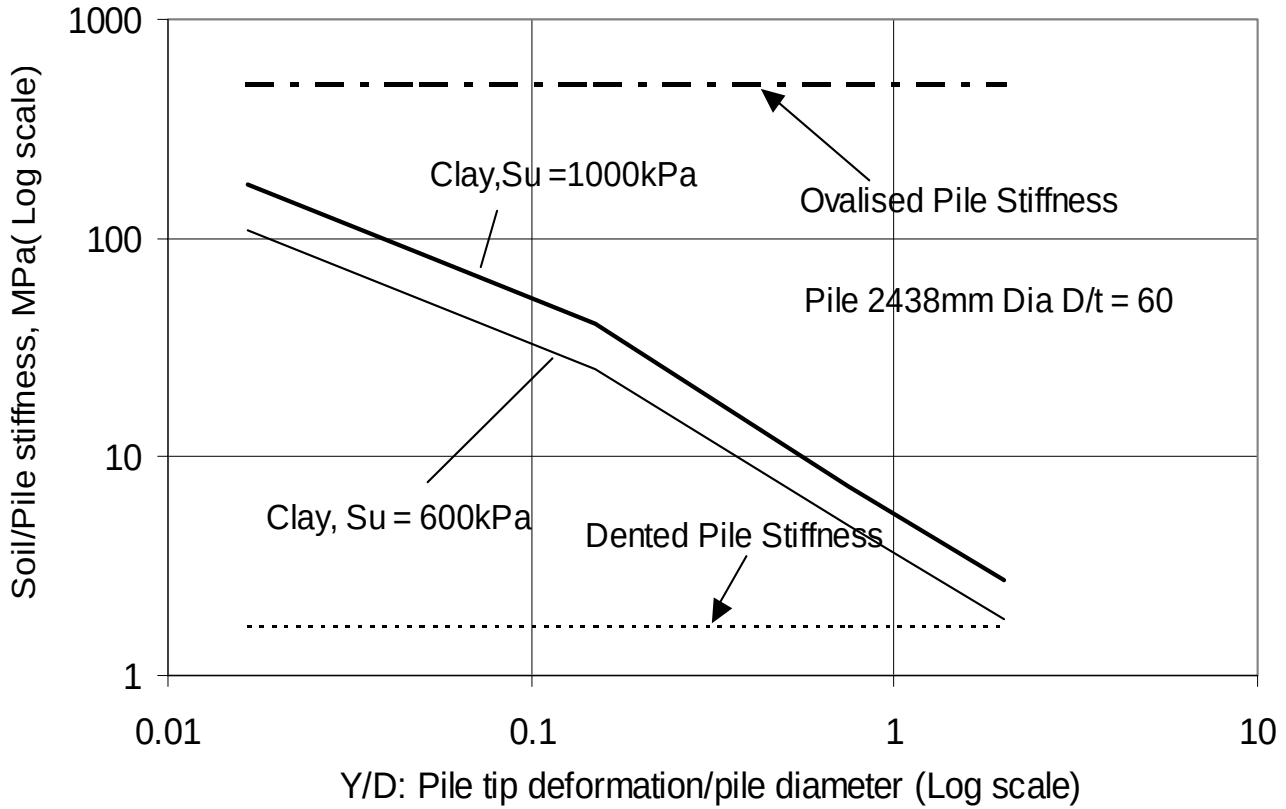

Figure 4-14
Comparison of Pile and Clay Stiffness D/t = 60

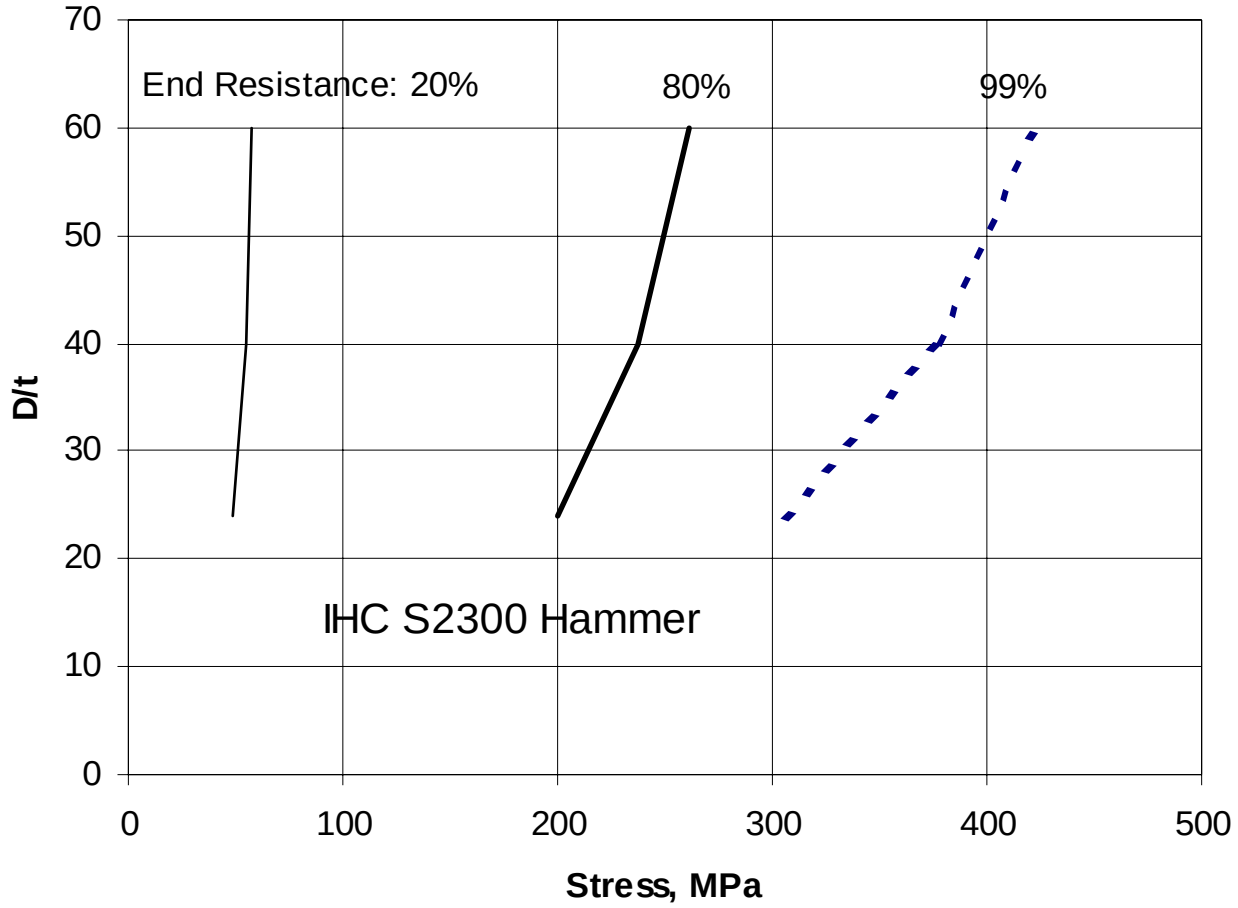

Figure 4-15
Pile Tip Stresses at Refusal , IHC S2300 Hammer

APPENDIX A

Survey of Pile Shoe Details

Authors	*Title*	*Published*	*Pile Size*	*Shoe Details*	*Comments*
API	13th-19th Edition	American Petroleum Institute	N/A	50% Thickening Length: 1.0xD	This could result in very high D/T ratios
Semple & Gemeinhardt	Stress History Approach to Analysis of Soil Resistance to Driving	Offshore Technology Conference OTC 3969, 1981	N/A	No recommendation given	These references provide recommendations on reduced skin friction for shoes
Toolan & Fox	Geotechnical Planning of piled Foundations for Offshore Structures	Proc ICE May 1977	N/A	No recommendation given	
Heerema E P	Pile Driving and Static Loads on Piles in Stiff Clay	Offshore Technology Conference OTC 3490, 1979	610mm Dia by 22.5mm D/T = 27.1	610mm Dia by 48.0mm Wall D/T = 12.7	Piles were test piles
Durning P J & Rennie I A	Determining Pile Capacity in Hard Overconsolidated North Sea Clay	Proc European Offshore Petroleum Conference 1979	1.52m Dia by 63.4mm D/T = 24.0	1.52m Dia by 90mm Wall by 0.482m length D/T = 16.9	The Heather Piles were provided with a very heavy shoe for hard clays
Rigden J and Semple	Design and Installation of the Magnus Foundation; Prediction of Behaviour	Proc Conf on Design of Offshore Structures ICE 1983	2.134m Dia by 63.5mm D/T = 33.6	80mm Wall by 1.4m Length D/T = 26.6	
Fox D A, Sutton V J R and Oksuzler Y	Development of Forties Piles from West Sole and Nigg Bay Experiences and Tests	Proc Conf Design and Construction of Offshore Structures ICE 1979	Not Reported	Not Reported	The authors note that shoes of various geometry were used

Authors	*Title*	*Published*	*Pile Size*	*Shoe Details*	*Comments*
Clarke J, Rigden W J and Senner D W	Re-interpretation of the West Sole Platform 'WC' Pile Load Tests	Geotechnique, Sept 1985	762mm Dia by 32mm Wall D/T= 23.6	762mm Dia by 51mm wall by 550mm long D/T = 15.0	Test Piles
Tagaka K, Heerema E P, Uchino T and Kusaka T	Pile Driveability Test on Actual Offshore Platform in Calcareous Clay for Qatar NGL Offshore Project	Offshore Technology Conference, Houston, 1979 OTC 3440	762mm Dia by 32mm and 915mm Dia by 32mm D/T = 23.6 and 28.6	762mm Dia and 915mm Dia by 45mm Wall by 0.68m long D/T = 16.9 and 17.9	Test Piles
Rennie I A and Fried P	An Account of the Piling Problems Encountered and the Innovative Solutions Devised During the Installation of the Maui 'A' Tower in New Zealand	Offshore Technology Conference, Houston, 1979 OTC 3442	1219mm Dia by 38mm D/T = 38.0	1219mm Dia by 45mm Wall 1.5m long and 1219mm by 51mm Wall 1.5m long D/T = 27.0 to 23.9	Various shoes were tried to overcome difficult driving in dense sand

Printed and published by the Health and Safety Executive
C0.5 5/01

MAIL ORDER
HSE priced and free
publications are
available from:
HSE Books
PO Box 1999
Sudbury
Suffolk CO10 2WA
Tel: 01787 881165
Fax: 01787 313995
Website: www.hsebooks.co.uk

RETAIL
HSE priced publications
are available from booksellers

HEALTH AND SAFETY INFORMATION
HSE InfoLine
Tel: 08701 545500
Fax: 02920 859260
e-mail: hseinformationservices@natbrit.com
or write to:
HSE Information Services
Caerphilly Business Park
Caerphilly CF83 3GG

HSE website: www.hse.gov.uk

OTO 2001/018

£15.00

ISBN 0-7176-2040-9

9 780717 620401